בס"ד

DEVELOPING CONDITIONAL PROTEIN RESCUE FOR SYNTHETIC PROTEN-BASED LOGIC CIRCUITS TOWARDS THE DETECTION AND TREATMENT OF CANCER

by

Andrew S. Gaynor

A dissertation submitted to the Faculty of the University of Delaware in partial fulfillment of the requirements for the degree of Doctor of Philosophy in Chemical Engineering

Summer 2020

DEVELOPING CONDITIONAL PROTEIN RESCUE FOR SYNTHETIC PROTEN-BASED LOGIC CIRCUITS TOWARDS THE DETECTION AND TREATMENT OF CANCER

by

Andrew S. Gaynor

Approved: _____
Eric Furst, Ph.D.
Chair of the Department of Chemical and Biomolecular Engineering

Approved: _____
Levi T. Thompson, Ph.D.
Dean of the College of Engineering

Approved: _____
Douglas J. Doren, Ph.D.
Interim Vice Provost for Graduate and Professional Education and
Dean of the Graduate College

I certify that I have read this dissertation and that in my opinion it meets the academic and professional standard required by the University as a dissertation for the degree of Doctor of Philosophy.

Signed: _____

Wilfred Chen, Ph.D.
Professor in charge of dissertation

I certify that I have read this dissertation and that in my opinion it meets the academic and professional standard required by the University as a dissertation for the degree of Doctor of Philosophy.

Signed: _____

April M. Kloxin, Ph.D.
Member of dissertation committee

I certify that I have read this dissertation and that in my opinion it meets the academic and professional standard required by the University as a dissertation for the degree of Doctor of Philosophy.

Signed: _____

Millicent O. Sullivan, Ph.D.
Member of dissertation committee

I certify that I have read this dissertation and that in my opinion it meets the academic and professional standard required by the University as a dissertation for the degree of Doctor of Philosophy.

Signed: _____

Sharon Rozovsky, Ph.D.
Member of dissertation committee

EPIGRAPH

"לא עליך המלאכה לגמור, ולא אתה בן חורין להבטל ממנה."

-פרקי אבות ב:טז

“It is not incumbent upon you to complete the work, yet you are not free to desist from it.”

-*Ethics of Our Fathers* 2:16

ACKNOWLEDGMENTS

A PhD, like most undertakings of importance, is not accomplished in a vacuum. I would not be where I am today without the help, support, guidance, friendship, and love of countless individuals. There are simply too many of you to count and recognize here without penning a document equal in size to the body of the work that follows this. Please know that just because you are not mentioned by name, does not mean you were forgotten or unworthy. If you read this dissertation closely, you will find your influence and guidance between the lines. That frustrating experiment you helped push me through is bound somewhere between the covers.

First and foremost, I would like to thank my advisor, Prof. Wilfred Chen. Inherently, there is a leap of faith when an advisor accepts a student, for perhaps that student will become the bane of existence for somewhere between 4-6 years. I sincerely hope that was not the case for me, but nonetheless, I appreciate the vote of confidence, both in acceptance to the PhD program and into the lab. Dr. Chen has been nothing but helpful and encouraging my entire time here. In his caring about me as his student, he demanded a personal investment of every fiber of my being. They say (whoever "they" are) a PhD program is whatever you put into it, and Dr. Chen ensured that I maximized my gain from my time at the University of Delaware. His unwavering passion and curiosity inspired me to leave no stone unturned in an effort to produce the best work possible, and his unequivocal rejection for any project that wasn't novel demonstrates a boldness uncommon in today's world. All of this and more has no doubt made me a better scientist, and I am forever grateful for this. I'm

so sorry that I "sold out" for industry (truly, I am), but I am confident that academia will carry on in good hands so long as you stay in the game.

Secondly, my dissertation committee has been instrumental in the success of this undertaking. I am fortunate to be in the unique position to have been more involved with my committee than most. My first interactions with Prof. April Kloxin were in her own lab as a CBI rotation student. It was a wonderful way to spend my first winter session, and I never could imagine it possible to be so productive in just six weeks fresh out of the gate. Prof. Millie Sullivan, along with Prof. Thomas Epps, was gracious enough to take me under her wings as the teaching fellow in Heat and Mass Transfer. Dr. Sullivan is a master lecturer, and I still have much to learn from her poise and fluid delivery at a chalkboard. Prof. Sharon Rozovsky and I attended many common seminars through the CBI program, and I always enjoyed the research updates from her group. Thank you April, Millie, and Sharon for the feedback and suggestions that brought out the best aspects of my project. The fault for any omissions, errors, or mistakes lies entirely with me and with me alone.

The main support in the Chen lab comes from the remarkable team of scientists and peers I was so fortunate with whom to work. Senior students and postdocs are so instrumental to early success when starting in a lab. I would like to thank Dr. Qing Sun, Dr. Qi Chen, Dr. Maryam Raeeszadeh, and Dr. Vince Price for blazing the trail before me. In particular, I would like to mention Dr. Heejae Kim, with whom I was fortunate to spend a longer amount of time in lab. Haeejae had a no holds barred approach to science that was enviable, and I appreciate the drive he instilled in me to "do it better" and to accept nothing less for myself.

My first mentor in the lab, Dr. Rebecca Chen, taught me almost everything I know about life in the Chen lab, and none of this dissertation would be possible without her patient and methodical pedagogy. She forced me to think and consider not just what I was doing, but more importantly why I was doing it. Her teaching gave me the ability to design my own experiments and lab activities in a way that maximized my productivity from my early years in the lab. This teacher-student relationship quickly gave way to a friendship I will value for life. We disagreed about almost everything in life, but I respect the way you debate calmly and rationally while never losing respect for me as I person (or at least so I think). I treasure so many of those late-night conversations in the lab and office, and of course the memes too.

Dr. Kay Siu made for many enjoyable conversations in the office, and I thoroughly enjoyed sharing space with him for many years. I've always been envious of his abilities to think outside the box and his desire for nothing short of personal perfection. We spent many enjoyable afternoons on slower days watching hilarious video clips online and reminiscing about the "Hopeless Place" as conferences became to be known for reasons that need not be repeated here. It also meant so much that you flew all the way out from California for my wedding as you were starting a postdoc. I hope you got enough to drink, and I'm pretty sure that guy is still waiting to start that biotech business venture with you. However, for the record (and this is published so it doesn't get more recorded than this) I will never understand your love of the *John Wick* series. I mean, just so much senseless violence. Why do people like it?

Emily Hartzell (♥zell) has now shared the office with me longer than anybody else, and she was an important go-to when I needed to let off steam caused be some

egregious action of one undergraduate or another. I still get a laugh out of sharing the trials and tribulations from my time as a teaching fellow with you (as I mentioned above, I still have a lot to learn about lecturing) and from all the *Saturday Night Live* skits we shared back and forth, particularly Chad. I think after Dr. Chen, nobody loved the science more than Emily in the lab, and it really showed in how much she demanded of herself and those around her. On this proclivity alone, you can build an entire academic career, should you chose to pursue that.

Dr. Andrew Swartz (aka Andrew #1) and I first had a chance to work together on the statistics semester project in our first year at Delaware. Right away, I recognized him as a force to be reckoned with, especially when it came to statistics. Andrew was one of the few students who could continuously impress Dr. Chen with his results, and it did seem that everything in his hands turned to scientific gold. It was no wonder that he graduated in record time, and I have no reservations that he will have an illustrious career. Andrew was also one of the few students in the program who know how to have fun, and never forgot about the world beyond the laboratory walls. It's an important lesson, and one that took me a while to learn. Once I did, I became a better, happier graduate student for it. I appreciate the example in work/life balance.

Rachel Lieser quickly became a good friend in the lab, and I'm so glad her office assignment was in the Chen block rather than downstairs in the Sullivan office. I could always turn to Rachel to brighten my day with her ever-present and infectious smile. Rachel is truly a happy person if I ever met one. She laughs frequently and genuinely cares about those around her. On top of all that, she's great scientist and quickly began making her mark in the lab. Rachel, thank you so much for letting me

interrupt your work on all those occasions, listening to me, and your steady friendship. The Chen Lab was truly a more enjoyable place to show up every morning because of you.

It is truly difficult to fully express the debt of gratitude I feel to Emily Berckman for her friendship. While likely most of our conversations should never be repeated (ever!), there were several of them, and "hanging out" was usually the high point in the work day. We spoke daily while we worked in lab, sometimes for hours on end. We spoke bluntly and openly in a most refreshing way. Emily had an ability to make me laugh in a way few others could, and she challenged me to actualize my potential in a way only a true friend could. For that reason and others, I thoroughly looked forward to our walks to the UPS store and subsequent side trips to 7/11 for energy drinks (Please lay off of those. They're so bad for you!). I hope Emily had the opportunity to learn everything she wanted about Judaism, and I guess I'm thankful for all of the worldly things you taught me over the years too. Had Emily not been in lab, I undoubtedly would have graduated at least a year earlier (kidding, we did work hard), but I wouldn't trade this friendship for anything in the world, and I honestly would have no regrets if there hypothetically were extra months added on to my PhD. Thank you for your kindness and generosity with your time, and I look forward to the continuation of Wednesday morning meeting times.

There were also several younger students who enhanced my time in the Chen lab. Thank you to Victoria Hunt and Hopen Yang for sharing the cell culture room with me and putting up with all the times I needed the microscope in absolute darkness. I enjoyed the relaxed atmosphere you created in that small room and working side-by-side with all of you. Thank you also to Alex Mitkas for several great

memories and for your humor. Thank you to Daniel Yur for always laughing; I appreciated looking up from my lab bench to see a constant smile from the other side of the room. Best of luck to the newest students, Antonio Goncalves and Anxhela Sinani, and thank you for making my last few months in the Chen lab even better. I look forward to hearing great things about all of you.

I would be remiss if I did not mention my adopted lab, the April Kloxin lab. Their office for me was like a tiny oasis in the middle of Colburn, a place I could go to relax and laugh where most people wouldn't think to look for me (except, of course, the members of the Kloxin lab themselves). I spent more hours than I care to admit joking around in their office. I would often tell the members that in all likelihood, I would not have very vivid memories of working in the lab; most of the activities are too rote and mundane to make an impact in my memory. However, what I will certainly remember is the meaningful conversations over a cup of tea. *Brew Haha* was oftentimes the exact escape I needed. Thank you to Dr. Kat Wiley, even though she claims she was completely detestable our first year (her exact phrasing need not be repeated here), I know a good person and a quality friend when I see one. I hope you enjoyed all the stories of a real life *Marvelous Mrs. Maisel*. I know I will miss telling them to you. Thank you to Dr. Amber Hilderbrand for your insight and support. In many ways, she was Colburn's chief therapist, and I am grateful for the many times I was able to be a "client". You definitely helped put so many things into a more positive perspective, and you kept me sane during the strain of a PhD. Thank you to Dr. Paige LeValley, who was never afraid to "tell it like it is" in a remarkably sensitive way when she knows it's within her power to better a situation. I enjoyed putting this into practice at qualifying practice talks, and I really do believe the two of

us saved a lot of graduate careers from catastrophe. Last but not least in the group, thank you to Eden Ford, who was almost never too busy to stop and say hello in the hallways. It's that kind of kindness that goes so unacknowledged in Colburn, yet it is the cornerstone of the chemical engineering community.

My first few months and Delaware, it was slightly awkward being one of the only few Jews around. This was rapidly alleviated by the original "Jew Crew", Dr. Elisa Ovadia (also a member of the abovementioned Kloxin group) and Amanda Czik. I always looked forward to our falafel trips to Philadelphia, mostly because of the company. Of course, the annual Shabbat dinner we would prepare together was a highlight of my year (again, mostly because of the company). I cannot even begin to explain how instrumental the two of you were to my success in Delaware. Just knowing that there were a few people around with the same heritage as me made the whole place more hospitable and warm, and I don't think I could have lasted without that comradery. On top of that shared connection, you are both quality people of the highest caliber. It's difficult to find friends like you anywhere, and who could have imagined it would happen in Delaware? While we've now dispersed literally across the entire country, I know we'll stay in touch long after we've all graduated, and I look forward to the day when we can get together and have a Shabbat dinner again (someway, somehow). Thank you to both of you just for being you and extending to me your steadfast friendship.

Of course, the road to the University of Delaware was a long one, and many friends who helped me along that path continued to be there for me during my time as a graduate student. While in high school, I shared the long magnet school bus ride to Wheeler with Shelby Lits, whom I annoyed incessantly for quite some time (sorry).

Nonetheless, a friendship blossomed and endured. I can always count on her for a Podcast recommendation or a spot-on, insightful, and funny quip. Our respective careers have come a long way since helping out at the local Hebrew School (aka glorified babysitting), but at its core, nothing much has really changed between us, and I look forward to taking Millie to the dog park with you on future trips to Atlanta.

For three whole years while at Tulane, Nick Lowe and I shared living space. As a result, we had a lot of hilarious adventures, and I seriously do hope to record those stories in "The Book" one day. From hosting Shabbat dinner in our house (and subsequently wrapping all my cans of seltzer in aluminum foil) to late-night trips to Rally's for multiple half-pound servings of chicken tenders (and avoiding the local New Orleans crack heads), we had quite an eventful four years. Even beyond that time, from Black Friday Blowouts and documentary filming to drinks at The Hudson Social, I knew college had gained me a friend for life. I enjoyed visiting when you lived in D.C. and our occasional (and often spontaneous) video calls. I am so glad to have met you, but any stories you tell my children in the future must be approved in advanced.

During my senior year of college, I shared the house with Nick with Michael Kevin McCarty, a fellow chemical engineering major. If memory serves me correctly, it was actually Kevin who convinced me to study chemical engineering in the first place, a decision that has obviously been to my benefit at every turn in life. From all of those hours in the ChemE computer lab doing homework and projects to the life discussions with our "advisor", Prof. Hank Ashbaugh, I probably spent more combined time with Kevin than almost anybody else at Tulane. His optimism and good spirits made majoring in ChemE a joy. Some days I really miss reclining on

Couchy and just shooting the breeze. I will forever be indebted for being the life of the party at my wedding. Whether you were Kevin or Arty that night, I will never know, and perhaps it's for the best that I don't.

While at Tulane, I probably spent equal shares of time in Boggs (which housed chemical engineering) and Chabad. I could find Erica Diamond in both places, and my life was much improved because of it. Erica was always smiley and bubbly in a most contagious way, and she almost always had a corny joke to share to brighten any occasion. Thank you for all those times you got GE to buy us pizza in Philadelphia. After all you have done for them and their sales numbers, I really did earn it (somehow in my mind as of this writing, that makes sense). I appreciate your willingness to share your stories of the strange, strange people you encounter in your many escapades. New Orleans is interesting like that. Our conversations are always delightful, and you're one of those friends with whom I can pick up exactly where we left off as if nothing happened. I hope to see you at a professional conference or training soon!

Also at Chabad of Tulane and the infamous crew of Butler 8, I had the privilege of meeting Ethan Abrams, one of the best senses of humor I've ever encountered. Chabad board meetings were much more fun with somebody with whom to exchange sarcastic comments, though I was admittedly in agreement with much of what was being discussed. Visits to New York City were made more enjoyable by latching on to a local, even though we did eat at the same restaurant every time (Mocha Burger for life) with the notable exception of our Xmas Day adventure to Brooklyn for kosher BBQ. Fortunately, I will likely be making many future journeys

to the other Promised Land, and so I look forward to sharing many more burger meals with you in the future.

Then there are those friendships that surprise you in how they develop over a distance after graduation once everybody has gone their separate ways. This could not be more true of (double doctor) Stephanie Hurwitz (MD, PhD), my "outside consultant" who understood so well the trials and tribulations of working in a lab yet could maintain such an objective outlook simultaneously. I honestly do not think I could have navigated graduate school so effectively without having Steph to bounce ideas, strategies, and solutions around. I hope you benefited from our conversations as much as I did. Of course, there's so much more to Steph than just a powerhouse academic, and I also liked somebody with whom to discuss the best jokes from *Wait Wait* and the human fascination of *This American Life*. Steph has a resolute determination that is unparalleled, and honestly might be one of the most driven, intelligent individuals I know. I hope to keep you and Mike in my life for many years to come, and I am so eager to see all that you accomplish in your own career, however you may choose to direct it.

While all of the above people have contributed so heavily to my psychological and emotional wellbeing, there are a select group of people who have maintained me spiritually along the way. These people have the distinct privilege of being emissaries of the Lubavitcher Rebbe, Rabbi Menachem Mendel Schneerson, to whom I am so indebted for the inspiration and motivation to live up to my potential and spread as much goodness as I possibly could while in Delaware. A huge thank you to Rabbi Yochanan Rivkin, who has done so much to improve my attitude and outlook on life into an overall more positive, happy person. I appreciate always having time to take

my phone calls when I needed to discuss something. Thank you to the dedicated emissaries who have served the University of Delaware since my arrival, who so selflessly serve the Jewish community on campus: Rabbi Eliezer Snederman, Rabbi Shruli Matusof, and Rabbi Avremel Vogel. Last but not least, thank you to Rabbi Levi Haskelevich and Rabbi Doniel Grodnitsky for your outstanding hospitality and warmth through countless Sabbaths and holidays; the impressions you and your families have left on me will not be forgotten, and they serve as a model to me on how to treat guests and others.

What is a person without family? As for me, I am blessed to have one that is loving and supportive, but at the same time, knows how to push somebody when there is that need. My parents raised me to have the persistent work ethic needed to complete a PhD, and they guided me affectionately towards my goals. Their home provided a refuge for breaks during my studies, and my trips there always left me recharged and focused to continue upon my return to lab. I looked forward to traveling back for holidays or for no reason at all, and I hope to spend many more celebrations with the both of them into the future. My parents invested themselves fully into my overall wellbeing, often looking out for me when I was guilty of not looking after myself. My brother and sister, Ryan and Jenna, made my visits with family extra special. Honestly, I don't keep in touch as much as I should, but I always enjoy the limited amount of time we get to spend together. Thank you both for being such good siblings, even when I seemed absent myself.

With marriage comes an entirely new family, and for this one too, I feel blessed. My mother-in-law and father-in-law accepted and loved me instantly, and I always feel welcomed at the Spadone residence as a full-fledged son. Thank you both

for being so nurturing and supportive during our first year of marriage. Zeissa, my new sister, has been instrumental in helping with gift selection for my wife, and also made my addition to the family seamless. I wish you and Mendel so much success in everything to come. To our neighbors and friends, Shimshie and Sarah Teitelman, thank you for your friendship and hospitality after our arrival in Baltimore. I loved Shabbat dinners at your house and the genuine interest you took into my studies; you both are true friends. Thank you also to Nechama Engel (and Rivka Liba), Shani Heifetz, Chenya Levitan, and Gitty Wolf (in alphabetical order by last name, not importance to me) for so readily accepting me into your friend group and the smiles you provided. I love when you visit for the Sabbath. I look forward to having you guys over throughout our lives, and I hope that soon you come with accompaniment and a different last name. There will always be a guest room waiting for you and a roll of sushi in the refrigerator wherever we might be living.

I saved the best and most importance for last, and I think everybody who knows me knows how important and special my wife, CM, is to me. I'm not sure she fully understood what she was signing up for by marrying a sixth year PhD student, but she jumped into the role of supporter, cheerleader, and confidant with the utmost grace. She took what is normally the most stressful time in a graduate student's career (the end stage), and she kept me calm and focused throughout. I do not know how I will ever repay you for what you have given me during this trying time in my life, and I hope you have benefited by having me in your life as much as I have from you. I promise you I will never do anything as crazy as attempt a PhD again in my life. Thank you also for bringing Gio the Mi-Ki Thing (and Beary Bear) into my life and sharing him with me as much as he is willing to be shared. Thank you for everything,

and I am so glad I get to traverse the adventures of life together with you. There truly is nobody else with whom I'd rather embark on such a journey. There is no doubt you are the partner and soulmate Divinely intended for me, and I am honored to be yours in return. CM, please always come as you, because that is always exactly what I need.

TABLE OF CONTENTS

LIST OF TABLES

LIST OF FIGURES

ABSTRACT

Cancer is a complicated set of diseases marked by drastic changes in the cellular proteome. To treat cancer, clinicians still strongly rely on chemotherapy, which kills mitotic cells indiscriminately, leaving formidable side effects in its wake. Recently, there has been a drive for "smart therapies" that can distinguish between healthy and cancerous cells. To head this call, several researches have sought to leverage proteomic differences to deploy a therapeutic protein, but most have focused on individual differences in expression levels of cell surface markers only. Probing intracellular proteins or multiple proteins simultaneously still remains challenging. This dissertation attempts to alleviate these barriers by engineering an autonomous protein switch triggered by intracellular proteomic information. To this end, we have developed a modular platform that enables the control of protein half-life based on the presence of a target protein. Important stages in the development of this technology and their broader implications are investigated herein.

First, foundational work was completed to determine that a prodrug converting enzyme, a commonly proposed option for a protein-based cancer therapy that enzymatically converts an innocuous prodrug into a cytotoxic drug, can be regulated via protein degradation. Using Traceless Shielding, a method for inducing the rescue of a protein of interest (POI) via a small molecule, we explored the kinetics of initial protein degradation and rescue. Next, we showed that cell viability was unaffected by the presence of the prodrug in the absence of the rescuing molecule. Thus, protein degradation is a viable strategy for managing prodrug converting enzymes.

With this important cornerstone laid, we sought a clever, facile method for translating cellular protein inputs into a POI rescue output. This lead to the development of conditional protein rescue, in which a degron is genetically fused to a POI followed by a short, sensing domain. In the absence of the sensing domain's target, the degron is exposed and the POI is fated for degradation. However, in the presence of the target, the degron is concealed and the protein is rescued. The first versions of this platform used SpyTag as the sensing domain, which resulted in a dramatic increase in POI concentration upon the co-expression of SpyCatcher, which spontaneously forms an isopeptide bond with SpyTag. We expanded upon this by using nanobodies—small, monomeric, and specific antigen-sensing domains—as the sensing domain. Nanobodies varied POI concentration based on the presence of co-expressed fluorescent proteins. Nicely, CPR is adept at distinguishing between cancer cells and non-cancer cells *in vitro*.

Finally, we further improve the capabilities of CPR by constructing Boolean AND gate architecture into the framework. Fluorescent protein targets are initially employed to block N- and C-terminal degrons. We show that both targets are necessary to raise the concentration of the POI. We prove the therapeutic feasibility of this design by detecting a synthetic cancer-model system: HeLa cells constitutively expressing GFP from both HeLa cells and HEK293T cells. This promising results shows that our design is an initial step at addressing some of the challenges impeding next-generation therapies.

This technology shows that the power of engineered protein degradation to yield rapid, definite changes in the concentration of a POI can be effectively harnessed to detect multiple, intracellular cancer protein targets. Paired with developments in

targeted delivery, it is now possible to offer a two-pronged cancer sensing device requiring both the overexpression of a cell surface receptor and multiple intracellular proteins to activate. This should result in low background in off-target cells and an overall reduction of side effects. Furthermore, multi-input CPR can be expanded to any system of interest, and it may be practical in the study of other biological systems as well.

Chapter 1 is adapted and reproduced with permission from Elsevier. Source:

Chen, R. P.*, Gaynor, A. S.* & Chen, W. Synthetic biology approaches for targeted protein degradation. *Biotechnol. Adv.* **37**, 107446 (2019).

*Authors contributed equally to this work

Chapter 1

INTRODUCTION

1.1 Biological Differences Between Cancer and Non-cancer Cells

At its simplest definition, cancer is defined as a collection of related diseases in which cells grow in an unregulated fashion and invade the surrounding tissue.[1] Healthy cells are regulated by a well-choreographed cascade of cell cycle checkpoints enforced by obligatory protein-protein interactions; only under the proper conditions is a healthy cell permitted to undergo mitosis.[2–5] By contrast, cancer cells evade this tight regulation by undergoing genetic mutations that bequeath the cells with acquired capabilities advantageous to their uncontrolled growth.[6,7] Recently, the fields of systems biology and bioinformatics have sought to characterize the numerous differences between cancer cells and healthy cells on genomic,[8,9] transcriptomic,[10] and proteomic levels.[11,12] Based on the recent wealth of knowledge, scientists have begun to classify cancer into different subcategories, each with its own responses to treatment and clinical outcomes.

Because each cancer subcategory has a different "Achilles's heal," a more personalized approach to medicine is appropriate. Under this treatment approach, a "smart therapy" would be used to treat cancer based on the information it presents through its unique –omics profile.[13,14] This would be a welcomed departure from the "one-size-fits-all" approach of chemotherapies and other small molecules, which often target healthy cell populations along with the cancer. Currently, monoclonal antibodies, which bind to overexpressed surface markers on cancer cells, have

achieved success in the treatment of certain cancers.[15] Other next-generation therapies are in development, including T-cell therapy,[16] oncolytic viruses,[17] and cancer vaccines.[18,19] While these are certainly advancements in the field, they are still only capable of interpreting one cancer marker, meaning the overwhelming majority of cellular information is left unutilized. We envision a platform in which multiple inputs can be processed simultaneously in a way that more accurately identifies cancer cells from their healthy counterparts. In this way, healthy cells could be avoided altogether while delivering an efficacious treatment to the cancer, resulting in cancer medicine free from side effects.

Towards this end, previous colleagues in this lab have developed synthetic protein switches powered by DNA strand displacement. These switches can control protein proximity with Boolean logic, including the use of cancer-specific microRNAs (miRNAs) as device inputs.[20] An alternative, parallel strategy is protein degradation to control the switch. To our knowledge, no strategy for executing cellular computations using endogenous proteins as inputs currently exists. However, the tools developed in synthetic biology, a field that specializes in the design of artificial biological systems,[21,22] offer the ideal method to engineer this proposed approach. Herein, we describe a general method for regulating the intracellular concentration of a protein of interest (POI) via conditional protein rescue (CPR): engineered proteins are fated for degradation unless required to fulfil a desired function. We further demonstrate that this strategy is applicable to differentiating between cancer and non-cancer cells, providing a novel avenue for personalized medicine.

1.1.1 Cancer-Specific Delivery Based on Differences in Protein Expression

Targeted delivery is one suggested way to introduce therapeutic proteins specifically to cancer cells. In this approach, targeting ligands are conjugated to therapeutic proteins to improve protein stability and cellular uptake.[23] For example, GE11 is a peptide known to have high affinity for the epidermal growth factor receptor (EGFR) overexpressed in inflammatory breast cancer (IBC) cells, amongst other cancer types.[24] This peptide has been successfully conjugated onto a prodrug converting enzyme (PCE), resulting in uptake and cytotoxicity in IBC cells but not MCF10A, a normal breast epithelial cell line.[25] While this approach is promising and specific, it fails to capitalize upon the abundance of proteomic information contained within the cell itself. Thus, the platform described herein aims to improve upon this technology. Furthermore, there is the potential for targeted delivery of the intracellular sensor such that more layers of information are accessible as device inputs (**FIGURE 1.1**).

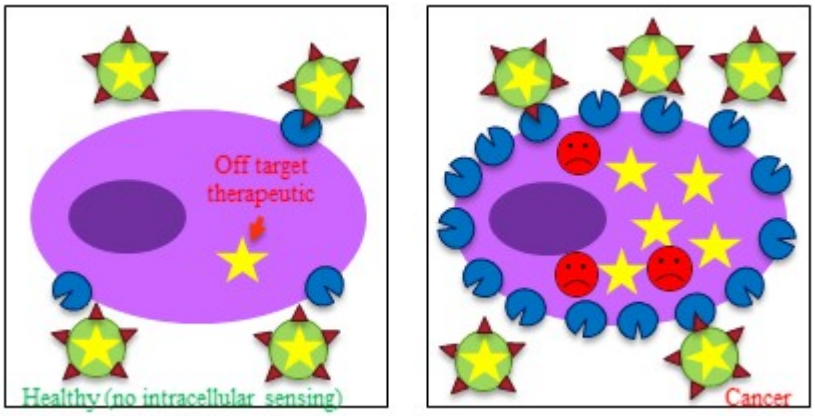

Figure 1.1 Receptor and intracellular protein information can be used to avoid off-target effects. In the healthy cell on the left, a lower concentration of cell surface receptors (blue) results in less recognition by the therapy carrier (green circle with triangular affinity probes), and therefore less uptake of the therapy (gold star). However, with no ability to sense the intracellular environment, therapy is promiscuously deployed. In the cancer cell on the right, the detection of both a high concentration of surface receptors and intracellular cancer markers yield a successful two-pronged activation.

1.2 Overview of Eukaryotic Proteasomal Protein Degradation

One of the fastest mechanisms of altering protein concentration in a cell is through proteasomal degradation of undesired proteins. As such, proteasomal degradation is an imperative process in maintaining cellular homeostasis and ensuring that the cell cycle is properly coordinated.[26–28] Many key regulatory proteins have specific chaperones responsible for their controlled degradation.[29–31] In general, degradation requires a means of trafficking the target protein to the 26S proteasome and an unstructured region to initiate its destruction.[32] Two major mechanisms, ubiquitination-dependent or ubiquitination-independent pathways, are primarily responsible for proteasomal degradation.[30,33]

1.2.1 Ubiquitin-Dependent Protein Degradation Pathway

Ubiquitination is a central mechanism of targeting proteins to the proteasome.[34–36] Typically, multiple ubiquitin (Ub) units are attached to a lysine residue on the target protein via the sequential action of a three-enzyme cascade: a ubiquitin-activating enzyme (E1), a ubiquitin-conjugating enzyme (E2), and a ubiquitin ligase (E3) (**FIGURE 1.2**), creating a polyubiquitin chain.[36] This tagging process leads to recognition of the polyubiquitin chain by the 26S proteasome to degrade the target proteins to small peptides.[37,38]

Generally, E3 ligase falls into two broad structural classes – either the monomeric homology to E6-AP C-terminus (HECT) domain or the larger really interesting new gene (RING) finger family.[39,40] HECT domain proteins consist of two functionally distinct regions that enable transfer of an activated Ub from E2—bound to N-terminus of the HECT E3—to the POI.[41,42] The RING finger E3 ligase family contains a canonical RING finger domain that is responsible for facilitating E2-dependent ubiquitylation.[43] The largest multi-subunit RING finger E3 ligases is the cullin (CUL) RING ligase (CRL),[44,45] which contains the SKP1-cullin-F-box protein (SCF) complex. The F-box protein is responsible for substrate binding and is attached to one end of CUL via the adaptor protein, Skp1.[46–49] To the other end of CUL, a RING finger E3 ligase binds to an ubiquitin-charged E2 to catalyze the transfer of ubiquitin to the target substrates. The ability to interchange F box proteins within the same cullin E3 framework allows for great flexibility in proteome management[50]

This proximity-driven ubiquitylation strategy provides a simple framework to hijack the native E3 ligase machinery for non-natural POIs for targeted degradation.[51–53] This idea has inspired the development of bifunctional chemical linkers called proteolysis targeting Chimeras (PROTACs) containing distinct substrate-binding and

E3 ligase-binding groups for hijacking the native E3 ligase machinery.[54–58] The conjugate molecule serves to assemble a ternary complex between the E3 ligase, target protein, and probe molecule, allowing the E3 ligase complex to ubiquitinate the non-natural substrate and promote proteasome-dependent degradation. While these drug-like PROTAC molecules allows targeted degradation of native proteins, it is often challenging to identify and synthesize the target-specific binding moiety.[56] Alternatively, purely protein-based strategies for targeted protein degradation based on proximity control have gained more attention due to the ease and flexibility of design.[59]

A minor category of E3, the RING-between-RING (RBR) family, shares features of both HECT and RING E3s. The name is derived from the presence of two RING domains (RING1 and RING2) that sandwich an in-between-ring (IBR) domain.[50] The first RING domain serves to recruit E2 as might be expected,[60] but the second RING domain contains a catalytic cysteine that complexes with Ub before being transferred to the target, similar to HECT E3s.[61] While no synthetic biology has been attempted using the RBR E3 ligases, the hybrid properties of this system might allow for future, novel applications.

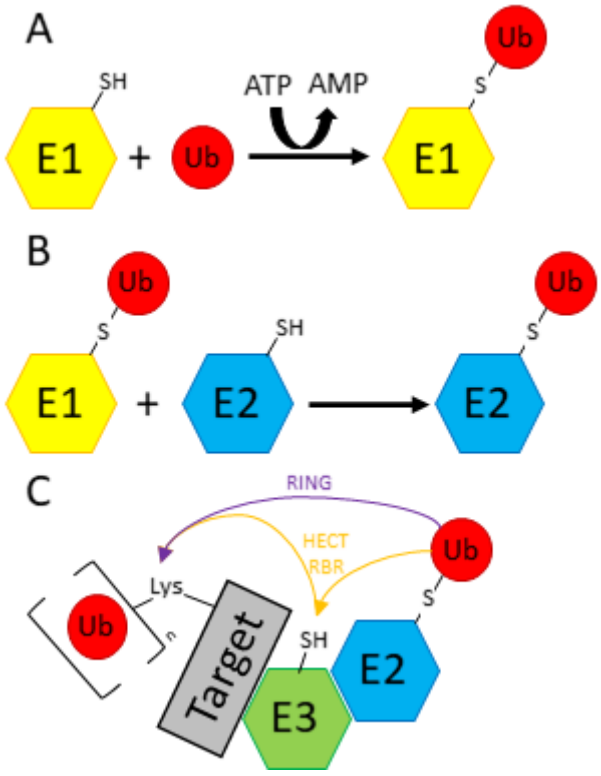

Figure 1.2 **The ubiquitination enzyme cascade.** A) Ubiquitin activating enzyme (E1) forms a thioester bond with ubiquitin at the expense of ATP. B) Ubiquitin conjugating enzyme (E2) accepts the activated ubiquitin from E1 in a transthioesterification reaction. C) Ubiquitin ligase (E3) is responsible for both target recognition and the transfer of Ub from the active site of E2 to a lysine on the target or growing polyubiquitin chain. RING E3s catalyse the transfer of Ub directly without first accepting it (purple arrow). Alternatively, HECT and RBR E3s first form a thioester with Ub before transferring it to the target (gold arrows).

1.2.2 The N-end Rule Degrons

The N-terminal amino acid residue of a protein plays a central role to its half-life by acting as a N-degron[62,63] that is recognized by a specialized E3 ligases, *N*-recognins.[64–68] Upon *N*-recognin binding, the target is polyubiquitinated at an internal lysine and targeted for degradation.[35,69] The in vivo stability of a protein is directly correlated to the identity of its N-terminal residue and can vary from a half-life of less

than 1 h (Arg) to longer than 100 h (Val).[70] This simple rule set provides a new strategy to engineer the half-life of POIs by artificially exposing the desired N-terminal residue.[62,71]

1.2.3 Ubiquitin-Independent Proteasomal Degradation

Not all proteins targeted to the proteasome are first ubiquitinated. The proteasomal degradation of ornithine decarboxylase (ODC), a well-folded protein, takes place without ubiquitination with the help of a C-terminal degradation tag (C-degron).[72] A second protein, antizyme 1 (AZ1), mediates the interaction between ODC and the 26S proteasome by exposing a stretch of amino acids at the C-terminus from which degradation begins.[73,74] Because the initiation sequence is relatively short and well-characterized, this C-terminal portion of ODC has been used extensively as a reliable, facile C-degron tag for a wide of protein targets.[75–78]

1.3 Engineered Protein Degradation Based on Stimuli Responsive Degrons

A common strategy to modulate protein stability is to insert a conditional degron tag either to induce degradation or to rescue the target from degradation (**FIGURE 1.3**). A wide range of external stimuli can be used to activate the desired phenotypes, making this a highly flexible and adaptable strategy for a wide array of POIs.

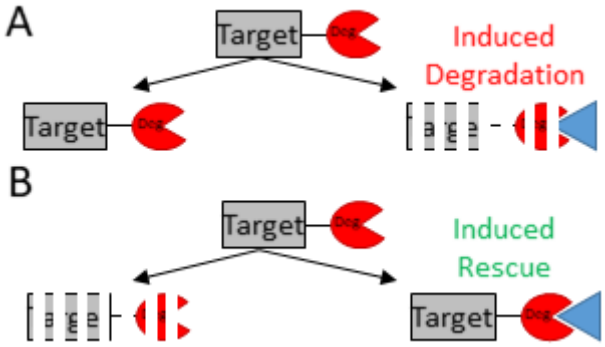

Figure 1.3 General scheme of controlled protein fate by a conditional degron. A) By default, the conditional degron (red circle with missing wedge) is stable (left), but upon addition of a small molecule cue (blue triangle), the degron becomes unstable and the target (grey rectangle) is degraded (right). B) By default, the conditional degron is unstable and the target is degraded (left). Upon addition of the small molecule, the degron is stabilized and the target is rescued from degradation.

1.3.1 Small-Molecule Induced Protein Degradation

Small molecules are frequently used to activate degron activities. The ligand-induced degradation (LID) system, a mutant of the rapamycin-binding protein FKBP, was first identified as a cryptic inactive degron.[79] Upon the addition of the synthetic small molecule Shield-1 (Shld1), a derivative of rapamycin that has no reported biological activity,[80] the cryptic degron is displaced and exposed for interaction, thereby inducing degradation of the corresponding fusion POI. While the LID system is able to degrade proteins of interest rapidly when activated, the stable version still necessarily contains a bulky FKBP fusion protein, which might interfere with the biology activity of the POI. To minimize this issue, small molecule-assisted shutoff (SMASh) was developed.[81] In this configuration, the POI contains a C-terminal fusion to the following components in order: a specific viral protease cut site, the viral protease for that cut site, and a degron tag. With no additional cues, the protease cuts

at its recognition site, releasing the target protein from the degron, and therefore the target is stable by default. Unlike the LID system, the POI does not contain a bulky fusion after protease cleavage, and therefore it is more likely that native activity will remain unimpaired. Upon the addition of a specific protease inhibitor, the degron is able to act upon the entire protein, including the target. SMASh demonstrated a strong signal-to-noise ratio, and spacers can be configured to allow SMASh to function from either the N- or C-terminus, offering flexibility to the end-user. These strategies allow easy deactivation of cellular phenotypes by using a small molecule and have been successfully applied in mammalian cell culture, transgenic mice, plants, and virus studies.[82,83]

1.3.2 Small-Molecule Induced Protein Rescue

In contrast to induced degradation, induced protein recue has also been made possible using a small molecule. A degron tag that is inherently unstable is fused to a POI to induce degradation. However, when bound to a highly specific small molecule ligand, stability is restored and the POI is rescued. Emphasis has been placed on developing degrons whose ligands are inexpensive, active at low concentrations, commercially available, and cell membrane permeable. One of the earliest examples was based on FKBP12. Rescue of various proteins could be induced by Shld1. An orthogonal strategy involved a mutated *E. coli* dihydrofolate reductase (ecDHFR), which is rescued specifically by trimethoprim (TMP). It was demonstrated that two different proteins could be rescued on cue by introducing either Shld1 or TMP,[84] expanding the toolkit and protein space that could be studied. The ability to execute orthogonal and conditional protein rescue lends itself to the possibility to create synthetic logical circuits to modulate protein functions and cellular activities.

1.3.3 Small-Molecule Induced Rescue by Removable Degron

To eliminate possible negative effects on protein activity caused by the degron fusion, technologies have been developed to cleave the degron tag once rescue is induced by the small molecule. The first such technology termed split ubiquitin for rescue of function (SURF) innovated the use of a split ubiquitin domain, which induces endogenous cleavage by the de-ubiquitination enzyme (DUB) after reconstitution.[85] The degron was an engineered FKBP12-rapamycin-binding protein (FRB) with point mutations that fated FRB and its fusions to degradation (**FIGURE 1.4**). Upon the addition of rapamycin, FRB is stabilized by its interaction with native FKBP, situated on a separate construct containing the second half of the split ubiquitin. Simultaneously, the two split ubiquitins are forced into proximity, allowing the POI to be cleaved from the degron. Different FRB mutants or native FRB fused to a separate degron could be used to offer varying kinetic properties.

An improved version of SURF was developed by using a mutant FKBP called FKBP*, and the native FRB was used to reconstitute the split ubiquitin. Both proteins were expressed under a single promoter using a viral "self-cleaving" 2A site.[86,87] This Traceless Shielding (TShld) method offers improvements over its predecessor both in terms of dynamic range and ease of use.[88] The same group placed TShld under a tetracycline inducible promotor, and showed that in this manner, they could completely eliminate any system background by adding a layer of transcriptional control as well.[89] In Chapter 2, we used TShld to control the prodrug converting enzyme, yCD, and found HeLa cell viability was only affected in cells that received both the prodrug and activating molecule. This demonstration shows the promise of engineered controlled degradation in therapeutic applications.

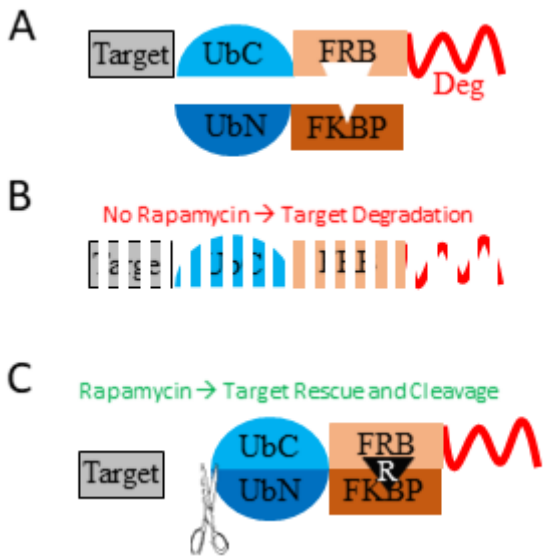

Figure 1.4 Split ubiquitin for rescue of function (SURF). A) SURF is composed of a target protein fused to the C-terminus of ubiquitin (UbC), FRB, and a degron tag. A second component is composed of the N terminus of ubiquitin (UbN) and FKBP. B) The default state in the absence of rapamycin is the degron leads to the complete proteolysis of the component to which it is fused, including the target. C) In the presence of rapamycin (black triangle), FRB and FKBP are drawn into proximity by binding to rapamycin. Consequently, UbC and UbN are complimented, leading to the rescue and cleavage of the target protein from SURF.

1.3.4 Protein Degradation by Revealing a Degron

Light is a popular optogenetic tool used in the field of synthetic biology because it offers the unparalleled combination of spatial and temporal control.[90–93] The light oxygen voltage (LOV2) domain is a light-sensitive protein that can reversibly interact with its C-terminus Jα-helix in the light (unbound) versus dark (bound) state.[94] By fusing an ODC degron to the C-terminus of the Jα-helix, researchers developed a degron tag that is hidden within the LOV2 domain in the dark state. Upon the application of blue light, release of the hidden ODC degron tag led to degradation of a

POI fused to the N-terminus of LOV2.[95] The use of light for conditional degradation is particularly attractive as it has no reported impact on cell physiology. However, delivering blue light in a developing embryo or a living animal is not trivial, and other alternative light-sensitive domains that are responsive to red or far red light[96,97] may be repurposed to broaden the use of light-responsive degrons.

Conditional degradation can also be achieved by using protease cleavage to reveal N-degrons. Protease cleavage sites are placed upstream of the N-end residue of a POI. Prior to cleavage the protein is stable, but upon cleavage a new N-end residue is exposed and degraded at a rate accordingly to the N-end rule (**FIGURE 1.5**). This concept was first explored by Taxis et al. in a system termed TEV protease induced protein inactivation (TIPI).[98] They designed a TDegX component that is fused to the N-terminus of the target protein. The TDegX contains a TEV protease cut site in which cleavage exposed a new N-terminal "X" residue of an N-degron. The implementation of TIPI in yeast resulted in rapid TEV-dependent degradation of target proteins fused to TDegD and TDegF. Although this strategy requires the fusion of synthetic components to the POI, it is powerful in establishing a framework for creating conditional protein modules. Subsequent works have utilized this concept with orthogonal and split proteases to establish post-translational control of genetic circuits,[99] and most recently programmable protein circuits capable of complex logic behavior.[100] This concept of hiding a concealing and revealing a degron under different conditions will be pivotal in Chapter 3.

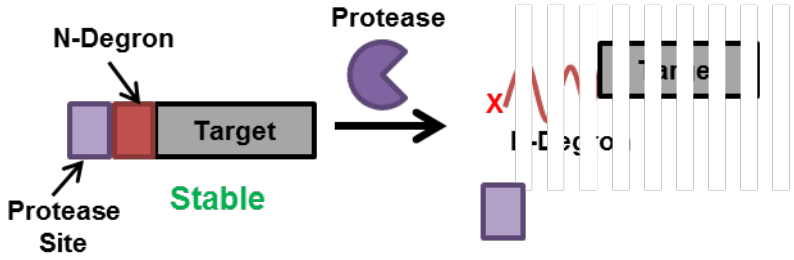

Figure 1.5 TEV protease induced protein inactivation (TIPI). Protease-dependent N-end degradation is achieved by using protease cleavage to create a newly exposed N-terminal residue that makes the target protein vulnerable to rapid degradation by the N-end rule.

A more complex design using TEV has also been demonstrated.[101] Site-directed cleavage by the TEV protease deprotected two degrons fused to two separate POIs, resulting in degradation of both parts of the processed protein. In this design, both target proteins act as a steric shield, blocking the degrons from interacting with the proteasomal degradation machinery. The deprotection of two orthogonal degrons provides the feasibility to execute Boolean logic gates for conditional degradation. These developments represent crucial progress towards repurposing artificial degrons from tools for the study of protein effects to useful components in synthetic biology platforms, an idea that will be explored further in Chapter 4.

1.4 Single-Domain Antibodies (Nanobodies)

While previous work lays the foundation for determining protein half-life, a method for translating cellular protein information into a degradation or rescue output is still lacking. Single-domain antibodies, commonly referred to as nanobodies, are the smallest known intact antigen-binding fragments discovered to date.[102,103] Due to

their relatively small size (12-15 kDa), ease of folding, and monomeric structure, they have been successfully expressed recombinently in bacterial, yeast, and mammalian hosts.[104,105] Nanobodies contain three complimentary determining regions (CDRs) involved in antigen binding, and advances in phage display technology have greatly expedited the discovery process of high-affinity, specific nanobodies against a new antigen.[106,107] For all of these reasons, nanobodies are the ideal biological intermediaries to modulate between protein inputs and degradation or rescue outputs of a POI. As time progresses, nanobodies against various cancer targets are expected to become more prevalent, and the adaptation of the technology described in this dissertation will thus become more facile.

1.5 Dissertation Overview

This dissertation describes a novel strategy for regulating proteins for cancer therapy by autonomous interpretation of cellular protein information. Each chapter will discuss one advancement towards this overall goal.

In Chapter 2, the simple concept of regulating the activity of a PCE through protein degradation will be explored. Using TShld (described in **Section 1.3.3** above) as a small-molecule inducible rescue model system, we show that kinetic rates of protein degradation can operate fast enough to outpace most enzymatic activity. Therefore, in the absence of the inducer but presence of the prodrug, cells remain viable. Only in the presence of both the prodrug and inducer do cells experience cytotoxicity. We coined this idea degradation dependent prodrug enzyme therapy (DDEPT). Since any strategy involving protein degradation of a PCE would be untenable if prodrug conversion occurred faster than degradation, this work lays the foundation for the rest of the dissertation.

In Chapter 3, we explore a technology we call conditional protein rescue (CPR) in which a degron fused to a POI is concealed by a target protein, rescuing the POI. CPR is the main driving force for translating cellular protein information into a therapeutic output. We first show that CPR is successful using a covalent-bond forming model system. By making strategic nanobody fusions, we also demonstrate the capability to detect GFP and use that as an input for both fluorescent proteins and PCE. Thus, we achieve an expansion of DDEPT. CPR can operate using both N- and C-terminal degron, and we show the capability to rescue a POI using cancer-specific proteins.

In Chapter 4, we tackle the challenge of multi-input CPR. Effective next-generation cancer therapies will require the examination of multiple protein targets simultaneously. Encouraged the success in both N- and C-terminal degrons, we combine both of these onto one POI to form a Boolean AND gate. Multiple inputs and their rescue efficiencies are studied, and a model system is used to explore cancer subtype recognition. We conclude that a relatively small addition to CPR allows for straightforward two-input recognition.

Finally, Chapter 5 will offer an overarching conclusion and examination of the work studied in this dissertation. The exciting future directions and therapeutic implications will be discussed, as well as future directions for additional research to expand upon the ideas and technologies addressed herein.

Chapter 2

INDUCED PRODRUG ACTIVATION BY CONDITIONAL PROTEIN DEGRADATION

Abstract

Enzyme prodrug therapies hold potential as a targeted treatment option for cancer patients. However, off-target effects can be detrimental to patient health and represent a safety concern. This concern can be alleviated by including a failsafe mechanism that can abort the therapy in healthy cells. This feature can be included in enzyme prodrug therapies by use of conditional degradation tags, which degrade the protein unless stabilized. We call this process Degradation-Directed Enzyme Prodrug Therapy (DDEPT). Herein, we use traceless shielding (TShld), a mechanism that degrades a protein of interest unless it is rescued by the addition of rapamycin, to test this concept. We demonstrated that TShld rapidly yielded only native protein products within 1 h after rapamycin addition. The rapid protection phenotype of TShld was further adapted to rescue yeast cytosine deaminase, a prodrug converting enzyme. As expected, cell viability was adversely affected only in the presence of both 5-fluorocytosine (5-FC) and rapamycin. We believe that the DDEPT system can be easily combined with other targeting strategies to further increase the safety of prodrug therapies.

Chapter 2 is adapted and reproduced with permission from Elsevier. Source:

Gaynor, A. S. & Chen, W. Induced prodrug activation by conditional protein degradation. *J. Biotechnol.* **260**, 62–66 (2017).

2.1 Introduction

Enzyme prodrug therapies are an attractive alternative to conventional chemotherapies due to their potential to elicit a localized, targeted toxic effect at the tumor site.[108,109] One example is use of yeast cytosine deaminase (yCD), which converts a non-toxic prodrug, 5-fluorocytosine (5-FC), to the clinically prevalent cytotoxic drug, 5-fluorouracil (5-FU), for the treatment of glioblastoma (**Figure 2.1**).[110,111] Proposed methods for introducing prodrug converting enzymes (PCEs) require the targeted delivery of the enzyme to the cancer, as any off-target activity would kill the benign cell upon addition of the prodrug.[112–115] While many methods have tested successful for targeting tumors in vitro, none are completely free of risk and safety concerns. Activation based on targeting extracellular cancer markers may lack the required specificity as these markers are presented at certain levels on healthy cells as well.[116] More importantly, we lack any means of regulating the intracellular protein levels after delivery as there is no innate mechanism for clearing the PCE in an event of promiscuous delivery.

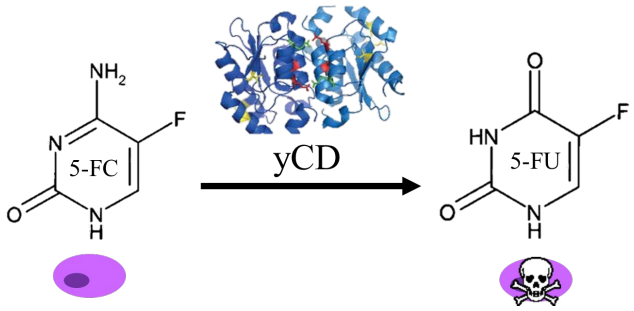

Figure 2.1 Yeast cytosine deaminase (yCD) catalyzes the enzymatic deamination of 5-fluorocytosine (5-FC) to 5-fluorouracil (5-FU). 5-FC is innocuous to cells, while 5-FU is an extremely cytotoxic chemotherapeutic agent that indiscriminately kills cells. Regulating yCD might allow selective cell killing.

One way to address this issue is to impose an additional layer of cell-specificity by controlling intracellular enzyme levels in a process we coin "Degradation-Directed Enzyme Prodrug Therapy (DDEPT): Healthy cells would quickly degrade the PCE and remain unscathed while cancerous cells, through a targeted activation mechanism, would preserve the PCE towards a therapeutic outcome. DDEPT is most conveniently executed by simply grafting a conditional degradation domain (DD) to the PCE,[79,81,84,85,117] which under normal circumstances is recognized and swiftly eliminated by the proteasome, but the DD can be stabilized by the introduction of a chemical cue. This approach is simple but leaves behind a DD-PCE fusion protein, which may affect its endogenous biological activity. An improved technology termed Traceless Shielding (TShld) was recently reported to generate native proteins, in which a chemical cue is used to both shield the target proteins from degradation and trigger their release from the DD.[88] Briefly, TShld consists of two separate constructs that function together to rescue the protein of interest. On the first construct, the protein payload is flanked by a conditional DD, FKBP, which is stabilized by the small molecule rapamycin,[80,118] and the C-terminus of ubiquitin (UbC, residues 35-76). In the absence of rapamycin, FKBP destabilizes the complex containing the payload, resulting in its degradation. In addition to stabilizing FKBP, rapamycin also induces complementation between FKBP and the second construct consisting of FRB, a domain from the mTOR protein, and the N-terminus of ubiquitin (UbN, residues 1-37), resulting in reconstitution of the split ubiquitin and separation of the protein of interest from the rest of the complex via ubiquitin hydrolases (**Figure 2.2**).[119,120] Intrigued by the dual capability of TShld to provide conditional PCE rescue in a native conformation, we demonstrated the principle of DDEPT using TShld for

the conditional rescue of yCD and controlled prodrug activation as an initial step towards a novel therapeutic direction.

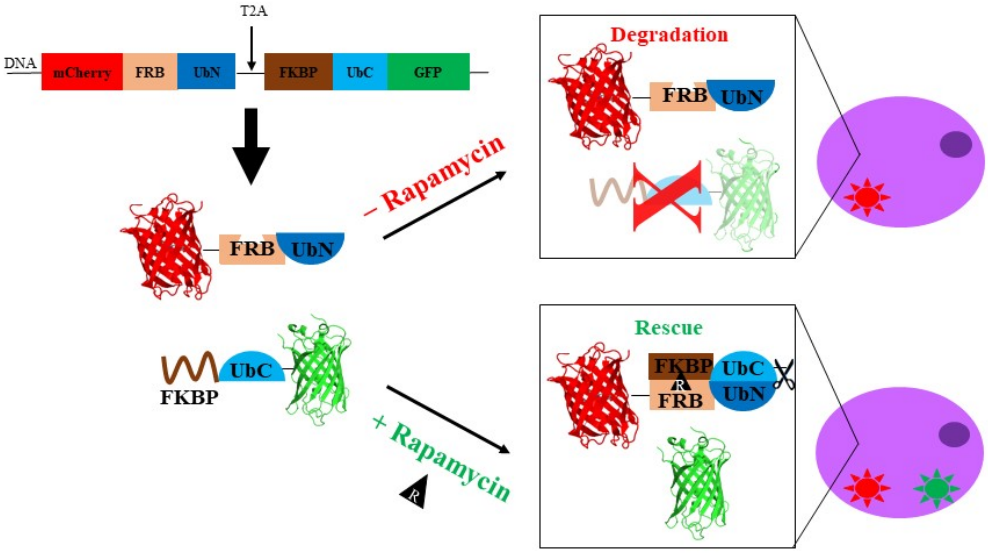

Figure 2.2 Schematic representation of mCherry TShld GFP protein product. The transcribed DNA includes the entirety of the protein under one promotor. A T2A site between the proteins forces the synthesis of two separate proteins due to ribosome skipping at the Gly-Pro junction of the T2A peptide (left). In the absence of rapamycin, FKBP is destabilized, targeting itself and its fusion partners, including GFP, towards degradation. The first part of the construct, including mCherry, does not contain a degradation tag and is not subject to induced degradation (top right). In the presence of rapamycin (black triangle containing the letter "R"), FKBP is stabilized and FRB is recruited to FKBP, promoting a close proximity between UbC and UbN. GFP is cleaved from the construct, rescuing it from possible degradation. Both mCherry and GFP can now be detected (bottom right).

2.2 Materials and Methods

2.2.1 Plasmid Construction

All constructs were prepared using standard molecular cloning techniques. pEntry TShld-GFP was a gift from Matthew Pratt (Addgene plasmid #53211). TShld GFP was cloned into pcDNA3.1 (Invitrogen), and mCherry was cloned onto the N-terminus. For cell viability experiments, GFP TShld yCD was cloned as follows: yCD was substituted for GFP and GFP was substituted for mCherry as the global protein expression control.

2.2.2 Cell Culture

HeLa cells were maintained in T150 tissue culture flasks (Thermo Fisher) in Minimum Essential Media (MEM, Cellgro) supplemented with 10% fetal bovine serum (FBS, Corning) and 1% penicillin/streptomycin (HyClone) at 37°C and 5% CO2.

2.2.3 Transfection

Plasmid DNA was prepared using ZymoPURE™ Plasmid Midiprep Kit (Zymo Research) according to the manufacture's protocol. HeLa cells were seeded at roughly 175,000 cells/well in 12-well plates (Corning) supplemented MEM as described above. One day after seeding, transfection was achieved with Lipofectamine® 3000 (Invitrogen) using 1 μg plasmid DNA per well and following the manufacture's protocol. Transfection occurred for a minimum of 12 hours.

2.2.4 Endpoint Cell Culture Experiments

Transfected cells were treated with the appropriate amount of rapamycin (LC Laboratories, >99% purity) and 5-FC (Sigma-Aldrich, >99% purity) to achieve the

desired final concentrations in a total volume of 1 mL for 24 hours. Cells were washed twice in 1 mL pre-warmed imaging buffer (140 mM NaCl, 2.5 mM KCl, 1.8 mM CaCl2, 1.0 mM MgCl2, 20 mM HEPES, pH 7.4). Cells were then incubated in 0.5 mL of pre-warmed imaging buffer throughout microscopy. For viability studies, 1 drop of NucRed® Dead 647 ReadyProbes® Reagent (Invitrogen) was added and allowed to incubate at room temperature for 2 minutes prior to imaging.

2.2.5 Fluorescent Microscopy and Image Analysis

All images were captured using an Observer Z.1 Inverted Microscope (Zeiss) with GFP, mCherry, or Cy5 filter cube sets (Chroma). For image analysis, five images were captured in each well. Image analysis was conducted using the "Measure" analysis in ImageJ with threshold set 10-255. Error bars represent the 95% confidence interval.

2.2.6 TShld Time Course Experiments

HeLa cells were seeded in individual 35 mm tissue culture-treated culture dishes (Corning) and transfected as described above. Transfected cells were treated with 500 nM rapamycin in a total of 1 mL of media. Each hour, one plate was removed from the incubator, washed twice in 1 mL pre-warmed cell imaging buffer, and imaged in 0.5 mL of imaging buffer.

2.2.7 Western Blotting

Following imaging, cells were incubated in ice-cold lysis buffer (50 mM Tris, 150 mM NaCl, 1% Triton X-100, pH 8.0) on ice for 20 minutes with protease inhibitor cocktail (Calbiochem). Cells were then removed from the plate with a cell scrapper (Genemate), and the lysate was clarified in a pre-cooled centrifuge at 12,000 rpm for

10 minutes at 4°C. Total protein concentrations were normalized through a Bradford assay (Bio-Rad) with a BSA standard. 15 μg of lysate was mixed with a 5x loading buffer and separated by 10% SDS-PAGE before being transferred to a nitrocellulose membrane (Bio-Rad).

Western blots were blocked in TBST (20 mM Tris, 500 mM NaCl, 0.05% Tween-20, pH 8.0) containing 5% non-fat milk overnight at room temperature with gentle shaking. Membranes were washed twice in TBST and incubated for 3 hours in anti-GFP (1:5000 dilution, Covance) or anti-mCherry (1:2000 dilution, Novus) in TBS. The blots were then washed twice in TBST and incubated with horseradish peroxidase (HRP)-conjugated secondary antibody (GenScript) for 2 hours in TBST. The blots were washed three times in TBST and developed using ECL reagents (GE) according to the manufactures protocol. Band intensities were quantified using ImageJ gel analysis tools.

2.3 Results and Discussion

2.3.1 Appending a Global Protein Expression Marker to TShld

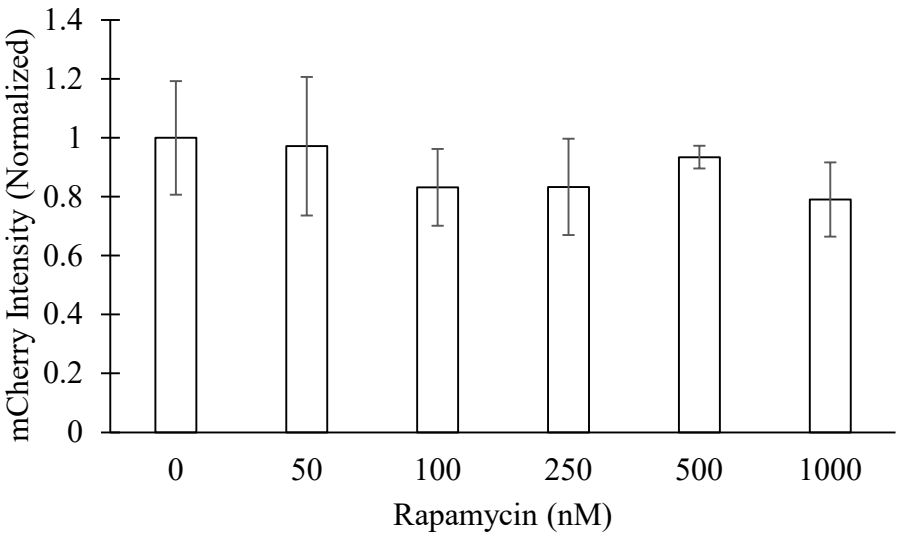

Figure 2.3 Quantification of mCherry intensity. mCherry intensity remained relatively constant regardless of the concentration of rapamycin (n=5 for each concentration).

Previous reports on the TShld system have clearly indicated the release of target proteins 48 h after rapamycin addition. However, it was unclear whether the initial protection was mainly due to DD stabilization or DD release. Since the two protein complexes are expressed under one promoter and are translated into two individual constructs using the T2A viral "self-cleaving" peptide,[86,121] we first fused mCherry to the N-terminus of FRB-UbN to allow direct monitoring of total protein synthesis. Similar to other reports, GFP was fused to the C-terminus of FKBP-UbC to enable easy tracking of protein rescue in a rapamycin dosage-dependent manner. HeLa cells were transfected with the mCherry-TShld-GFP construct. Cells were then cultured in a specified concentration of rapamycin ranging from 0-1000 nM in media for 24 h, and the abundance of mCherry and GFP was probed by both Western blotting and microscopy. As expected, the levels of mCherry fluorescence were

unaffected by the rapamycin concentration in the media (**Figure 2.3**). However, only a low level of GFP fluorescence was detected in the absence of rapamycin, which increased significantly in a dosage-responsive manner until 500 nM of rapamycin, at which point the maximum signal was observed (**Figure 2.4A** and **Figure 2.5**). Overall, a 11.2-fold difference in normalized GFP fluorescence was observed between 0 and 1000 nM of rapamycin (**Figure 2.4B**).

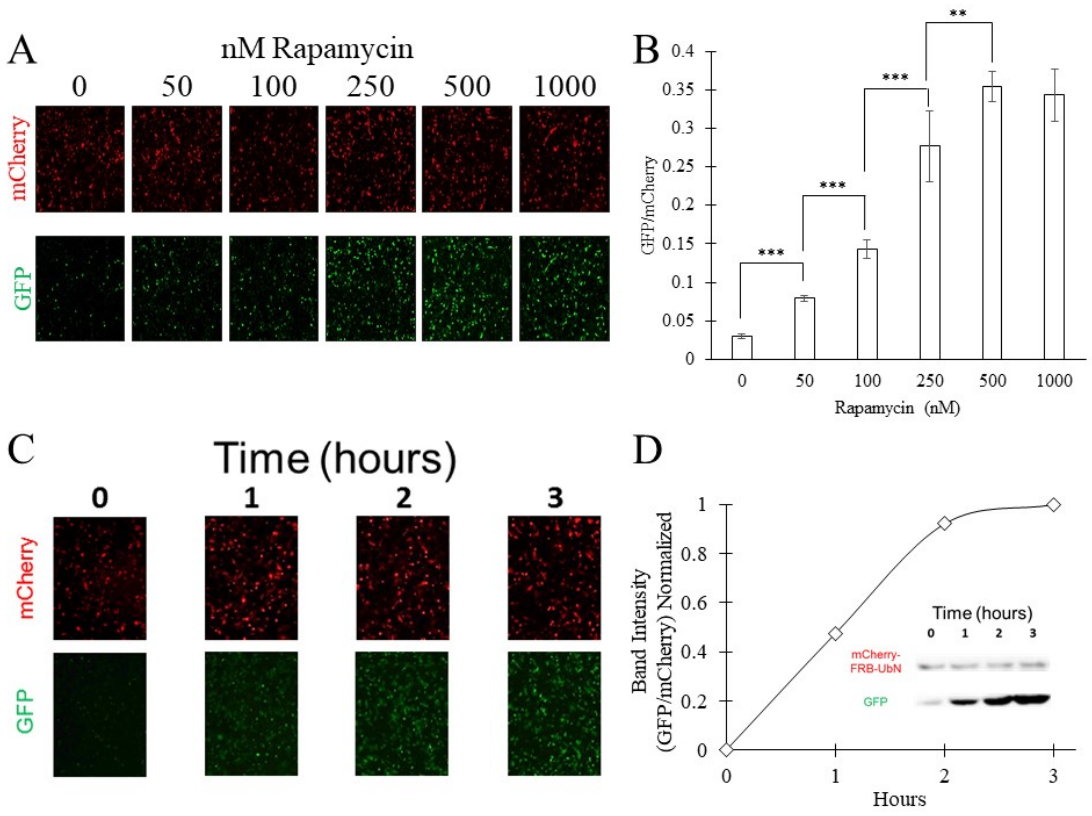

Figure 2.4 mCherry serves as a marker for protein synthesis in the TShld system and can be used to probe the initial mechanism of protection. (a) Microscopy of HeLa cells demonstrates the dosage response of GFP levels to rapamycin while mCherry levels are maintained as constant. Images were obtained 24 hours following the addition of rapamycin. (b) Quantification of fluorescent images showing statistically significant increases in GFP level relative to the mCherry transfection marker between all doses of rapamycin through 500 nM ($n = 5$, ** $p < 0.01$, *** $p < 0.001$). (c) Western blots probing for mCherry and GFP reveals constant mCherry-FRB-UbN expression with GFP protein levels quickly increasing over time. The response is rapid, leaving no uncleaved GFP detected, indicating that initial protection results from DD release. Quantification of the western blot band intensities shows the GFP time profile immediately following rescue initiation. The absolute intensity was different for the two proteins as mCherry-FRB-UbN was probed with anti-mCherry primary antibody and GFP was probed with anti-GFP antibody. (d) Fluorescent microscopy corroborates the findings of the western blot analysis.

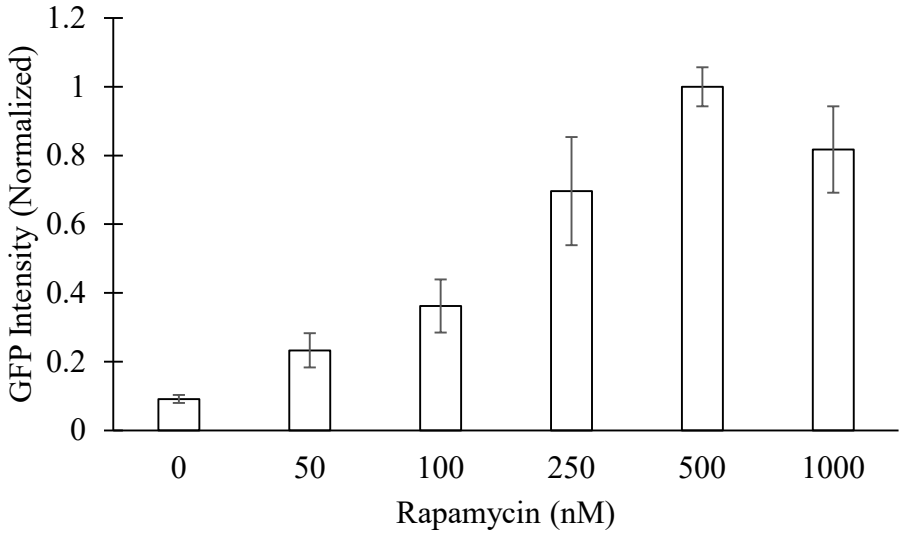

Figure 2.5 Quantification of GFP intensity for mCherry TShld GFP. GFP intensity increased with increasing concentrations of rapamycin. The decrease for 1000 nM of rapamycin is due to an overall decrease in global protein expression as seen in the parallel decrease in mCherry intensity. This highlights the importance of an internal fluorescent control when making direct comparisons (n=5 for each concentration).

2.3.2 Protein Release from DD Occurs Rapidly

Western blotting was used to further probe the mechanism of GFP rescue. Only a small quantity of cleaved GFP product was detectable before rapamycin addition, indicative of efficient degradation and a low level of background cleavage. However, the DD tag cleavage via ubiquitin hydrolase was extremely rapid, and only cleaved GFP was detected even 1 h after rapamycin addition (**Figure 2.4C**). The level of cleaved GFP increased slightly with time after the addition of rapamycin, while the level of mCherry-FRB-UbN remained constant (**Figures 2.4C** and **2.4D**). It is clear that the initial DD (FKBP) stabilization by rapamycin is also very rapid, a condition

necessary for the subsequent quick release of GFP from the reconstituted ubiquitin by ubiquitin hydrolase.

2.3.3 DDEPT Requires both Protein Rescue and Prodrug to Reduce Cell Viability

Having demonstrated the rapid rescue and release of native GFP by rapamycin addition, we next sought to execute DDEPT through the dynamic control of yCD levels using the TShld system in order to regulate the degree of 5-FC conversion to 5-FU and the corresponding cell viability. We first replaced mCherry with GFP as the expression marker because of the higher fluorescence intensity and yCD as the TShld payload. After transfection, the levels of GFP expression and cell viability were compared in the presence or absence of rapamycin ranging from 0-1000 nM and/or 300 μM 5-FC. To distinguish healthy cells from dead cells, we employed the NucRed® Dead 647 ReadyProbes® Reagent, which stains the genomic DNA of non-viable cells whose membrane integrity is compromised. No discernible difference in the GFP level was observed regardless of 5-FC and/or rapamycin addition, indicating their addition has no effect on protein expression. The addition of rapamycin by itself had no impact on cell viability across the spectrum of rapamycin added, and these levels were statistically similar to the group that received only 5-FC (**Figures 2.6A** and **2.6C**). These results again support the need of both 5-FC and active yCD for prodrug activation. In contrast, cell viability decreased in a rapamycin dosage-responsive manner in the presence of 5-FC as reflected by the higher number of purple fluorescent cells (**Figures 2.6B** and **2.6C**). Since the GFP level remained fairly constant independent of rapamycin and 5-FC addition, this observation implies that

the increase in cytotoxicity is not a result of increased protein synthesis but a direct effect of yCD rescue by rapamycin addition.

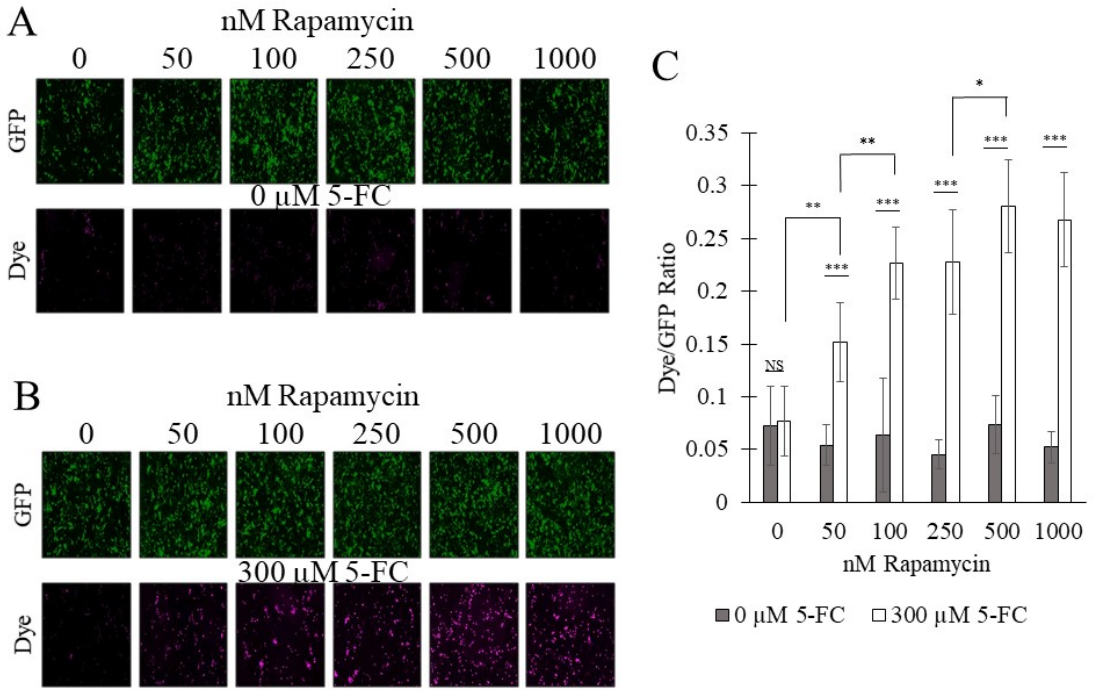

Figure 2.6 Cell death is only induced by the presence of both rapamycin and 5-FC. All images were obtained 24 hours after the addition of rapamycin and/or 5-FC. (a) Images of HeLa cells demonstrating that rapamycin alone is insufficient to induce cell death. GFP indicates high levels of protein synthesis, yet cell viability is maintained at all doses of rapamycin. (b) Images of HeLa cells demonstrating that the combination of rapamycin-induced yCD rescue and the prodrug 5-FC results in dosage-responsive cell killing. (c) Quantification of the fluorescent images with nuclear dye (cell death) normalized to GFP (transfection). All concentrations of rapamycin $\geq$ 50 nM are statistically different between each 0 µM 5-FC group and its corresponding 300 µM 5-FC group. Cell killing is dosage responsive to rapamycin concentration (n = 5, * $p < 0.05$, ** $p < 0.01$, *** $p < 0.001$, NS $p > 0.05$).

2.4 Discussion

In summary, we reported here a new DDEPT approach to provide conditional prodrug activation based on controlled protein degradation. This approach capitalized on the well-known feature of the TShld system to both rescue the prodrug activating enzyme, yCD, from degradation as well as its release from the DD upon rapamycin addition. By tagging the two TShld components with fluorescence proteins, we were able to discern that protein rescue was mainly the result of rapid DD release as only native proteins were detected even 1 h after rapamycin addition. The small background levels in the absence of rapamycin can be attributed to the low level of split ubiquitin complementation as previously reported.[89] For prodrug activation, this low level of background yCD rescue did not impact cell viability as even the introduction of 5-FC was not sufficient to cause cytotoxicity. Only in the presence of both 5-FC and rapamycin did we observe significant cell death. This approach allows the advantages of both targeted prodrug therapy in addition to a mechanism for clearing PCEs from healthy cells. This work represents an important first step in utilizing the DDEPT concept towards targeted prodrug activation. Looking forward, DDEPT would further benefit from autonomous switching such that the presence or absence of a specific cancer marker would determine the fate of the PCE thus rendering it independent of a small molecular trigger. For example, yCD has been engineered to accumulate only in cells that overexpress hypoxia-inducible factor 1α, common in many cancers.[122] Furthermore, delivery platforms have been developed that specifically target unique markers of the surface of cancer cells. For example, overexpressed human growth factor receptor 2 has been used for targeted gene delivery to breast cancer,[123] allowing DDEPT to be used as a gene therapy combined

with the additional failsafe of the PCE degradation. These represent a few means by which DDEPT could function as a therapy independent of outside intervention.

Chapter 3

CONDITIONAL PROTEIN RESCUE (CPR) BY BINDING-INDUCED PROTECTIVE SHIELDING

Abstract

An effective method to modulate the stability of proteins is essential to biological research. Herein, we describe a new technology that allows conditional stabilization of proteins based on masking of a degron tag by a specific intracellular protein cue. A target protein is fused to a degron tag and an affinity sensor domain. When the sensor detects its target protein, the degron is effectively concealed and the target protein is rescued. By introducing nanobodies as the sensor, we allow for virtually any endogenous protein to be targeted. In a model system using yeast cytosine deaminase, we demonstrate low cell death background yet maintain the ability to elicit strong activation and prodrug-mediated cell killing using GFP as the rescue protein. The flexibility in choosing different masking targets provides a straightforward method to generalize the strategy for conditional protein rescue in a wide range of biological contexts, including oncoprotein detection.

3.1 Introduction

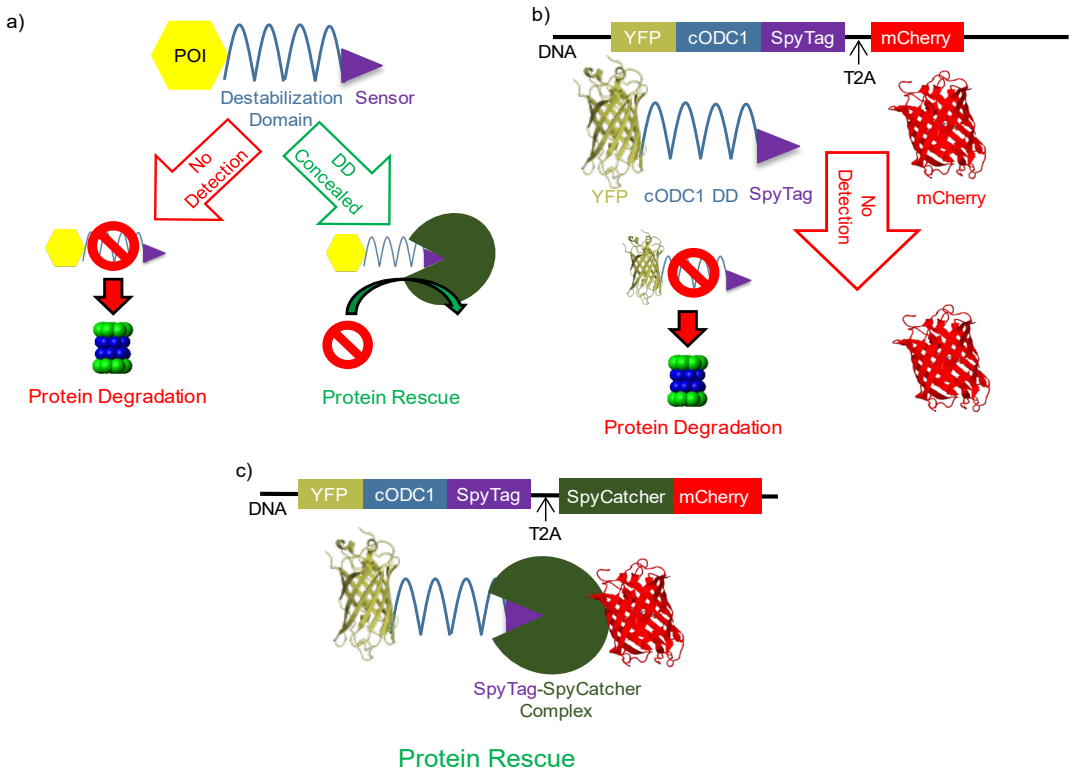

Figure 3.1 Conditional protein rescue (CPR) via masking the DD. a) The DD (blue squiggle) contains a small sensor domain (purple triangle) fused to its C-terminus. In the absence of the corresponding binding target to the sensor, the POI (yellow hexagon) is recruited to the proteasome via DD interaction (red symbol) and degradation proceeds (left). Interaction with the target (green cut-out circle) conceals the DD from the proteasomal recruitment, and the POI is rescued from degradation (right). b) YFP is fused to the cODC1 DD and SpyTag (sensor) and co-expressed with mCherry as a transfection marker. YFP is degraded by proteasome recognition of cODC1, and mcherry remains. c) When mcherry is fused to the SpyCatcher (target), the SpyTag sensor recruits SpyCatcher-miRFP670, sterically concealing cODC1 and rescuing YFP by CPR.

Conditional control of protein levels remains elusive for many biological applications. RNA interference (RNAi) destroys mRNA, but it can frequently be off-target or partially potent.[124] While small molecule-responsive transcriptional switches

are frequently used to regulate mRNA levels, the overall dynamic is limited by the half-life of the target protein.[125–127] Another common method is the fusion of a degradation domain (DD) to a protein of interest (POI),[76] which drastically reduces its half-life and allows faster fluctuations in the intracellular level.[128,129] As we recently reviewed,[130] while several approaches can modulate protein degradation in response to a small molecule,[81,84,88] they do not allow protein concentration control in response to native cellular environments. Ideally, a modular platform that combines rapid protein turnover by DDs with temporal and autonomous responsiveness to cellular environments will greatly expand our ability to generalize the strategy for conditional protein rescue (CPR) in a wide range of biological contexts.

Coordinated degradation of cyclins is a key mechanism to ensure correct progression through the cell cycle.[27,28,131] This exquisite control between accumulation and depletion of cyclins is tightly regulated by changes in cellular protein information, suggesting a possible framework for CPR. One potential strategy is based on the Ac/N-End Rule pathway used for protein quality control, which recognizes and targets certain Nα-terminally acetylated resides for degradation.[132–134] Remarkably, the same acetylated residue is also necessary for proper interaction with cellular chaperones, which sterically shield the degradation domain and preserve properly folded proteins. The intriguing ability to shield the DD from initiating degradation has inspired the design of a new generation of artificial protein stability switches for conditional degradation. Insertion of a DD into the Jα-helix successfully shielded the DD-Jα-helix peptide within the LOV domain and arrested degradation. Irradiation with blue light unmasked the Jα-helix and restored degradation.[95] Similarly, a DD placed between two proteins was only activated upon release by

protease cleavage.[98,135] While these reports represent a first step towards CPR, they are unable to couple endogenous cellular cues to modulate degradation.

We sought to increase the practicality of CPR by using cellular protein cues to provide masking and unmasking of DDs. In this design, a small sensor domain is appended to the DD. When a binding target is present, the DD is effectively concealed, and the target protein is rescued (**Figure 3.1a**). We demonstrated that effective CPR can be executed using both covalent SpyTag/SpyCatcher conjugation and non-covalent nanobody/antigen interaction. Selective rescue of the yeast cytosine deaminase enabled strong prodrug activation and targeted cell killing.

3.2 Materials and Methods

3.2.1 Plasmid Construction

All constructs were prepared using standard molecular cloning techniques and cloned into pcDNA3.1(+) (Invitrogen). All oligonucleotides were ordered from Integrated DNA Technology (Coralville, IA) and purified via standard desalting. A list of primers can be found in Appendix A. All enzymes were purchased from New England Biolabs (Ipswich, IA) and used per the manufacturer's protocol with the provided buffers. All overlapping oligos were first 5' phosphorylated with T4 polynucleotide kinase (PNK) treatment, and then were heat denatured and slow cooled to allow for proper hybridization before ligation.

3.2.1.1 mCherry:T2A:YFP-cODC1-SpyTag

YFP was PCR amplified and double digested with *AflII* and *XhoI*. The DNA sequences for oCDC1-SpyTag were ordered as overlapping oligonucleotides as ultrameres with appropriate overhangs to make them complimentary to *XhoI* and *ApaI*.

The vector pcDNA3.1(+) was double digested with *AflII* and *ApaI* to generate the backbone, and YFP and cODC1-SpyTag were ligated simultaneously using T4 DNA Ligase per the manufacturer's protocol to generate YFP-cODC1-SpyTag. Finally, mCherry was PCR amplified with a reverse primer that included the T2A region in the non-overlapping region, and this product was double digested with *NheI* and *AflII*. YFP-cODC1-SpyTag was double digested with *NheI* and *AflII*, and mCherry:T2A was ligated, generated mCherry:T2A:YFP-cODC1-SpyTag.

3.2.1.2 SpyCatcher-mCherry:T2A:YFP-cODC1-SpyTag

SpyCatcher was codon optimized and ordered as a gBlock gene fragment. SpyCatcher was then PCR amplified and double digested with *NheI* and *EcoRI*. mCherry:T2A was PCR amplified with the same reverse primer as above, but the forward primer provided an N-terminal *EcoRI* site, and this product was double digested with *EcoRI* and *AflII*. mCherry:T2A:YFP-cODC1-SpyTag was double digested with *NheI* and *AflII* to remove mCherry:T2A and generate the backbone into which SpyCatcher and mCherry:T2A were simultaneously ligated, generating SpyCatcher-mCherry:T2A:YFP-cODC1-SpyTag.

3.2.1.3 miRFP670 Constructs

miRFP670 was PCR amplified and double digested with *NheI* and *HindIII*. The T2A polycistronic site was ordered as two overlapping oligonucleotides with overhangs to provide *HindIII* and *AflII* complimentary sites. mCherry:T2A:YFP-cODC1-SpyTag was double digested with *NheI* and *AflII* to remove mCherry:T2A. miRFP670 and T2A were simultaneously ligated with the backbone to generate miRFP670:T2A:YFP-cODC1-SpyTag. Next, miRFP670 was PCR amplified with

overhangs providing *EcoRI* and *HindIII* sites, and the product was double digested at those sites. The human codon optimized SpyCatcher was PCR amplified and double digested with *NheI* and *EcoRI* as described above. miRFP670:T2A:YFP-cODC1-SpyTag was double digested with *NheI* and *HindIII* to remove miRFP670, and SpyCatcher and miRFP670 was simultaneously ligated into the backbone, generating SpyCatcher-miRFP670:T2A:YFP-cODC1-SpyTag. Finally, SH3 was PCR amplified. SH3 and SpyCatcher-miRFP670:T2A:YFP-cODC1-SpyTag were double digested with *NheI* and *EcoRI* to remove SpyCatcher, and SH3 was ligated to generate SH3-miRFP670:T2A:YFP-cODC1-SpyTa*SH3* and *SH3Lig constructs*. SH3 was PCR amplified and double digested with *NheI* and *EcoRI*. SH3Lig was ordered as a pair of overlapping oligonucleotides with overhangs providing for *XbaI* and *ApaI* complementation sites. Previous plasmids could be double digested with *NheI* and *EcoRI* (to install SH3) or *XbaI* and *ApaI* (to install SH3Lig) to generate SpyCatcher-mCherry:T2A:YFP-cODC1-SH3Lig, SH3-mCherry:T2A:YFP-cODC1-SpyTag, or SH3-mCherry:T2A:YFP-cODC1-SH3Lig.

3.2.1.4 miRFP670-cODC1-SpyTag-GBP1

SpyTag was ordered as a pair of overlapping oligonucleotides providing overhangs with *XbaI* and *BamHI*. The GFP Nanobody, *aka* GFP Binding Protein 1 (GBP1), was PCR amplified and double digested with *BamHI* and *ApaI*. mCherry:T2A:YFP-cODC1-SpyTag was double digested with *XbaI ApaI* to remove SpyTag, and SpyTag and GBP1 were simultaneously ligated into the backbone generating mCherry:T2A:YFP-cODC1-SpyTag-GBP1. Next, miRFP670 was PCR amplified and double digested with *AflII* and *XhoI*¸and mCherry:T2A:YFP-cODC1-SpyTag-GBP1 was double digested with *XhoI* and *ApaI* in order to purify cODC1-

SpyTag-GBP1. pcDNA3.1(+) was double digested with *AflII* and *ApaI*, and miRFP670 and cODC1-SpyTag-GBP1 were simultaneously ligated into the vector to generate miRFP670-cODC1-SpyTag-GBP1.

3.2.1.5 yCD Constructs

BFP was PCR amplified and double digested with *NheI* and *ClaI*. A T2A site was ordered as overlapping ultramers with overhangs providing *ClaI* and *AflII* complementation sites. mCherry:T2A:YFP-cODC1-SpyTag-GBP1 was double digested with *NheI* and *AflII* to remove mCherry:T2A. BFP and T2A were simultaneously ligated into the cut vector to generate BFP:T2A:YFP-cODC1-SpyTag-GBP1. A second BFP was PCR amplified and double digested with *EcoRI* and *ClaI*. SH3 was again PCR amplified similar to above and double digested with *NheI* and *EcoRI*. BFP:T2A:YFP-cODC1-SpyTag-GBP1 was then double digested with *NheI* and *ClaI*, and SH3 and BFP were ligated to generate SH3-BFP:T2A:YFP-cODC1-SpyTag-GBP1. yCD was PCR amplified and double digested with *AflII* and *Xho*I. SH3-BFP:T2A:YFP-cODC1-SpyTag-GBP1 was also double digested with *AflII* and *XhoI* to remove YFP, and yCD was ligated in its place generating SH3-BFP:T2A:YFP-cODC1-SpyTag-GBP1. To generate the rescuing construct, EGFP was PCR amplified and double digested with *NheI* and *EcoRI*. The previous construct was double digested with the same enzymes to remove SH3, and GFP was ligated in its place generating GFP-BFP:T2A:YFP-cODC1-SpyTag-GBP1.

3.2.1.6 UbL Constructs

A single copy of the UbL domain was PCR amplified and double digested with *AflII* and *ClaI*. YFP was also PCR amplified and double digested with *ClaI* and *XhoI*.

Both mCherry:T2A:YFP-cODC1-SpyTag and SpyCatcher-mCherry:T2A:YFP-cODC1-SpyTag were double digested with *AflII* and *XhoI* to remove YFP, and UbL and YFP were simultaneously ligated into the cut vector to generate mCherry:T2A:UbL-YFP-cODC1-SpyTag and SpyCatcher-mCherry:T2A:UbL-YFP-cODC1-SpyTag, respectively.

3.2.1.7 N-end Rule Constructs

Ub-R-GFP was a gift from Nico Dantuma (Addgene plasmid # 11939 ; http://n2t.net/addgene:11939 ; RRID:Addgene_11939). Site directed mutagenesis was performed to generated Ub M-GFP and Ub-L-GFP using Q5 Hot Start High-Fidelity Polymerase New England Biolabs (Ipswich, IA) according to the manufacture's protocol. KpnI and BamHI restriction sites were introduced via mutagenesis between the N-terminal amino acid and GFP, and GBP1 was inserted into these sites. Finally, GFP was excised using BamHI and NotI, and miRFP670 was ligated in its place to generate Ub X-GBP1-miRFP670.

3.2.1.8 LaM4 Constructs

To generate EGFP-cODC1-LaM4, EGFP was PCR amplified to include AflII and XhoI restriction sites. miRFP670-cODC1-GBP1 was digested with AflII and XhoI, and EGFP was ligated to generate EGFP-cODC1-GBP1. GBP1 was excised using BamHI and ApaI, and LaM4 was ligated in its place. N-End rule constructs were generated by excising GBP1 from Ub X-GBP1-EGFP using KpnI and BamHI; LaM4 was ordered as a gene fragment and PCR amplified to include the same restriction sites, and the ligation product yielded Ub X-LaM4-EGFP.

3.2.1.9 nE7 Constructs

Ub R-GBP1-miRFP670 was digested with KpnI and BamHI. The nE7 nanobody was ordered as a gene fragment from IDT, PCR amplified to include KpnI and BamHI restriction sites, and ligated into the vector. This subclone was subsequently digested with AgeI and NotI, and mCherry was PCR amplified and cloned into place to yield Ub R-nE7-mCherry. To generate the control construct, Ub R-GBP1-miRFP670 was digested with AgeI and NotI, and mCherry was PCR amplified and ligated into the vector to yield Ub R-GBP1-mCherry.

3.2.2 Cell Culture

HeLa cells were maintained in T150 tissue culture flasks (Thermo Fisher) in complete media, *i.e.* Minimum Essential Media (MEM, Cellgro) supplemented with 10% fetal bovine serum (FBS, Corning), 10 U mL^{-1} penicillin (HyClone), and 10 U mL^{-1} streptomycin (HyClone) at 37°C and 5% CO_2. Cell passaging occurred upon reaching confluency in the flask by treating with 0.05% trypsin-EDTA for 4 minutes at 37°C and 5% CO_2. Cells were pelleted at 500 *g* for 10 minutes, resuspended in 5 mL of complete media, and counted. HeLa cells were seeded in 12-well plates at 175,000 cells/well and 6-well plates at 750,000 cells/well. HEK293T cells were seeded in 6-well plates at 250,000 cells/well.

3.2.3 Transfection

Plasmid DNA was prepared using ZymoPURE™ Plasmid Midiprep Kit (Zymo Research) according to the manufacture's protocol. One day after seeding, transfection was achieved with Lipofectamine® 3000 (Invitrogen) using 1 μg total plasmid DNA per well for 6-well plates and 2.5 μg total plasmid DNA for 12-well plates in complete media and following the manufacture's protocol. Where more than

one plasmid was transfected, the total DNA was split evenly among all plasmids unless otherwise noted.

3.2.4 Fluorescent Microscopy and Image Analysis

All images were captured using an Observer Z.1 Inverted Microscope (Zeiss) with GFP, mCherry, BFP, or Cy5 filter cube sets (Chroma). For image analysis, five images were captured in each well. Image analysis was conducted using the "Measure" analysis in ImageJ with threshold set 10-255. Error bars on all plots represent the 95% confidence interval.

3.2.5 Western Blotting

Following imaging, cells were incubated in ice-cold lysis buffer (50 mM Tris, 150 mM NaCl, 1% Triton X-100, pH 8.0) on ice for 20 minutes with protease inhibitor cocktail (Calbiochem). Cells were then removed from the plate with a cell scrapper (Genemate), and the lysate was clarified in a pre-cooled centrifuge at 12,000 rpm for 10 minutes at 4°C. Total protein concentrations were normalized through a Bradford assay (Bio-Rad) with a BSA standard. 15 μg of lysate was mixed with a 5x loading buffer and separated by 10% SDS-PAGE before being transferred to a nitrocellulose membrane (Bio-Rad).

Western blots were blocked in TBST (20 mM Tris, 500 mM NaCl, 0.05% Tween-20, pH 8.0) containing 5% non-fat milk overnight at room temperature with gentle shaking. Membranes were washed twice in TBST and incubated for 3 hours in anti-GFP (1:5000 dilution, Covance) or anti-mCherry (1:2000 dilution, Novus) in TBS. The blots were then washed twice in TBST and incubated with horseradish peroxidase (HRP)-conjugated secondary antibody (GenScript) for 2 hours in TBST.

The blots were washed three times in TBST and developed using ECL reagents (GE) according to the manufactures protocol. Band intensities were quantified using ImageJ gel analysis tools.

3.2.6 Flow Cytometry

Most flow cytometry was conducted on the Novocyte Benchtop Flow Cytometer (Acea Biosciences, San Diego, CA). Experiments involving mCherry (Ub R-nE7-mCherry and Ub X-LaM4-EGFP rescued with mCherry) were conducted on BD FACSAria Fusion High Speed Cell Sorter (BD Biosciences, San Jose, CA). All flow cytometry experiments involved $\geq$50,000 transfected cells as determined by forward- and side-scatter profiles of recorded events and fluorescent gating to exclude cells not transfected by at least the rescuing protein for each respective experiment. Cells were prepared for flow cytometry by washing twice in warm PBS. Trypsin treatment was applied for 3 minutes, and the reaction was quenched by warm media. Cells were collected in microcentrifuge tubes and spun at 0.8g for 5 minutes. The supernatant was aspirated, and cells were resuspended in cold PBS. This solution was then passed through a cell strainer into a flow cytometer tube and stored on ice until analysis.

3.2.7 yCD Viability Studies

HeLa cells were seeded as above in 6-well plates and transfected with the appropriate constructs as above. Approximately one day post-transfection, wells either received no treatment, 5-FC, or 5-FU for 48 hours. Viability was determined using NucRed Dead 647 ReadyProbes Reagent (Thermo Fisher) per the

manufacturer's instruction. Fluorescent microscopy was used for analysis as described above.

3.2.8 E7 Detection Studies

HeLa cells and HEK293T cells were seeded as described above. Transfection was conducted for 6 hours, and then replaced with normal media. Flow cytometry analysis was conducted 24 hours post-transfection as described above.

3.2.9 Statistical Analysis

All the experiments were performed in triplicates and results were expressed as means ± standard deviations (SD). Statistical significance was analyzed using the student *t*-tests. $P < 0.05$ was considered statistically significant throughout the study.

3.3 Results and Discussion

3.3.1 Conditional Protein Rescue by Covalent SpyTag/SpyCatcher Conjugation

To evaluate the feasibility of CPR, we first utilized the SpyCatcher and SpyTag system, which provides the most stable *in vivo* interaction because of covalent conjugation.[136] A well-characterized synthetic cODC1-like C-degron tag was used as an effective DD with kinetics that allow for rescue to occur.[95] By fusing the DD-SpyTag to a fluorescent reporter, we generated YFP-cODC1-SpyTag, an unstable complex that can be rescued by SpyCatcher. We employed mCherry as an orthogonal transfection reporter (**Figure 3.1B**). Both the YFP fusion and mCherry were expressed under one promotor by use of a polycistronic viral T2A self-cleaving sequence.[86,121] To induce rescue of YFP, SpyCatcher was fused to mCherry for easy tracking (**Figure 3.1C**).

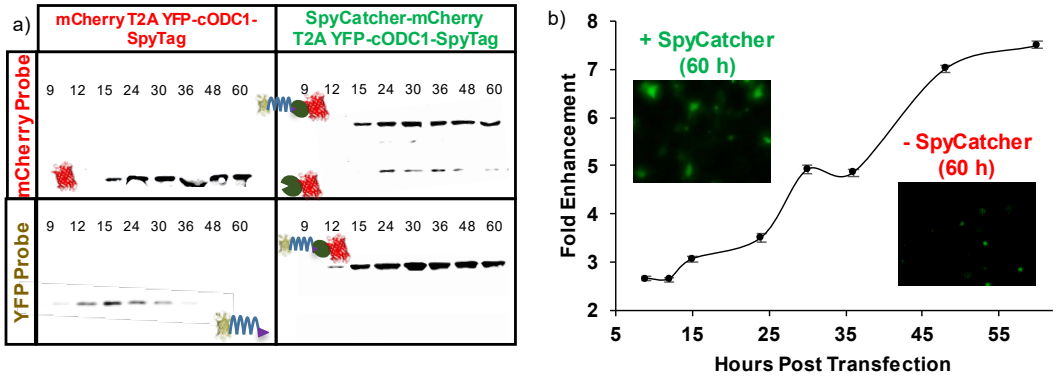

Figure 3.2 YFP rescue from cODC1-mediated degradation via SpyTag-SpyCatcher interaction. a) Western blotting of HeLa cell lysate. Expression of YFP and mCherry/mCherry-SpyCatcher were probed by their respective antibodies. The upward shift in the protein size for the mcherry-SpyCatcher samples was the result of SpyTag-SpyCatcher conjugation. b) Flow cytometry quantification of YFP enhancement by CPR. miRFP670, a near-infrared fluorescent protein with a completely orthogonal signal to YFP on the flow cytometer, was used in place of mcherry. Fold enhancement is the YFP signal normalized to miRFP670 expression in the SpyCatcher-miRFP670 fusion sample relative to the control with no SpyCatcher expression. Error bars represent 95% confidence intervals.

To evaluate the rescue efficiency, HeLa cells were transfected with SpyCatcher-mCherry:T2A:YFP-cODC1-SpyTag or the control, mCherry:T2A:YFP-cODC1-SpyTag, without SpyCatcher. Expression of both proteins was tracked by fluorescent microcopy and western blot over 60 h. Western blot analysis (**Figure 3.2A**) demonstrated that mCherry was detected consistently in both constructs roughly 15 h post-transfection. YFP gradually disappeared in cells expressing only mCherry, while a strong band corresponding only to the ligated YFP products was detected for

cells expressing SpyCatcher-mCherry. The absence of any un-ligated YFP with SpyCatcher-mCherry co-expression highlights that ligation between SpyTag and SpyCatcher is solely responsible for YFP rescue due to shielding of the DD (**Figure 3.2A**, top right box). This is further supported by the fluorescent images (**Figure 3.3**) demonstrating efficient YFP rescue due to DD shielding by SpyTag-SpyCatcher ligation.

To quantify CPR more accurately, miRFP670 — a near-infrared, monomeric, fluorescent protein with a completely orthogonal signal to YFP on the flow cytometer[137] — was fused similarly to mCherry to generate SpyCatcher-miRFP670:T2A:YFP-cODC1-SpyTag and the control, miRFP670:T2A:YFP-cODC1-SpyTag. Flow cytometry showed that CPR enhancement increased throughout the entire time course, with roughly 7.5-fold increase in the YFP signal after 60 h (**Figure 3.2B**). Western blots confirmed a similar size increase as a result of the covalent conjugation between SpyCatcher and SpyTag (**Figure 3.4**).

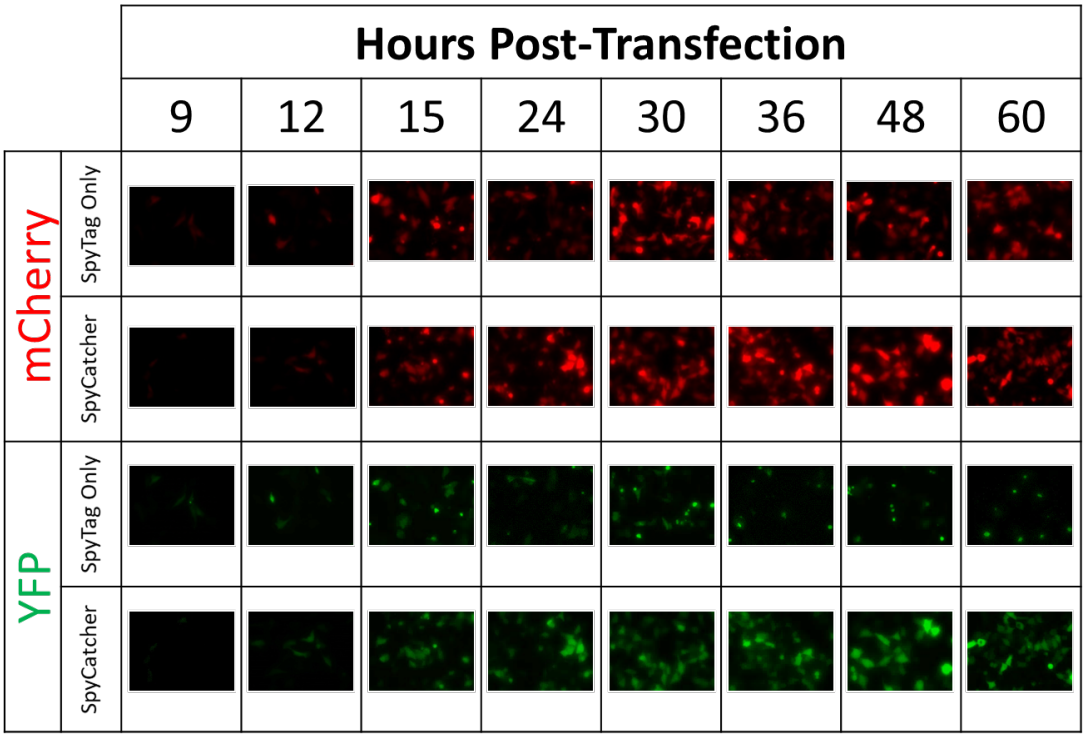

Figure 3.3 Fluorescent images of YFP rescue in the presence or absence of SpyCatcher-SpyTag ligation. Representative images of HeLa cells transfected with mCherry T2A YFP-cODC1-SpyTag (SpyTag Only) or SpyCatcher-mCherry T2A YFP-cODC1-SpyTag (SpyCatcher) were captured over a 60-hour time course. While mCherry expression is consistent regardless of the presence of SpyCatcher, YFP expression is many-fold higher when SpyCatcher is co-expressed, suggesting that concealing the DD hinders the degradation of YFP.

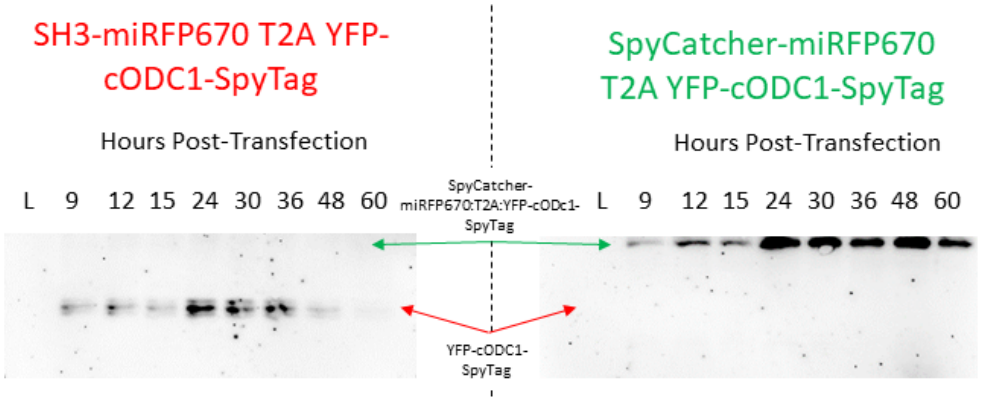

Figure 3.4 Western blot analysis demonstrating the rescue of YFP by ligating to SpyCatcher-miRFP670. Substituting miRFP670 for mCherry in order to perform flow cytometry analysis has no effect on the level of YFP rescue. As with mCherry, the YFP signal degrades over time in the absence of SpyCatcher. When SpyCatcher is fused to miRFP670, there is a shift up in protein size indicative of SpyCatcher/SpyTag reaction, and the YFP signal persists strongly throughout the time course. The YFP signal increase is also reflected in the flow cytometry data in Figure 3.2b.

3.3.2 Use of Non-Covalent Interactions for CPR

Although CRP was correctly executed using covalent conjugation between SpyTag and SpyCatcher, most intracellular interactions are non-covalent in nature. To show that non-covalent interaction can also be used to provide similar shielding effects, we replaced the SpyTag/SpyCatcher pair with the well-known Src homology 3 (SH3) domain and its corresponding binding ligand, wLig (k_D = 10 μM).[138,139] A similar shielding effect was observed albeit at reduced efficiencies, confirming that even a weak non-covalent interaction is sufficient to provide adequate masking of the DD (**Figure 3.5**). Again, no rescue was observed when the SH3 domain is absent, highlighting again the importance of specific interaction for proper DD masking (**Figure 3.5**).

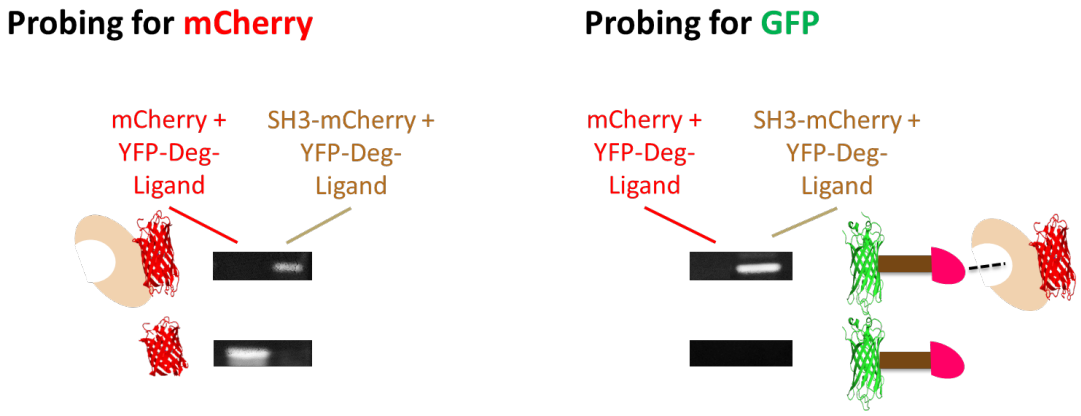

Figure 3.5 **Non-covalent interactions resulting in protein rescue.** Western blots were generated after expressing mCherry T2A YFP-cODC1-Ligand (left lane in each pair) and SH3-mCherry T2A YFP-cODC1-Ligand (right lane in each pair) for 60 hours. These blots demonstrate the ability to rescue protein from degradation using an exogenous, non-covalent interacting pair. In this instance, the interacting protein pair is the SH3 domain and one of its known peptide ligands. When mCherry is expressed without an SH3 fusion, YFP is degraded by the degradation tag cODC1 (brown line). The close association between SH3 and its ligand is sufficient to induce YFP rescue by concealing the degradation tag from the proteasome.

In order to adapt this technology towards more relevant cellular targets, a small, monomeric sensor capable of interacting with endogenous proteins with high specificity is required. Camel single-domain antibody fragments, or nanobodies, are ideal because of their relative small size (~13kDa) and the ability to generate high-affinity nanobodies for virtually any protein target.[140,141] To investigate whether the degradation phenotype could be preserved even after addition of a nanobody near the DD, an anti-GFP nanobody (GBP1, k_D ~1 nM) was first fused to the C-terminus of an miRFP670-cODC1 fusion (**Figure 3.6A**). Unlike conjugation of a SpyCatcher-fusion onto an adjacent SpyTag to cOCD1, no masking of the DD was observed as virtually

no miRFP670 signal was detected (**Figure 3.7**, left side). This is somewhat unexpected as a small structural nanobody was physically tethered next to the DD. We speculate that the steric masking of the DD may be size dependent. To test this hypothesis, we fused a larger maltose-binding protein (MBP; 43 kDa) to the C-terminus of GBP1. This resulted in improved miRFP670 signal (**Figure 3.7**, right side), an outcome consistent with the proposed enhanced DD masking and miRFP670 rescue.

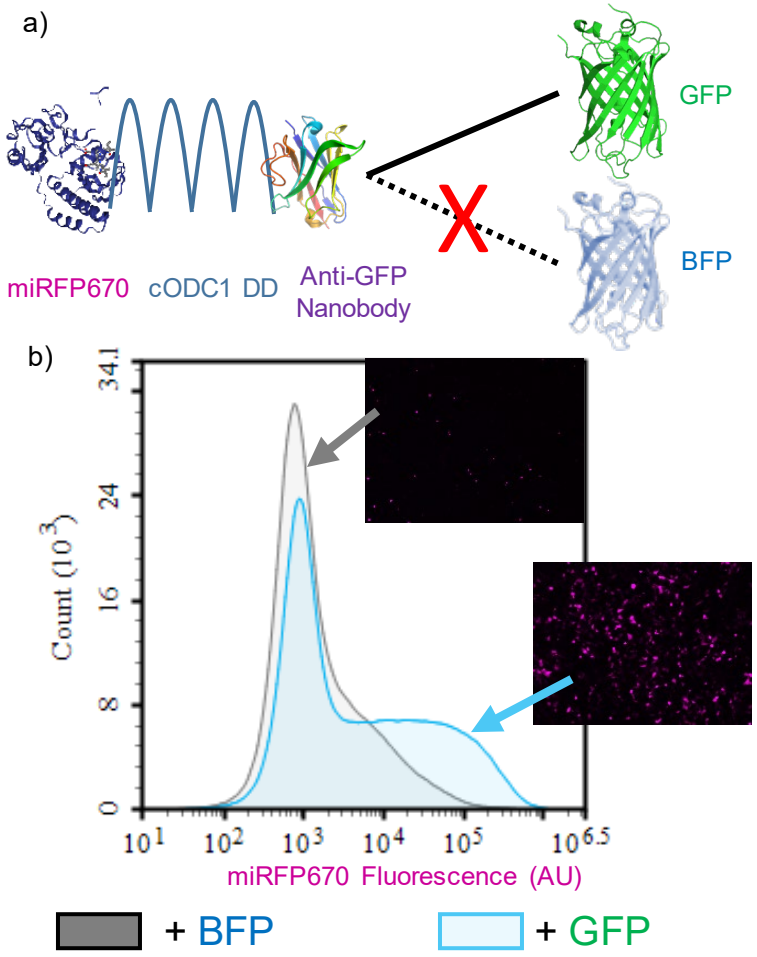

Figure 3.6 Rescuing a POI using non-covalent nanobody-antigen interactions. a) miRFP670 is fused to the cODC1 DD and an anti-GFP nanobody (GBP1), which still maintains its inherently unstable feature. HeLa cells expressing miRFP670-cODC1-GBP1 were co-transfected with either BFP or GFP for CPR. Co-expression with BFP alone did not result in miRFP670 rescue due to a lack of interaction with GBP1, while co-expression with GFP restored miRFP670 signal due to DD masking. b) Flow cytometry quantification of miRFP670 fluorescence in the presence of BFP (grey) and GFP (blue) after 48 h. Inserts show fluorescent microscopy images of miRFP670 of each sample.

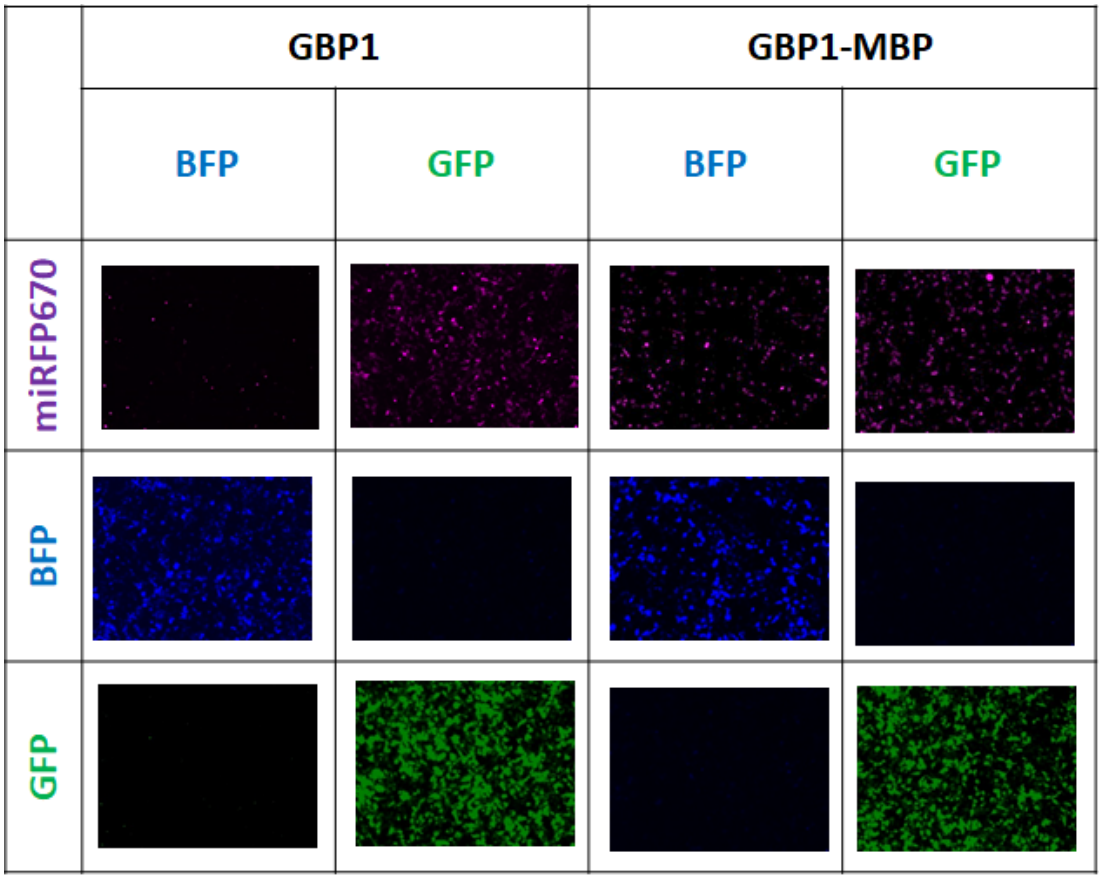

Figure 3.7 The use of nanobody-antigen interaction as an efficient sensing mechanism to control protein rescue. Representative images of HeLa cells expressing either miRFP670-cODC1-GBP1 (left) or miRFP670-cODC1-GBP1-MBP (right) after 60 hours of transfection. The level of miRFP670 rescue was compared when either BFP or GFP was co-expressed at the same time. The miRFP670-cODC1-GBP1 sample receiving BFP shows low levels of miRFP670 due to its degradation. Both samples receiving GFP show rescue of miRFP670 from degradation, suggesting that the interaction between GFP and its nanobody concealed the degradation tag and rescued miRFP670. The direct fusion of MBP also stabilized miRFP670 even in the absence of GFP, suggesting a size-dependent steric interference model for CPR.

After establishing that a small nanobody GBP1 can be fused after the DD without impacting degradation, we next investigated whether protein rescue could be attained based on GBP1 and GFP interaction. In the presence of BFP, which could not associate with GBP1, miRFP670 was still efficiently degraded. In contrast, expression of GFP efficiency rescued miRFP670 from degradation due to GFP shielding of the DD (**Figure 3.6B** and **Figure 3.7**). Somewhat surprisingly, GFP failed to induce as effective CPR when we used GBP6, a nanobody that binds GFP at a different epitope than GBP1,[142] suggesting that interacting orientation, in addition to the size of the rescuing protein, is also important for CPR (**Figure 3.8**). These results provide the feasibility to repurpose nanobody-antigen interactions to elicit CPR for many different synthetic biology applications of practical interest.

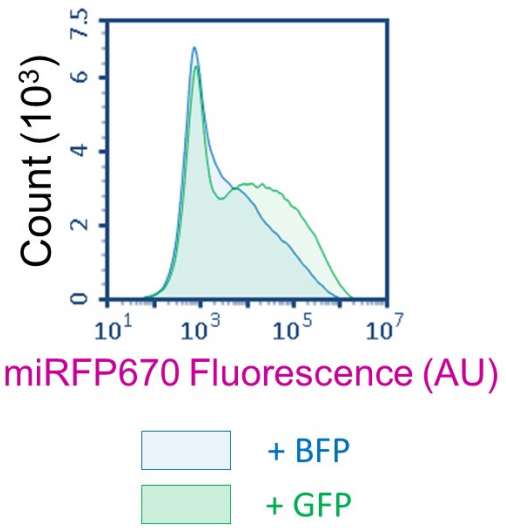

Figure 3.8 GBP6 fails to induce protein rescue effectively. When GBP6, a nanobody that binds GFP at a different epitope than GBP1 (see Fig. 3 in the main text), is used to rescue miRFP670-cODC1-GBP6, the rescue efficiency is extremely low. This implies that GFP must interact at an orientation conducive to CPR in order to rescue miRFP670 from cODC1-mediated degradation.

3.3.3 Engineering CPR for Prodrug Activation

One of the most pressing needs in cancer treatment is to distinguish cancer versus healthy cells. Prodrug targeting offers a layer of therapeutic control due to the innocuous nature of prodrugs. Yeast cytosine deaminase (yCD) is a prodrug-converting enzyme (PCE) that transforms the innocuous 5-fluorocytosine (5-FC) into the cytotoxic 5-fluorouracil (5-FU), and it has been used successfully for the treatment of glioblastoma.[110,111] Previously, we demonstrated the ability to regulate yCD activity using a small molecule-dependent rescue system, but this approach lacked any autonomous ability to distinguish cancer cells from healthy cells.[143] To adapt CPR for prodrug targeting, yCD was used as the POI to test how well this strategy can control 5-FC activation. GFP again served as a visually trackable surrogate for a cancer-relevant protein. The ability to trigger cell death by 5-FU was used to indicate the overall efficiency of the conditional PCE therapy. A dye that only crosses the leaky cell membrane of dead cells was used as a visible indicator of cell viability. As expected, 5-FU killed large quantities of cells regardless of GFP, while cell viability was high when no drugs were administered (**Figure 3.9**). When treated with 5-FC, only cells co-expressing GFP were killed in similar quantities to those being treated directly with 5-FU (**Figure 3.9**). Although the degree of cell killing in the absence of GFP but with 5-FC is slightly higher than cells without 5-FC addition (**Figure 3.9B**), this undesired outcome can be rectified by using a stronger degradation signal (*e.g.* UbL) or a combination of multiple DDs.

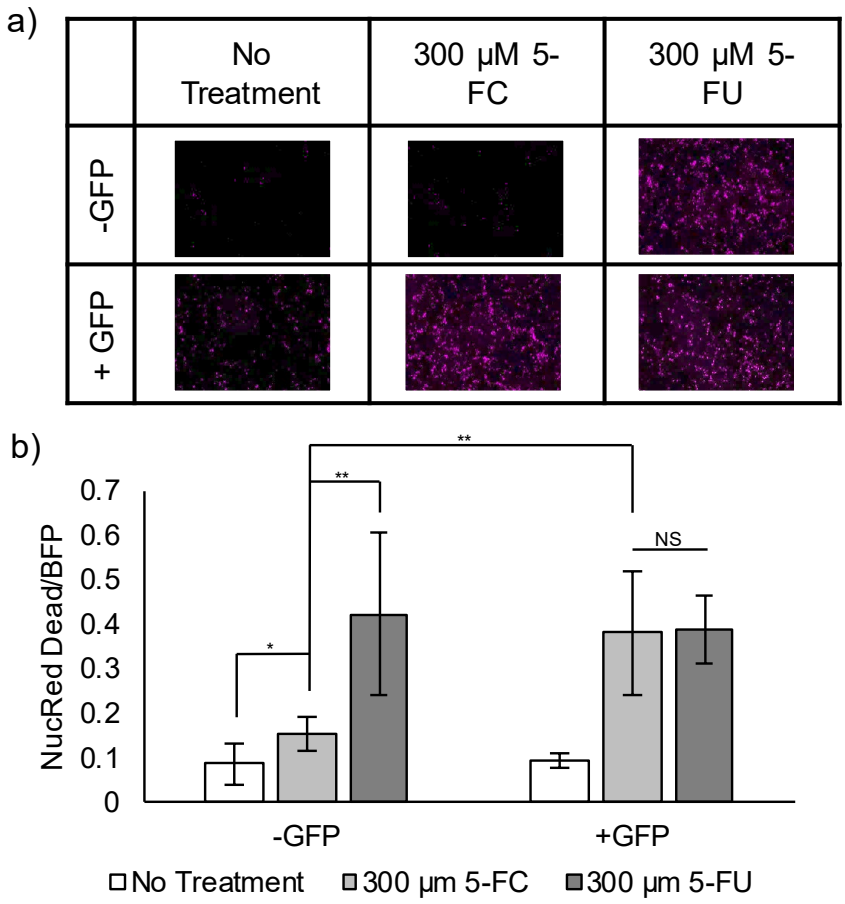

Figure 3.9 Controlling yCD activity via protein-nanobody interaction-mediated rescue. a) Fluorescent images of cell viability. Uptake of the NucRed Dead (pink) dye is indicative of cell death by the action of 5-FU. Cell viability was reduced in the presence of the prodrug, 5-FC, only when GFP rescued yCD by stabilizing the DD-nanobody fusion. b) Quantification of all fluorescent images, normalizing NucRed Dead dye to BFP, the protein transfection marker. Cells were transfected and either treated with no drugs (No Treatment), 5-FC, or 5-FU (n = 10; * = p < 0.05; ** = p < 0.01; NS = no statistical significant difference).

3.3.4 Tuning CPR by using a stronger proteasome binding motif

We next sought to improve the design to eliminate the background further. Previously, it has been reported that an unstructured domain and a proteasomal

targeting moiety are both necessary for efficient proteasomal degradation.[144] To determine if our CPR design could block access to the unstructured cOCD1 domain in the presence of a second proteasomal targeting moiety, we fused one copy of the ubiquitin-like (UbL) domain to the N-terminus of YFP.[145] UbL is derived from the Rad23 protein and has been shown to target its fusion partners directly to the proteasome more effectively than the cODC1 tag.[146,147] Fusing a UbL domain to the N-terminus of YFP enhanced the overall degradation, demonstrating that CPR can be tuned to achieve varying activation levels and signal to background ratios (compare the disappearance of YFP bands in **Figure 3.10B** with **Figure 3.2A**). Neither fluorescent microscopy (**Figure 3.10A** and **Figure 3.11**) nor western blot (**Figure 3.10B**) could detect YFP in the absence of SpyCatcher-mCherry. Co-expression of SpyCatcher-mCherry was again able to rescue YFP, although the rescued YFP level was lower than without the UbL domain (**Figure 3.10A**). The increase in protein degradation kinetics competes more aggressively with the SpyTag-SpyCatcher reaction, resulting in less rescue. This result highlights the modularity of our approach in adjusting signal background and rescue intensity and its ability to conceal unstructured domains from a proteasome in a UbL-tagged target.

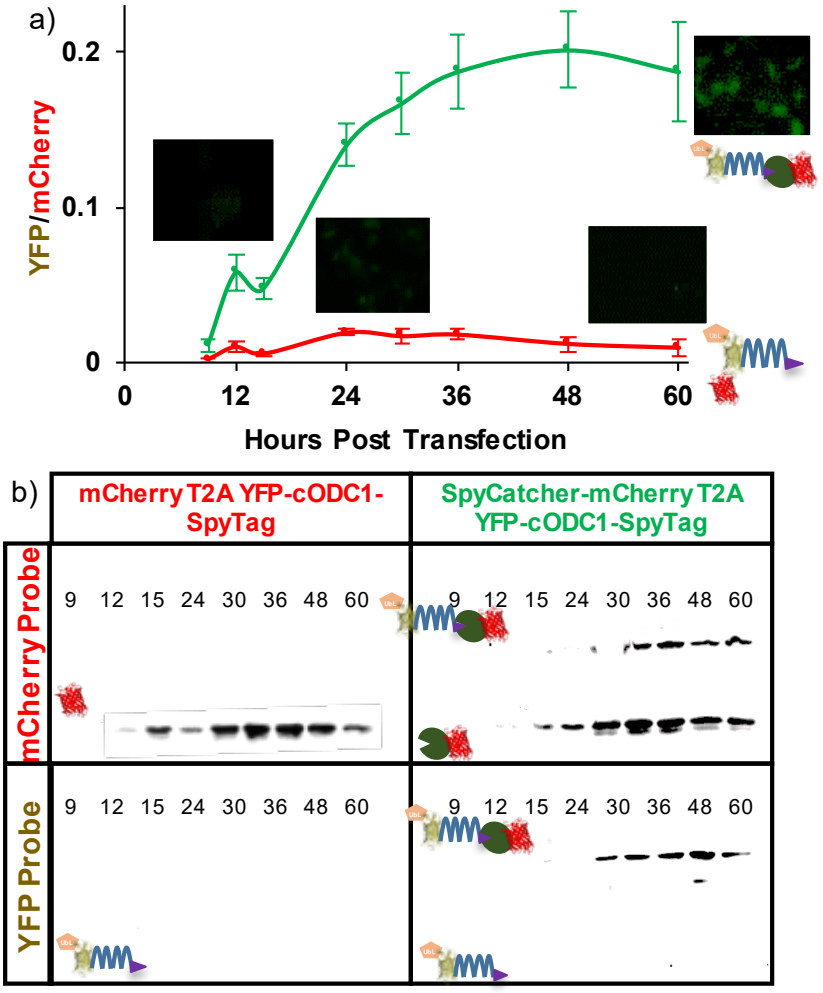

Figure 3.10 Tuning YFP rescue using the stronger proteasome binding UbL domain to improve degradation kinetics. a) Quantification of fluorescent microscopy measuring YFP intensity normalized by mCherry intensity. Compared to designs without UbL (see Figure 2), background YFP intensity was decreased (red line), but the ability of YFP to be rescued decreased as well (green line). The images show HeLa cells with the YFP signal (green) 9 h and 60 h post transfection. Error bars represent $\pm$ 95% confidence interval (n = 5). b) Western blotting of HeLa cell lysate. The UbL domain is effective in eliminating any detectable traces of YFP expression without rescue (lower left box). Co-expression with SpyCatcher rescued YFP from degradation (lower right box).

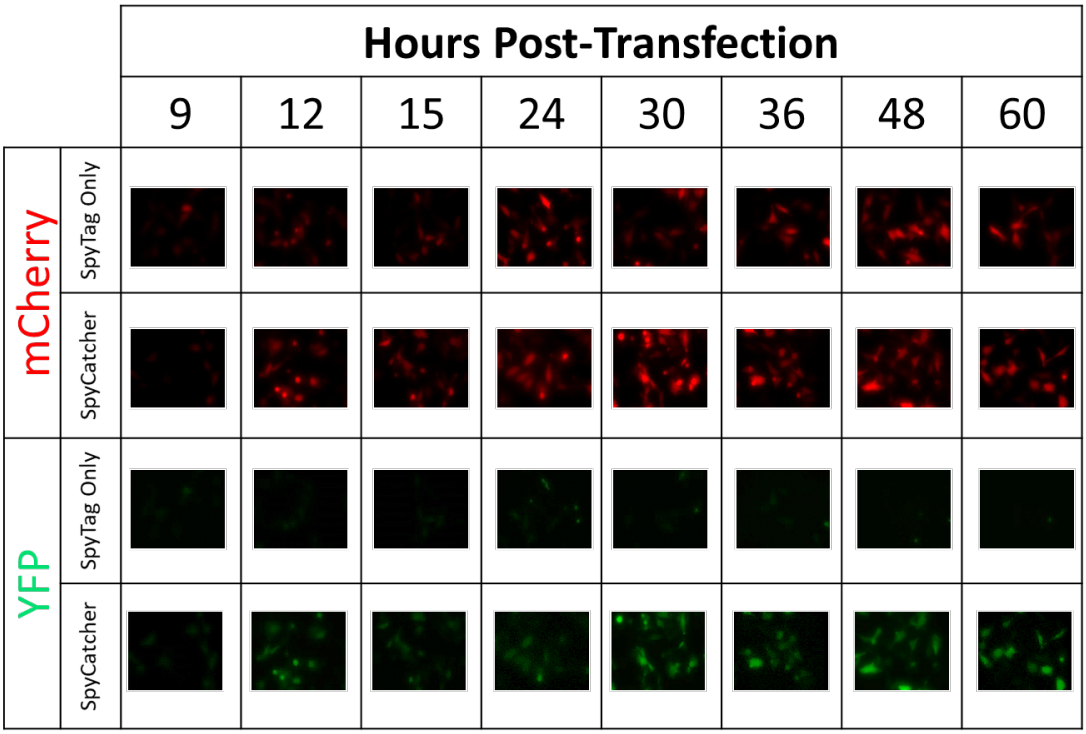

Figure 3.11 UbL-fusion speeds the degradation kinetics, resulting in lower background with efficient rescue. Representative images of HeLa cells transfected with mCherry T2A UbL-YFP-cODC1-SpyTag (SpyTag Only) or SpyCatcher-mCherry T2A UbL-YFP-cODC1-SpyTag (SpyCatcher) were captured over a 60-hour time course. While overall YFP levels are lower when rescued compared to when UbL is not fused to its N-terminus, the background when SpyCatcher is not co-expressed is virtually non-existent.

3.3.5 CPR for N-End Rule Degrons

Encouraged by the CPR results using the cOCD1 C-degron, we next turned our attention to the N-end rule protein degradation pathway. Because the N-end rule substrates are recognized by specific binding proteins known as N-recognins, which deliver these substrates to the 26S proteasome for destruction,[148,149] chaperones are able to protect their targets via steric interference.[133] We reasoned that expressing a sensing nanobody directly following a destabilizing N-terminus residue as a fusion to

a POI should result in rescue when the corresponding nanobody's target is co-expressed.

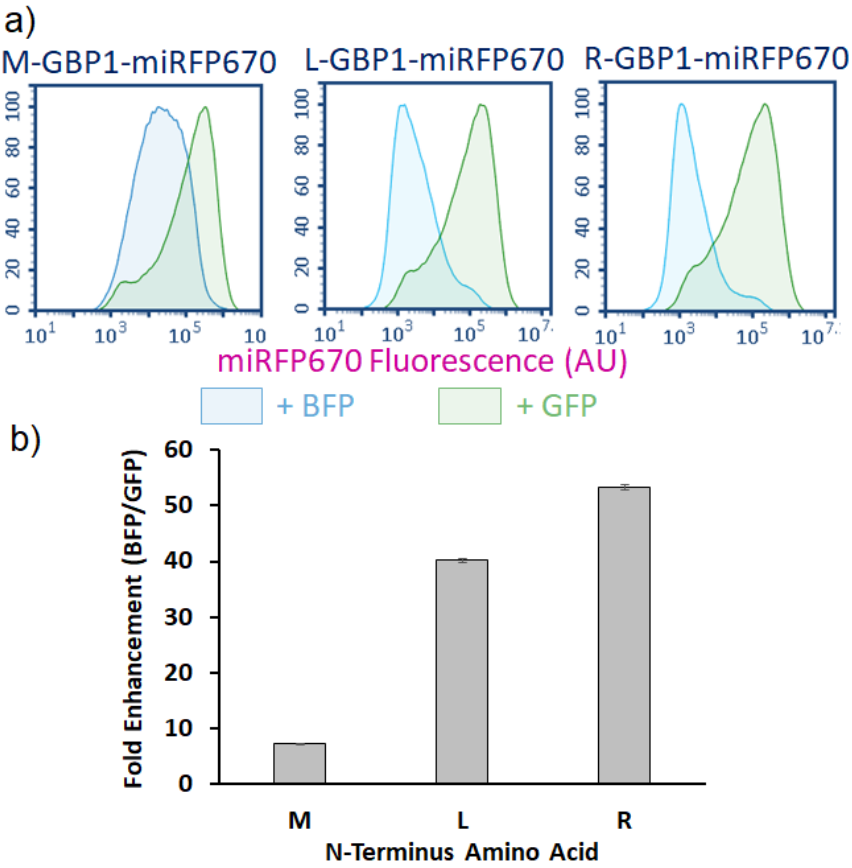

Figure 3.12 Rescuing protein by blocking N-end rule-mediated degradation. a) When only BFP was co-expressed, no miRFP670 rescue was detected; the residual fluorescence levels scaled well with the reported half-lives of proteins with the respective N-terminus residues. However, co-expression of GFP resulted in a significant increase in miRFP670 fluorescence levels. Furthermore, fluorescence levels of rescued protein are comparable regardless of which N-terminus residue was used. b) The fold enhancement measured for each N-terminus residue is plotted as a function of the median miRFP670 fluorescence when co-expressed with GFP divided by the median when co-expressed with BFP (background fluorescence). Met does not result in a large fold enhancement because it is a stabilizing residue. Error bars represent a 95% confidence interval.

To conduct CPR using an N-end rule degron, we relied upon the ubiquitin (Ub) fusion technique, in which Ub is added to the N-terminus of a POI. The Ub domain is subsequently cleaved by an endogenous deubiquitylase, exposing the desired N-terminus residue for destablization.[150] Using this strategy, we generated three Ub:X-GBP1-miRFP670 fusions, where X is the resulting N-terminal residue: methionine (M, half-life = 30 hr), leucine (L, half-life = 5.5 hr), or arginine (R, half-life = 1.0 hr).[151] These constructs were co-expressed with either BFP or GFP. Co-expression of BFP resulted in weak miRFP670 fluorescence scaling to the reported half-lives of the N-terminus residues tested. In contrast, co-expressing with GFP resulted in a dramatic rescue of miRFP670, showing more fluorescence than rescuing with the cODC1 degron (**Figure 3.12a** and **Figure 3.13**). Due to its extremely low background yet high level of rescue, an Arg N-terminus degron elicited an unprecedented >50-fold increase in protein fluorescence (**Figure 3.12b**). Not surprisingly, a Met N-terminus did not result in much fold increase since it is a stabilizing residue. To ensure that CPR was not a phenomenon specific to GBP1 and GFP-mediated rescue, we replaced GBP1 with LaM4, a nanobody that detects mCherry,[152] to create EGFP-cODC1-LaM4 and three different Ub:X-LaM4-EGFP fusions. For all constructs, only co-expression with mCherry resulted in higher EGFP fluorescence, and the N-end rule CPR outperformed C-end rule (**Figure 3.14**).

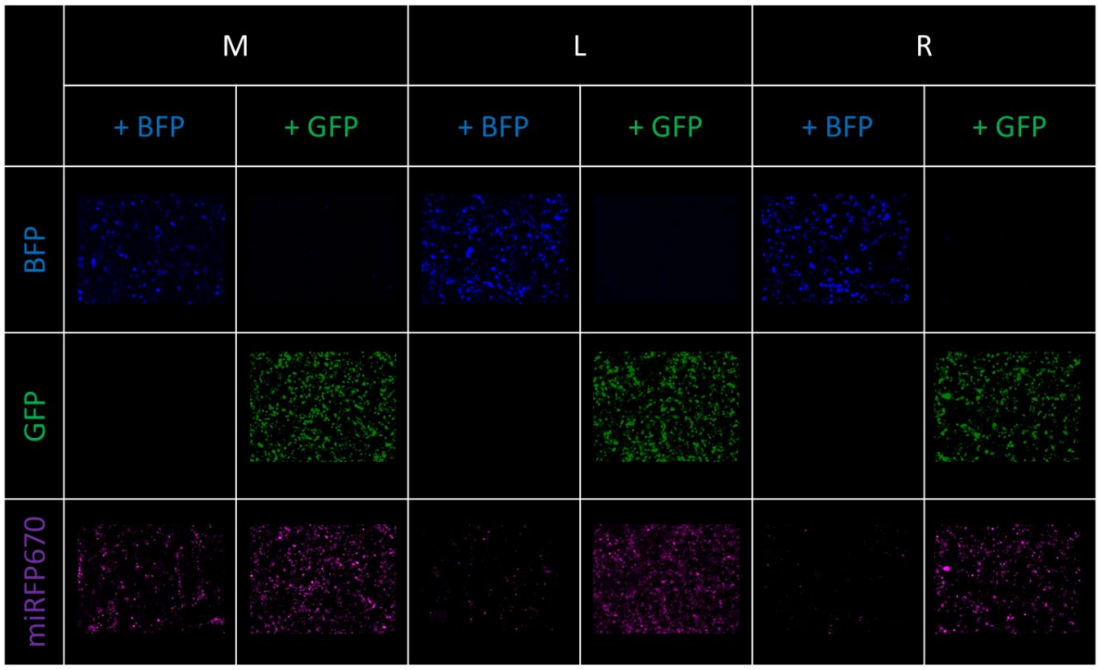

Figure 3.13 GFP is able to rescue miRFP670 tagged with degradation-inducing N-terminal amino acids by interacting with a GBP1. Representative images of HEK293T cells transfected with X-GBP1-miRFP670, where X represents the N-terminal amino acids listed above. Co-expression with BFP resulted in low protein levels except when Met is the N-terminal amino acid, consistent with reported half-lives. Co-expression with GFP results in a visible increase in miRFP670 in the case of all N-terminal amino acids.

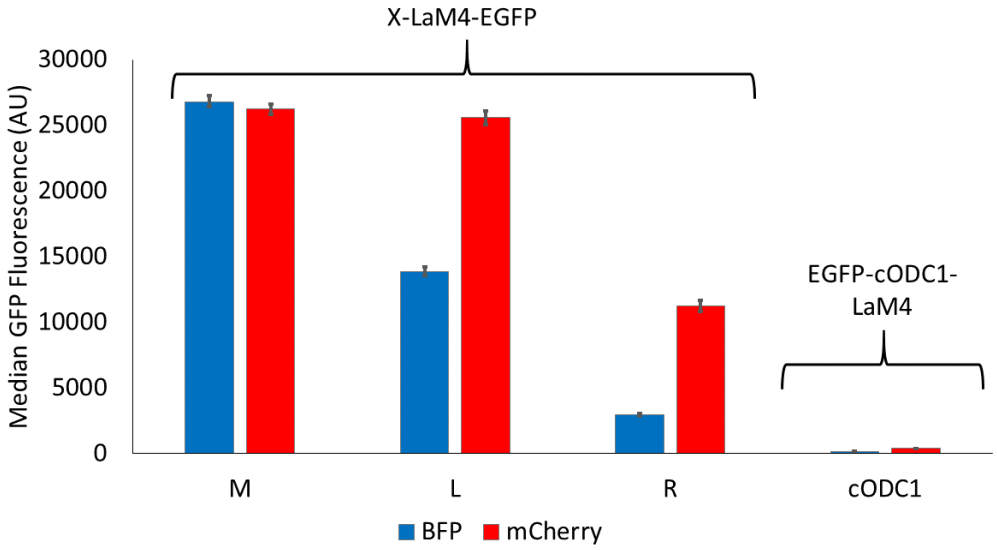

Figure 3.14 mCherry is able to rescue EGFP by interacting with a LaM4. When co-expressed with BFP, levels of EGFP scale well with the reported half-lives of the N-terminal amino acids, and EGFP-cODC1-LaM4 exhibits low levels of EGFP fluorescence. However, co-expression with mCherry results in levels of EGFP in all samples. Results graphed represent the median fluorescence values measured by flow cytometry, and error bars represent 95% confidence intervals.

3.3.6 CPR for the Detection of HPV-Positive Cells

To illustrate the broader applicability of our CPR approach toward native protein targets, we next extended our design to detect human papillomavirus (HPV)-positive cells. HPV is a known oncovirus that mainly relies on two proteins to induce carcinogenesis in cervical cells : E6, a major suppressor of apoptosis, and E7, a driver of the cell cycle.[153–155] Using E7 as a HPV marker, we exploited nE7, a nanobody that detects E7,[156] to generate Ub:R-nE7-mCherry to execute CPR. We transfected this construct and the control Ub:R-GBP1-mCherry into both HPV-positive HeLa cells and HPV-negative HEK293T cells. The HEK293T cells showed

similar low levels of mCherry fluorescence regardless of which nanobody was used to perform CPR (**Figure 3.15**). However, while GBP1 resulted in low levels of mCherry in the HeLa cells, nE7 resulted in a roughly 3-fold increase in mCherry, demonstrating that CPR is a powerful technique for detecting even low cellular levels of a cellular target protein.

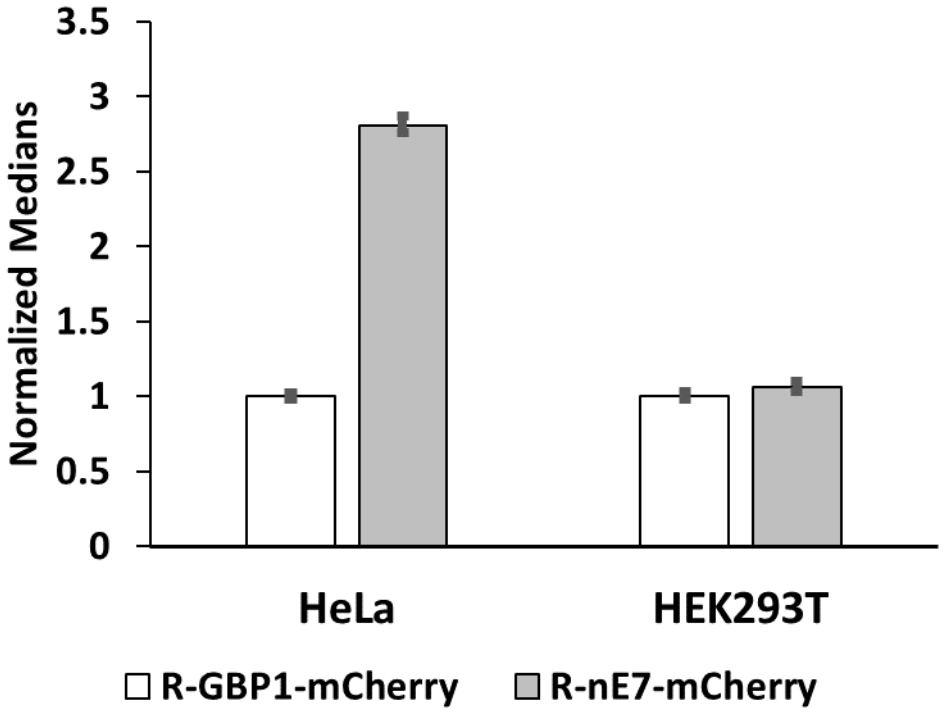

Figure 3.15 Executing CPR using an endogenous cancer marker. HeLa cells are cancerous as a consequence of infection with HPV. These viral proteins provide a specific marker for HeLa cells that can be detected by the HPV E7-specific nE7 nanobody (left). HEK293T cells do not contain this marker, and therefore no statistically significant difference in the mCherry signal was observed. For both cell types, median fluorescence is normalized to R-GBP1-mCherry fluorescence (background). Error bars represent 95% confidence intervals.

3.4 Discussion

We report here a new synthetic biology framework to elicit CPR based on proteomic information. To our knowledge, this is the first report that allows for the rescue of a target protein from degradation using a second protein as a masking agent. Although the initial feasibility was demonstrated using the SpyTag/SpyCatcher bioconjugation pair, even non-covalent interactions can be used to achieve similar rescue efficiencies. The modularity of the design allows the addition of a UbL proteasome-targeting domain to eliminate background while still allowing rescue of a POI. The use of nanobodies as a small sensing domain removes the limit on the potential target pool and creates a new synthetic biology framework by allowing endogenous cellular proteins to decide the fate of a POI. We demonstrated this feasibility by detecting E7, a protein unique to HPV-positive cells. The availability of DDs with a wide range of degradation kinetics, including the N-end rule, offers the possibility to elicit rescue by an endogenous protein in a threshold-dependent manner. By combining different DDs and sensing domains, it may be possible to generate more complex, multi-input protein logic gates to help further differentiate between disease and healthy cells for therapeutic applications.

Chapter 4

CONDITIONAL PROTEIN RESCUE WITH MULTIPLE INPUTS

Abstract

Cancer is a disease driven by the participation of multiple dysregulated proteins to drive the cell cycle forward inappropriately. To further complicate matters, many of these proteins are needed individually in certain cells for their continued health. Thus, therapies that are able to distinguish between cancer and healthy cells will be required to consider multiple protein signals simultaneously. Towards this end, we present a platform for multi-input conditional protein rescue (CPR) in which each input is necessary but insufficient to increase the half-life of a protein of interest (POI). Only the combination of both proteins together can execute CPR and rescue the POI from proteasomal degradation. Herein, based on the success of single-input CPR, a proof-of-concept is demonstrated in which two exogenous proteins are used in combination to rescue a third. Future directions are suggested in the conclusion towards improving the technology described and prospective cancer targets that might increase the probability of a successful therapeutic application are submitted.

4.1 Introduction

Human diseases are often the sum of additive cellular malfunctions, resulting in their complexity and difficulty to treat. Synthetic biology, in an effort to equip scientists with the ability to tackle this challenge, has long been interested in the design and execution of artificial cellular circuits.[21,22] Towards this ambition, researchers have been developing components that mimic their biological counterparts with predictable outcomes, such that design heuristics can be employed for facile "plug and play" circuit construction.[157–160] Owing to its predictability of hybridization, DNA is easily programmable both spatially and temporally,[161,162] and thus it served as a logical starting point. For example, relying on DNA toehold-mediated strand displacement (TMSD) technology,[163–165] a multi-input miRNA detector for cancer was constructed, and the end result was the reconstruction of a split prodrug converting enzyme.[20]

While proteins do not have predictable hybridization and folding rules, many protein domains have known binding peptides, and therefore protein interaction can be similarly programmed to provide predictable outcomes. In this way, some headway has been made in the construction of synthetic protein circuits. For example, in a corollary to DNA TMSD, coiled-coil structures interact in a thermodynamically driven manner to bring fusion partners into close proximity, and a third coiled-coil with the ability to displace one of the original pair results in the separation of the fusion partners.[166] Proteins also have the advantage of being enzymatic: Proteases act on their target sequences in a consistent manner, and protein cleavage can thus be programmed. In one study, proteases can be fused to an inhibitory peptide with an intervening, orthogonal protease cleavage site. When the inhibitory peptide is cleaved off, the first protease can then cleave a downstream target.[167] In another case, multiple

degron domains (DDs) can be cleaved from a protein of interest (POI) using orthogonal proteases such that its stability is determined by Boolean logic calculations.[100] However, none of the currently available technologies has the ability to drive a protein circuit from multiple endogenous inputs.

Much of the information that distinguishes a healthy cell from a cancerous one is contained within the proteome.[11,12] Therefore, sensors and modulates that are sensitive to the protein information space and can signal the circuit appropriately are strongly desirable. Conditional Protein Rescue (CPR), the subject of Chapter 3, is well-suited to address this challenge because of the ease with which targeting nanobodies can be introduced to detect endogenous proteins. Briefly, a POI is fated for proteasomal degradation by virtue of a DD fusion; however, a small sensing domain is also fused to the DD, and in the presence of a specific target to the sensing domain, the DD is concealed from the cell and the POI is stabilized. Based on the reliable behavior of both N- and C-end CPRs, it stands to reason that Boolean AND gate architecture can easily be constructed using two orthogonal protein inputs to protect both degrons simultaneously. To illustrate this feasibility, we constructed a model system by using an anti-GFP nanobody as the sensing domain for the N-end degron and a SpyTag as the sensing domain for the C-end degron, respectively. In this design, two orthogonal rescuing proteins, GFP and SpyCatcher, are necessary for POI stability (**Figure 4.1**). Since it was shown previously that nanobodies can be incorporated at both ends, this design can be further extrapolated to detect two different endogenous proteins.

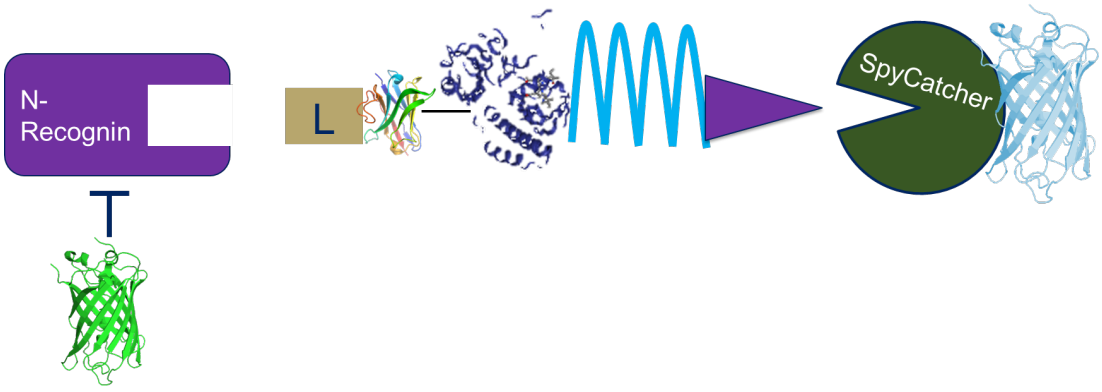

Figure 4.1 Protein-based Boolean AND gate constructed from CPR components. A POI is fused to both and N- and C- end degron, both of which independently fate the POI for degradation. The N-end degron contains an anti-GFP nanobody, and thus GFP acts as a synthetic inhibitor for the N-recognin. The C-end degron is fused to a SpyTag, such that SpyCatcher conceals that degron. In this design, GFP or SpyCatcher alone is insufficient to rescue the POI. However, the combination of the two can perform CPR.

4.2 Materials and Methods

4.2.1 Plasmid Construction

All constructs were prepared using standard molecular cloning techniques and cloned into pcDNA3.1(+) (Invitrogen). All oligonucleotides were ordered from Integrated DNA Technology (Coralville, IA) and purified via standard desalting. All enzymes were purchased from New England Biolabs (Ipswich, IA) and used per the manufacturer's protocol with their provided buffers.

4.2.1.1 Ub:L-GBP1-miRFP670-FLAG-cODC1-SpyTag Construction

Using Ub:L-GBP1-miRFP670 as a template, PCR was performed to amplify Ub:L-GBP1 using the primers in Table 1. This was double digested with *NheI* and

AflII. Similarly, miRFP670-FLAG-cODC1-SpyTag was PCR amplified and double digested with *AflII* and *ApaI*. The vector pcDNA3.1(+) was double digested with *NheI* and *ApaI*, and all three digested components were ligated together in a one-pot reaction.

Table 1 PCR primers used for Ub:L-GBP1-miRFP670-FLAG-cODC1-SpyTag molecular cloning

Name	**Category**	**Sequence (5'→3')**
NheI Ub:L-GBP1	Forward PCR Primer	ATATATGCTAGCGCTACCGGACTCAGATCTCG
Ub:L-GBP1 *AflII*	Reverse PCR Primer	ATATATCTTAAGCTTGCTGCTCACGGTCACCT
AflII miRFP670-FLAG-cODC1-SpyTag	Forward PCR Primer	ATATATCTTAAGATGGTGGCTGGACACGCTTC CGG
miRFP670-FLAG-cODC1-SpyTag *ApaI*	Reverse PCR Primer	ATATATGGGCCCTTACTTCGTCGGCTTGTAGG
XhoI → *NotI*	Mutagenesis Forward Primer	CGCTATGTCTTGTGCCCAAGAG
XhoI → *NotI*	Mutagenesis Reverse Primer	GCCGCTTTATCATCATCATCTTTATAATCGC

4.2.1.2 Mutagenesis to Remove the Redundant *XhoI* Restriction Site

While the procedure above results in a viable plasmid, there are multiple *XhoI* restriction sites throughout the vector, including one in the desired protein product, that will impair future cloning. To rectify this, the *XhoI* site directly following the FLAG tag was replaced with a *NotI* site (plus an additional thymine to keep the

remainder of the protein in frame). The plasmid resulting from the above protocol was amplified via PCR using Q5 Hot-Start DNA Polymerase and the mutagenesis primers listed in Table 1. This PCR product was purified and further processed with *DpnI*, T4 PNK, and DNA Ligase in the provided DNA Ligase buffer (supplemented with ATP) at room temperature for 3 hours. This processed DNA was transformed into NEB5α competent cells and screened for the presence of a *NotI* site via restriction digest.

4.2.1.3 Cloning SpyCatcher-BFP

SpyCatcher was human codon optimized and ordered as a gene fragment from Integrated DNA Technology (Coralville, IA). SpyCatcher and BFP were PCR amplified such that there was a common restriction enzyme site at the C-terminus of SpyCatcher and the N-terminus of BFP. The two PCR products were ligated together with a pcDNA3.1(+) backbone in a one-pot reaction.

4.2.2 Cell Culture

HEK293T cells were maintained in T75 tissue culture flasks (Celltreat) in complete media, *i.e.* Dulbecco's Modified Eagle Medium (DMEM, Cellgro) supplemented with 10% fetal bovine serum (FBS, Corning), 5% L-glutamine (Gibco), 10 U mL-1 penicillin (HyClone), and 10 U mL^{-1} streptomycin (HyClone) at 37°C and 5% CO_2. Cell passaging occurred upon reaching confluency in the flask by treating with 0.05% trypsin-EDTA for 4 minutes at 37°C and 5% CO_2. Cells were pelleted at 500 *g* for 10 minutes, resuspended in 5 mL of complete media, and counted. For experiments, HEK293T cells were seeded in 6-well plates at 250,000 cells/well.

4.2.3 Transfection

Plasmid DNA was prepared using ZymoPURE™ Plasmid Midiprep Kit (Zymo Research) according to the manufacture's protocol. One day after seeding, transfection was achieved with Lipofectamine® 3000 (Invitrogen) using 2.5 μg total plasmid DNA per well for 6-well plates in complete media and following the manufacture's protocol. The total DNA was split evenly among all plasmids as follows: 0.5 μg DNA with the POI to be rescued (*ex.* Ub:L-GBP1-miRFP670-cODC1-SpyTag) and 1.0 μg DNA of each rescuing protein (*ex*. GFP and/or SpyCatcher-BFP). For control experiments in which one rescuing protein was not transfected, the remaining balance of transfected DNA was completed using empty vector, pcDNA3.1(+).

4.2.4 Flow Cytometry

Flow cytometry was conducted on the Novocyte Benchtop Flow Cytometer (Acea Biosciences, San Diego, CA). All flow cytometry experiments involved $\geq$50,000 transfected cells as determined by forward- and side-scatter profiles of recorded events and fluorescent gating to exclude cells not transfected by at least the rescuing protein(s) for each respective experiment. Cells were prepared for flow cytometry by washing twice in warm PBS. Trypsin treatment was applied for 3 minutes, and the reaction was quenched by warm media. Cells were collected in microcentrifuge tubes and spun at 0.8g for 5 minutes. The supernatant was aspirated, and cells were resuspended in cold PBS. This solution was then passed through a cell strainer into a flow cytometer tube and stored on ice until analysis.

4.3 Results and Discussion

As a proof-of-concept for multi-input CPR, we operated with a protein which, based on single-input CPR, offered the highest probability of success. For the N-end CPR, we used GBP1, an anti-GFP nanobody,[140] as the rescuing sensor, which is rescued by GFP. Concerned that aggressive degradation might lead to minimal levels of rescue even after blocking of the DD, we chose leucine as the N-end residue, which has a reported half-life of ~5 h.[151] For C-end CPR, SpyCatcher/SpyTag pair was used as it forms a stable isopeptide bond providing efficient protein rescue.[136] To visualize SpyCatcher, BFP was fused to the C-terminus, generating SpyCatcher-BFP. Using miRFP670 — a near-infrared, monomeric, fluorescent protein[137] — as the POI, we created Ub:L-GBP1-miRFP670-FLAG-cODC1-SpyTag (**Figure 4.1**). This protein was transfected into HEK293T cells either by itself, with GFP only, with SpyCatcher-BFP only, or with both GFP and SpyCatcher-BFP.

As expected, Ub:L-GBP1-miRFP670-FLAG-cODC1-SpyTag had an extremely low half-life due to both DD domains working simultaneously with no rescuing agent, and fluorescent levels were similar to untrasnfected cells when measured by flow cytometry. Co-transfecting only with SpyCatcher-BFP did result in a small amount of miRFP670 rescue, suggesting that cODC1 is the dominant DD in this AND-gate design. This is further confirmed by co-transfecting with GFP alone as miRFP670 fluorescence did not raise much above background levels. In contrast, co-transfection with both GFP and SpyCatcher-BFP resulted in a 22-fold enhancement in miRFP670 fluorescent levels over the background (**Figure 4.2**). Thus as expected, both inputs are necessary to execute CPR, and either input alone is insufficient.

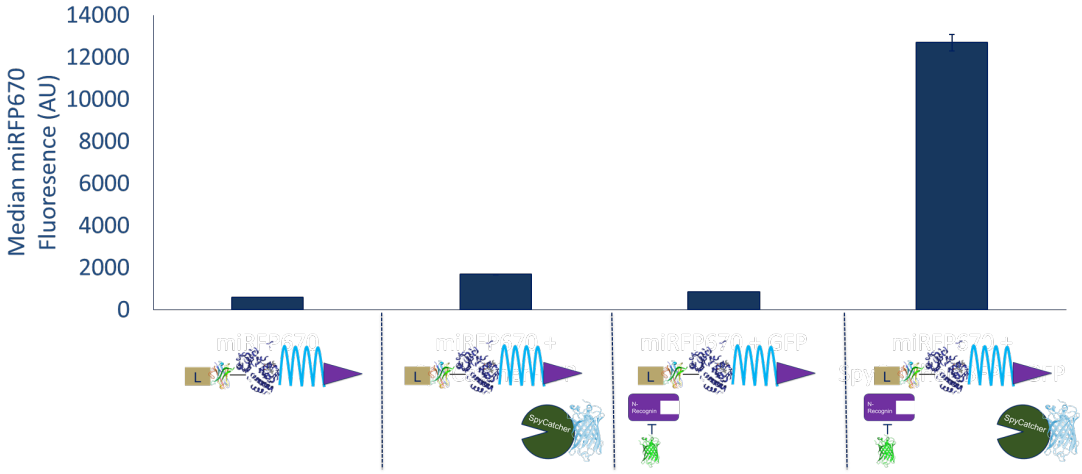

Figure 4.2 Flow cytometry results for multi-input CPR. Without any inputs, miRFP670 measures very low background levels similar to untransfected HEK293T cells. Co-transfection with SpyCatcher-BFP only resulted in a slight increase in miRFP670, and co-transfection with GFP only barely raised the levels of miRFP670. Only when co-transfected with both GFP and SpyCatcher-BFP is there a significant increase in the amount of miRFP670, suggesting that both inputs are needed simultaneously.

4.4 Discussion

Herein, we have demonstrated a purely protein-based Boolean AND gate that is not dependent upon a small molecule input. Rather, two orthogonal protein inputs are independently obligated to achieve the rescue of a third POI. To our knowledge, the proof-of-concept achieved here is the first of its kind, and presents a route to progress towards next-generation "smart therapeutics." While the multi-input CPR executed here utilized two exogenously transfected proteins, this work did establish the basis to extend the framework for a dual input system specific to two (or possibly more) cancer targets similar to the single-input systems described in Chapter 3.

One of the shortcomings of this design was the background achieved when only SpyCatcher-BFP was co-transfected. This demonstrates that cODC1 is the

dominating DD, and a leucine N-end residue is not sufficient to achieve complete degradation. Fortunately, there are other N-end residues, such as arginine, that result in an even shorter protein half-life. Indeed, earlier it was observed that a POI with an arginine N-end residue can still undergo rescue via CPR (Section 3.3.5). An appropriate N-end residue should reduce the background across all single-input cases without impairing the robust rescue observed.

In order to advance forward, there must be cancer-specific protein targets with available nanobodies. As time progresses, nanobody discovery will fill this void,[168,169] and screening libraries will facilitate the rate at which this occurs.[170–172] However, as it currently stands, CPR is best suited for detecting proteins unique to cancer, not just upregulated. More engineering will be required before CPR is capable of a threshold response, in which a certain intracellular concentration of a protein is required to rescue a POI, and below this concentration the POI is not rescued above background. For this reason, E7 made an ideal target since it is only introduced in HPV positive cervical cancer by virtue of the viral infection, and it is therefore absent in every other healthy cell.[153–155] Some proteins are unstable in most healthy cells, and they only persist in limited situations when they are required or once the cell becomes cancerous. For example, hypoxia inducible factor-1α (HIF-1α) is stabilized by the lack of oxygen typical of tumor environments, and several labs have developed specific nanobodies that bind this protein when present.[173–175] Unique disease states also exist for native proteins. For example, β-catenin is involved in the genesis of many types of cancer in a hypo-phosphorylated state, and nanobodies have been developed that specifically recognize the hypo-phosphorylated regions.[176,177] In

addition to therapeutic applications, CPR is also ideally suitable for real-time monitoring of disease- or cell-cycle-related protein changes.

Chapter 5

DISSERTATION CONCLUSIONS AND FUTURE WORK

The work in this dissertation seeks to harness the speed and responsiveness of mammalian protein degradation towards regulating protein cancer therapeutics. Protein degradation is a well-understood process, and natural cellular mechanisms for stabilizing proteins already exist. For example, cyclins are a class of proteins that drive the cell cycle.[27] At certain phases of the cell cycle, some cyclins are needed, while the presence of others would be detrimental to proper progression. On the other hand, when certain cyclins are necessary, they must appear quickly, and their degradation must occur just as rapidly once their purpose is served. To accomplish this feat, cells express cyclins constitutively and with a conditional degradation domain.[28] In this manner, the cyclin is constantly degraded, but when required, chaperone proteins protect the degradation domain (DD) via steric hindrance and stabilize the cyclin.[131,178,179] This paradigm served as an inspiration in our synthetic design. Likewise, therapeutic proteins must be at minimal to nonexistent levels in healthy cells, and yet they must be able to respond to high concentrations of their targets.

In Chapter 2, it was necessary to ascertain if a model cancer therapeutic, the prodrug converting enzyme yeast cytosine deaminase (yCD),[110,111] could be regulated on the basis of conditional degradation. If yCD could accomplish enough prodrug to drug conversion prior to being degraded, then the drug could approach lethal cytotoxic levels. While the kinetics of protein degradation have been engineered to be faster

than enzymatic activity, our overall approach still needed validation. To examine this, we used a model protein degradation system in which an exogenous small molecule served to inhibit protein degradation.[89] We could use this small molecule to simulate a "cancer state" while a control "healthy group" would not receive it. We found that the prodrug was necessary but insufficient to cause cell death, even when yCD was transfected. Only the combination of prodrug and rescuing small molecule could result in cell death.[143] Along the way, we recognized the importance of internal transfection markers as a means of normalizing protein degradation data, a lesson that eased future analysis.

From this demonstration, it was desirable to move away from the small molecule to create a degradation device that exploits proteins as the rescuing signal. Towards this goal, we developed conditional protein rescue (CPR) based on the principles of cyclin regulation mentioned above in Chapter 3. As a first attempt, it was desirable to have a "synthetic chaperone" that binds its target with extremely high affinity. Since there is no stronger binding affinity than a covalent bond, we used the SpyCatcher/SpyTag system[136] with a C-end cODC1 DD.[95] When SpyTag was fused to cODC1 and SpyCatcher was co-expressed, we demonstrated a remarkable ability to rescue a protein of interest (POI).

In a pivot towards endogenous targets that do not involve covalent bond formation, we next employed nanobodies, single-domain antibody fragments that can be screened for recognition of any desired target.[140,141] Starting with an anti-GFP nanobody, we again demonstrated the ability to rescue a POI from cODC1-induced degradation by co-expressing GFP. Furthermore, we were able to replicate our yCD experiment in a set up that allowed GFP to serve as a visually traceable "cancer

protein" while BFP served as the "healthy cell" control. Only the combination of GFP and the prodrug resulted in increased cell death. Cells co-transfected with BFP, on the other hand, maintained good viability even in the presence of the prodrug.

In order to expand the CPR repertoire, we sought to include other DDs in the toolbox. The native N-end rule protein degradation pathway provides a framework to modulate the half-life of any target protein simply by inserting an appropriate N-terminal amino acid residue.[148,149] From a synthetic biology standpoint, this simple rule allows for a convenient method for tuning degradation, and a competing protein binding near the N-terminal residue should rescue a protein fated for degradation. We indeed found this to be the case by installing an anti-GFP nanobody near the adjacent N-end rule residue. While C-end CPR was limited by the size and binding orientation of the rescuing protein, N-end CPR appeared to be more generous. Thus, it should be possible to execute CPR with a greater number of proteins when operating in the N-end configuration. As a demonstration of the power of CPR, we used a nanobody that targets E7, a human papillomavirus (HPV) protein that leads to oncogenesis in cervical tissue,[153,154] to execute CPR specifically in HPV positive cells but not in HPV negative cells. Using mCherry as a reporter detectable by flow cytometry, CPR was used to distinguish HeLa cells (HPV positive) from HEK293T cells (HPV negative).

However, cancer is a complicated disease that often requires the effort of multiple proteins to dysregulate the cell cycle and divide unchecked.[6,7] In order to eliminate off-target effects and treat only diseased cells, a robust protein therapy must be able to examine multiple protein targets before eliciting the correct therapeutic outcome. To reduce the likelihood of false positives, we lastly developed multi-input CPR, the combination of N- and C-end CPR. Configured in this way, only the

simultaneous presence of two different protein markers is capable of inhibiting both DDs for efficient protein rescue.

Unlike other protein-based cancer therapy strategies which examine expression patterns of cell surface receptors, CPR stands alone in its ability to probe the cytosolic proteome. Thus, this dissertation has unlocked the potential to examine a much broader information space, increasing the probability that the therapy can achieve a proper diagnosis. As such, CPR can be combined with other methods that probe surface receptors or other properties of cancer. For example, viral delivery can be used to encode a CPR device as a gene therapy. Similarly, since the DDs involved do not function outside of mammalian cell, therapies can be synthesized in an expression host and delivered to the cell via a targeted protein delivery vehicle. Working as a nucleic acid-protein hybrid, engineers might gain the ability to sense both cancer miRNAs and proteins simultaneously, giving an unprecedented level of control across multiple biomolecular categories simultaneously. For example, one could imagine a device that uses toehold-mediated strand displacement (TMSD) to detect the presence of cancer-specific miRNAs and assemble a split yCD as the desired output.[20] If the split yCD proteins are also configured for CPR, then the absence of cancer proteins would negate split yCD reconstitution and arrest a potential false positive. We envision a CPR-based cancer therapy enhancing the function of previously established methods to supplement additional layers of cell analysis in the decision making process. In this way, the inputs are additive over those required for accurate protein delivery and CPR execution, and one could design a therapy that requires the correct combination of surface receptors, miRNAs, and proteins as a three-layered checklist before deploying the therapeutic.

The multi-input CPR technique we have developed here is capable of executing a Boolean AND architecture with two inputs in the most complicated case. However, it should be feasible to engineer different architectures with multiple inputs. One way to accomplish this is through cascading CPR through multiple levels. Some example architectures assembled in this manner include:

- For OR gate architecture, one could envision a primary output with C-end CPR such that a SpyCatcher is necessary to stabilize the POI. Additionally, two separate SpyCatcher constructs could be synthesized, each with N-end CPR and different nanobodies serving as input detectors. If any one of the inputs is present, that SpyCatcher will be stabilized, and it in turn will stabilize the POI. Theoretically, in this configuration one could build an OR gate with as many targets as there are available nanobodies.

- For NOT gate architecture, one could build a construct with the POI followed by a DD, protease cut site, and a stabilizing protein fusion. Then, the protease for that cut site could be designed with either N- or C-end CPR with a nanobody to rescue it. In the absence of the nanobody's target, the POI will be stable since the DD is blocked by the larger stabilizing protein. When the nanobody's target is present, the protease will be stabilized, and this will cleave the stabilizing protein from the POI, revealing the DD and fating the POI for destruction.

- For more than two input AND gate architecture, the POI can be configured as demonstrated in Chapter 4 with N- and C-end CPR. Instead of sensing constitutively expressed proteins, the protein inputs for the POI can themselves be dependent upon AND gate CPR design. To use the example above, if both GFP and SpyCatcher are each expressed with N- and C-end CPR with rescuing nanobodies, then two unique targets can be required to rescue GFP, and two additional unique targets are needed to rescue SpyCatcher. Both GFP and SpyCatcher, once stabilized by their inputs, can then continue down the cascade to rescue the POI. In this example, four unique inputs are each necessary for POI rescue.

Since it has been established that a POI can be rescued through a nanobody-antigen interaction, changing the concentration of antigen over time ought to make

CPR a dynamic process. In the simplest example, if an exogenous rescue protein (*ex.* GFP) is expressed with an inducible promotor, the inducer level can be varied over time. Therefore, the level of GFP can be changed over time, which should effect the amount of POI present. One could imagine building an autonomous CPR-based protein oscillator based on this concept and in tandem with other previously built synthetic oscillator designs. In the more interesting case, CPR can be used as a means to probe endogenous protein levels at different phases of the cellular life cycle. A fluorescent POI creates an easily detectable output to inform an observer how the target protein's levels range in time.

CPR is a fledging technology with optimistic potential. In this dissertation, the objective was for cancer therapy. In this regard, CPR offers a novel approach towards next generation therapeutics, and it meets all the requisite requirements to address the shortcomings of current clinical treatment methods. The protein engineering community is well equipped to tackle the challenges already acknowledged, such as cell delivery and background off-target apoptosis, to transform this technology from its infancy to a final product. Ultimately, CPR has broader applications beyond just cancer treatment, such as detection and cellular protein probing. This dissertation introduces just the first-generation of the technology, and it is the author's aspiration that with the right ingenuity and creativity, this technology can be applied to a vast plethora of biological systems in exciting, innovative contexts.

REFERENCES

1. What Is Cancer? - National Cancer Institute. Available at: https://www.cancer.gov/about-cancer/understanding/what-is-cancer. (Accessed: 18th March 2020)

2. Barnum, K. J. & O'Connell, M. J. Cell cycle regulation by checkpoints. *Methods Mol. Biol.* **1170**, 29–40 (2014).

3. Sullivan, M. & Morgan, D. O. Finishing mitosis, one step at a time. *Nature Reviews Molecular Cell Biology* **8**, 894–903 (2007).

4. Murray, A. W. & Kirschner, M. W. Dominoes and clocks: The union of two views of the cell cycle. *Science* **246**, 614–621 (1989).

5. Morgan, D. O. *The cell cycle : principles of control*. (New Science Press, 2007).

6. Hanahan, D. & Weinberg, R. A. The hallmarks of cancer. *Cell* **100**, 57–70 (2000).

7. Hanahan, D. & Weinberg, R. A. Hallmarks of cancer: The next generation. *Cell* **144**, 646–674 (2011).

8. Stratton, M. R., Campbell, P. J. & Futreal, P. A. The cancer genome. *Nature* **458**, 719–724 (2009).

9. Garraway, L. A. & Lander, E. S. Lessons from the cancer genome. *Cell* **153**, 17–37 (2013).

10. Valdes-Mora, F. *et al.* Single-cell transcriptomics in cancer immunobiology: The future of precision oncology. *Frontiers in Immunology* **9**, 2582 (2018).

11. Doll, S., Gnad, F. & Mann, M. The Case for Proteomics and Phospho-Proteomics in Personalized Cancer Medicine. *Proteomics - Clinical Applications* **13**, e1800113 (2019).

12. Simpson, R. J. & Dorow, D. S. Cancer proteomics: from signaling networks to tumor markers. *Trends Biotechnol.* **19**, S40-8 (2001).

13. Gonzalez-Angulo, A. M., Hennessy, B. T. J. & Mills, G. B. Future of personalized medicine in oncology: A systems biology approach. *Journal of Clinical Oncology* **28**, 2777–2783 (2010).

14. Kalia, M. Personalized oncology: Recent advances and future challenges. *Metabolism.* **62**, (2013).

15. Pento, J. T. Monoclonal antibodies for the treatment of cancer. *Anticancer Research* **37**, 5935–5939 (2017).

16. June, C. H., O'Connor, R. S., Kawalekar, O. U., Ghassemi, S. & Milone, M. C. CAR T cell immunotherapy for human cancer. *Science* **359**, 1361–1365 (2018).

17. Twumasi-Boateng, K., Pettigrew, J. L., Kwok, Y. Y. E., Bell, J. C. & Nelson, B. H. Oncolytic viruses as engineering platforms for combination immunotherapy. *Nature Reviews Cancer* **18**, 419–432 (2018).

18. Hu, Z., Ott, P. A. & Wu, C. J. Towards personalized, tumour-specific, therapeutic vaccines for cancer. *Nature Reviews Immunology* **18**, 168–182 (2018).

19. Sahin, U. & Türeci, Ö. Personalized vaccines for cancer immunotherapy. *Science* **359**, 1355–1360 (2018).

20. Chen, R. P., Blackstock, D., Sun, Q. & Chen, W. Dynamic protein assembly by programmable DNA strand displacement. *Nat. Chem.* **10**, 474–481 (2018).

21. Lemke, E. A. & Schultz, C. Principles for designing fluorescent sensors and reporters. *Nature Chemical Biology* **7**, 480–483 (2011).

22. Hartwell, L. H., Hopfield, J. J., Leibler, S. & Murray, A. W. From molecular to modular cell biology. *Nature* **402**, (1999).

23. Mitragotri, S., Burke, P. A. & Langer, R. Overcoming the challenges in administering biopharmaceuticals: Formulation and delivery strategies. *Nature Reviews Drug Discovery* **13**, 655–672 (2014).

24. Li, Z. *et al.* Identification and characterization of a novel peptide ligand of epidermal growth factor receptor for targeted delivery of therapeutics. *FASEB J.* **19**, 1978–1985 (2005).

25. Lieser, R. M., Chen, W. & Sullivan, M. O. Controlled Epidermal Growth Factor Receptor Ligand Display on Cancer Suicide Enzymes via Unnatural Amino Acid Engineering for Enhanced Intracellular Delivery in Breast Cancer

Cells. *Bioconjug. Chem.* **30**, 432–442 (2019).

26. Sherr, C. J. & Roberts, J. M. CDK inhibitors: positive and negative regulators of G1-phase progression. *Genes Dev.* **13**, 1501–12 (1999).

27. Morgan, D. O. CYCLIN-DEPENDENT KINASES: Engines, Clocks, and Microprocessors. *Annu. Rev. Cell Dev. Biol.* **13**, 261–291 (1997).

28. Harper, J. W., Burton, J. L. & Solomon, M. J. The anaphase-promoting complex: it's not just for mitosis any more. *Genes Dev.* **16**, 2179–2206 (2002).

29. Saeki, Y. Ubiquitin recognition by the proteasome. *J. Biochem.* **161**, mvw091 (2017).

30. Schrader, E. K., Harstad, K. G. & Matouschek, A. Targeting proteins for degradation. *Nat. Chem. Biol.* **5**, 815–822 (2009).

31. Yu, H. & Matouschek, A. Recognition of Client Proteins by the Proteasome. *Annu. Rev. Biophys.* **46**, 149–173 (2017).

32. Prakash, S., Inobe, T., Hatch, A. J. & Matouschek, A. Substrate selection by the proteasome during degradation of protein complexes. *Nat. Chem. Biol.* **5**, 29–36 (2009).

33. Erales, J. & Coffino, P. Ubiquitin-independent proteasomal degradation. *Biochim. Biophys. Acta - Mol. Cell Res.* **1843**, 216–221 (2014).

34. Wilkinson, K. D. Ubiquitination and deubiquitination: Targeting of proteins for degradation by the proteasome. *Semin. Cell Dev. Biol.* **11**, 141–148 (2000).

35. Chau, V. *et al.* A multiubiquitin chain is confined to specific lysine in a targeted short-lived protein. *Science* **243**, 1576–83 (1989).

36. Komander, D. & Rape, M. The Ubiquitin Code. *Annu. Rev. Biochem.* **81**, 203–229 (2012).

37. Deshaies, R. J. & Joazeiro, C. A. P. RING Domain E3 Ubiquitin Ligases. *Annu. Rev. Biochem.* **78**, 399–434 (2009).

38. Berndsen, C. E. & Wolberger, C. New insights into ubiquitin E3 ligase mechanism. *Nat. Struct. Mol. Biol.* **21**, 301–307 (2014).

39. Metzger, M. B., Hristova, V. A. & Weissman, A. M. HECT and RING finger families of E3 ubiquitin ligases at a glance. *J. Cell Sci.* **125**, 531–537 (2012).

40. Lorick, K. L. *et al.* RING fingers mediate ubiquitin-conjugating enzyme (E2)-dependent ubiquitination. *Proc. Natl. Acad. Sci. U. S. A.* **96**, 11364–9 (1999).

41. Kamadurai, H. B. *et al.* Insights into Ubiquitin Transfer Cascades from a Structure of a UbcH5B~Ubiquitin-HECTNEDD4L Complex. *Mol. Cell* **36**, 1095–1102 (2009).

42. Huang, L. *et al.* Structure of an E6AP-UbcH7 complex: insights into ubiquitination by the E2-E3 enzyme cascade. *Science* **286**, 1321–6 (1999).

43. Zheng, N., Wang, P., Jeffrey, P. D. & Pavletich, N. P. Structure of a c-Cbl-UbcH7 complex: RING domain function in ubiquitin-protein ligases. *Cell* **102**, 533–539 (2000).

44. Skowyra, D., Craig, K. L., Tyers, M., Elledge, S. J. & Harper, J. W. F-box proteins are receptors that recruit phosphorylated substrates to the SCF ubiquitin-ligase complex. *Cell* **91**, 209–19 (1997).

45. Feldman, R. M., Correll, C. C., Kaplan, K. B. & Deshaies, R. J. A complex of Cdc4p, Skp1p, and Cdc53p/cullin catalyzes ubiquitination of the phosphorylated CDK inhibitor Sic1p. *Cell* **91**, 221–30 (1997).

46. Jin, J. *et al.* Systematic analysis and nomenclature of mammalian F-box proteins. *Genes Dev.* **18**, 2573–2580 (2004).

47. Skaar, J. R., Pagan, J. K. & Pagano, M. SnapShot: F Box Proteins I. *Cell* **137**, 1160-1160.e1 (2009).

48. Skaar, J. R., D'Angiolella, V., Pagan, J. K. & Pagano, M. SnapShot: F Box Proteins II. *Cell* **137**, 1358.e1-1358.e2 (2009).

49. Skaar, J. R., Pagan, J. K. & Pagano, M. Mechanisms and function of substrate recruitment by F-box proteins. *Nat. Rev. Mol. Cell Biol.* **14**, 369–381 (2013).

50. Lydeard, J. R., Schulman, B. A. & Harper, J. W. Building and remodelling Cullin-RING E3 ubiquitin ligases. *EMBO Rep.* **14**, 1050–1061 (2013).

51. Fulcher, L. J. *et al.* An affinity-directed protein missile system for targeted proteolysis. *Open Biol.* **6**, (2016).

52. Clift, D. *et al.* A Method for the Acute and Rapid Degradation of Endogenous Proteins. *Cell* **171**, 1692-1706.e18 (2017).

53. Nishimura, K., Fukagawa, T., Takisawa, H., Kakimoto, T. & Kanemaki, M. An auxin-based degron system for the rapid depletion of proteins in nonplant cells.

Nat. Methods **6**, 917–922 (2009).

54. Gu, S., Cui, D., Chen, X., Xiong, X. & Zhao, Y. PROTACs: An Emerging Targeting Technique for Protein Degradation in Drug Discovery. *BioEssays* **40**, 1700247 (2018).

55. Toure, M. & Crews, C. M. Small-Molecule PROTACS: New Approaches to Protein Degradation. *Angew. Chemie Int. Ed.* **55**, 1966–1973 (2016).

56. Collins, I., Wang, H., Caldwell, J. J. & Chopra, R. Chemical approaches to targeted protein degradation through modulation of the ubiquitin–proteasome pathway. *Biochem. J.* **474**, 1127–1147 (2017).

57. Lai, A. C. & Crews, C. M. Induced protein degradation: an emerging drug discovery paradigm. *Nat. Rev. Drug Discov.* **16**, 101–114 (2017).

58. Sakamoto, K. M. *et al.* Protacs: Chimeric molecules that target proteins to the Skp1-Cullin-F box complex for ubiquitination and degradation. *Proc. Natl. Acad. Sci.* **98**, 8554–8559 (2001).

59. Fulcher, L. J., Hutchinson, L. D., Macartney, T. J., Turnbull, C. & Sapkota, G. P. Targeting endogenous proteins for degradation through the affinity-directed protein missile system. *Open Biol.* **7**, (2017).

60. Wenzel, D. M., Lissounov, A., Brzovic, P. S. & Klevit, R. E. UBCH7 reactivity profile reveals parkin and HHARI to be RING/HECT hybrids. *Nature* **474**, 105–108 (2011).

61. Duda, D. M. *et al.* Structure of HHARI, a RING-IBR-RING ubiquitin ligase: Autoinhibition of an Ariadne-family E3 and insights into ligation mechanism. *Structure* **21**, 1030–1041 (2013).

62. Bachmair, A., Finley, D. & Varshavsky, A. In vivo half-life of a protein is a function of its amino-terminal residue. *Science* **234**, 179–86 (1986).

63. Hwang, C.-S., Shemorry, A. & Varshavsky, A. N-Terminal Acetylation of Cellular Proteins Creates Specific Degradation Signals. *Science (80-.).* **327**, 973–977 (2010).

64. Tasaki, T. *et al.* The Substrate Recognition Domains of the N-end Rule Pathway. *J. Biol. Chem.* **284**, 1884–1895 (2009).

65. Hwang, C.-S. & Varshavsky, A. Regulation of peptide import through phosphorylation of Ubr1, the ubiquitin ligase of the N-end rule pathway. *Proc.*

Natl. Acad. Sci. **105**, 19188–19193 (2008).

66. Xia, Z. *et al.* Substrate-binding Sites of UBR1, the Ubiquitin Ligase of the N-end Rule Pathway. *J. Biol. Chem.* **283**, 24011–24028 (2008).

67. Xie, Y. & Varshavsky, A. The E2-E3 interaction in the N-end rule pathway: the RING-H2 finger of E3 is required for the synthesis of multiubiquitin chain. *EMBO J.* **18**, 6832–6844 (1999).

68. Varshavsky, A. The N-end rule: functions, mysteries, uses. *Proc. Natl. Acad. Sci. U. S. A.* **93**, 12142–9 (1996).

69. Bachmair, A. & Varshavsky, A. The degradation signal in a short-lived protein. *Cell* **56**, 1019–32 (1989).

70. Varshavsky, A. The N-end rule pathway and regulation by proteolysis. *Protein Sci.* **20**, 1298–1345 (2011).

71. Varshavsky, A. Ubiquitin Fusion Technique and Related Methods. in *Methods in enzymology* **399**, 777–799 (2005).

72. Murakami, Y. *et al.* Ornithine decarboxylase is degraded by the 26S proteasome without ubiquitination. *Nature* **360**, 597–599 (1992).

73. Zhang, M., MacDonald, A. I., Hoyt, M. A. & Coffino, P. Proteasomes begin ornithine decarboxylase digestion at the C terminus. *J. Biol. Chem.* **279**, 20959–65 (2004).

74. Zhang, M., Pickart, C. M. & Coffino, P. Determinants of proteasome recognition of ornithine decarboxylase, a ubiquitin-independent substrate. *EMBO J.* **22**, 1488–96 (2003).

75. Zhao, W., Pferdehirt, L. & Segatori, L. Quantitatively Predictable Control of Cellular Protein Levels through Proteasomal Degradation. *ACS Synth. Biol.* **7**, 540–552 (2018).

76. Li, X. *et al.* Generation of destabilized green fluorescent protein as a transcription reporter. *J. Biol. Chem.* **273**, 34970–5 (1998).

77. Hsieh, C.-H. *et al.* Construction of Mutant TKGFP for Real-Time Imaging of Temporal Dynamics of HIF-1 Signal Transduction Activity Mediated by Hypoxia and Reoxygenation in Tumors in Living Mice. *J. Nucl. Med.* **50**, 2049–2057 (2009).

78. Joshi, R. G., Kulkarni, S. & Ratna Prabha, C. Engineering degrons of yeast

ornithine decarboxylase as vehicles for efficient targeted protein degradation. *Biochim. Biophys. Acta - Gen. Subj.* **1850**, 2452–2463 (2015).

79. Bonger, K. M., Chen, L. C., Liu, C. W. & Wandless, T. J. Small-molecule displacement of a cryptic degron causes conditional protein degradation. *Nat. Chem. Biol.* **7**, 531–537 (2011).

80. Banaszynski, L. A., Chen, L. chun, Maynard-Smith, L. A., Ooi, A. G. L. & Wandless, T. J. A Rapid, Reversible, and Tunable Method to Regulate Protein Function in Living Cells Using Synthetic Small Molecules. *Cell* **126**, 995–1004 (2006).

81. Chung, H. K. *et al.* Tunable and reversible drug control of protein production via a self-excising degron. *Nat. Chem. Biol.* **11**, 713–720 (2015).

82. Yan, D. *et al.* Replication-Competent Influenza Virus and Respiratory Syncytial Virus Luciferase Reporter Strains Engineered for Co-Infections Identify Antiviral Compounds in Combination Screens. *Biochemistry* **54**, 5589–5604 (2015).

83. Lemmens, B. *et al.* DNA Replication Determines Timing of Mitosis by Restricting CDK1 and PLK1 Activation. *Mol. Cell* **71**, 117-128.e3 (2018).

84. Iwamoto, M., Björklund, T., Lundberg, C., Kirik, D. & Wandless, T. J. A general chemical method to regulate protein stability in the mammalian central nervous system. *Chem. Biol.* **17**, 981–988 (2010).

85. Pratt, M. R., Schwartz, E. C. & Muir, T. W. Small-molecule-mediated rescue of protein function by an inducible proteolytic shunt. *Proc. Natl. Acad. Sci.* **104**, 11209–11214 (2007).

86. Szymczak, A. L. *et al.* Correction of multi-gene deficiency in vivo using a single 'self-cleaving' 2A peptide-based retroviral vector. *Nat. Biotechnol.* **22**, 589–594 (2004).

87. Holst, J., Vignali, K. M., Burton, A. R. & Vignali, D. A. A. Rapid analysis of T-cell selection in vivo using T cell-receptor retrogenic mice. (2006). doi:10.1038/NMETH858

88. Lau, H. D., Yaegashi, J., Zaro, B. W. & Pratt, M. R. Precise control of protein concentration in living cells. *Angew. Chemie - Int. Ed.* **49**, 8458–8461 (2010).

89. Lin, Y. H. & Pratt, M. R. A Dual small-molecule rheostat for precise control of protein concentration in mammalian cells. *ChemBioChem* **15**, 805–809 (2014).

90. Zhang, H. & Cohen, A. E. Optogenetic Approaches to Drug Discovery in Neuroscience and Beyond. *Trends Biotechnol.* **35**, 625–639 (2017).

91. Kim, C. K., Adhikari, A. & Deisseroth, K. Integration of optogenetics with complementary methodologies in systems neuroscience. *Nat. Rev. Neurosci.* **18**, 222–235 (2017).

92. Liu, Z. *et al.* Programming Bacteria With Light—Sensors and Applications in Synthetic Biology. *Front. Microbiol.* **9**, (2018).

93. Goglia, A. G. & Toettcher, J. E. A bright future: optogenetics to dissect the spatiotemporal control of cell behavior. *Curr. Opin. Chem. Biol.* **48**, 106–113 (2019).

94. Harper, S. M., Neil, L. C. & Gardner, K. H. Structural basis of a phototropin light switch. *Science (80-.).* **301**, 1541–1544 (2003).

95. Renicke, C., Schuster, D., Usherenko, S., Essen, L. O. & Taxis, C. A LOV2 domain-based optogenetic tool to control protein degradation and cellular function. *Chem. Biol.* **20**, 619–626 (2013).

96. Ochoa-Fernandez, R. *et al.* Optogenetics in Plants: Red/Far-Red Light Control of Gene Expression. in *Methods in molecular biology (Clifton, N.J.)* **1408**, 125–139 (2016).

97. Kawano, F., Shi, F. & Yazawa, M. Switching with red and blue. *Nat. Chem. Biol.* **13**, 573–574 (2017).

98. Taxis, C., Stier, G., Spadaccini, R. & Knop, M. Efficient protein depletion by genetically controlled deprotection of a dormant N-degron. *Mol. Syst. Biol.* **5**, 267 (2009).

99. Fernandez-Rodriguez, J. & Voigt, C. A. Post-translational control of genetic circuits using *Potyvirus* proteases. *Nucleic Acids Res.* **44**, 6493–6502 (2016).

100. Gao, X. J., Chong, L. S., Kim, M. S. & Elowitz, M. B. Programmable protein circuits in living cells. *Science* **361**, 1252–1258 (2018).

101. Jungbluth, M., Renicke, C. & Taxis, C. Targeted protein depletion in Saccharomyces cerevisiae by activation of a bidirectional degron. *BMC Syst. Biol.* **4**, 176 (2010).

102. Hamers-Casterman, C. *et al.* Naturally occurring antibodies devoid of light chains. *Nature* **363**, 446–448 (1993).

103. Muyldermans, S. Muyldermans, S. (2013). Nanobodies: Natural Single-Domain Antibodies. Annual Review of Biochemistry, 82(1), 775–797. http://doi.org/10.1146/annurev-biochem-063011-092449Nanobodies: Natural Single-Domain Antibodies. *Annu. Rev. Biochem.* **82**, 775–797 (2013).

104. Rahbarizadeh, F., Ahmadvand, D. & Sharifzadeh, Z. Nanobody; an old concept and new vehicle for immunotargeting. *Immunol. Invest.* **40**, 299–338 (2011).

105. Dumoulin, M. *et al.* Single-domain antibody fragments with high conformational stability. *Protein Sci.* **11**, 500–515 (2009).

106. Khodabakhsh, F., Behdani, M., Rami, A. & Kazemi-Lomedasht, F. Single-Domain Antibodies or Nanobodies: A Class of Next-Generation Antibodies. *International Reviews of Immunology* **37**, 316–322 (2018).

107. Reader, R. H., Workman, R. G., Maddison, B. C. & Gough, K. C. Advances in the Production and Batch Reformatting of Phage Antibody Libraries. *Molecular Biotechnology* **61**, 801–815 (2019).

108. Altaner, C. Prodrug cancer gene therapy. *Cancer Lett.* **270**, 191–201 (2008).

109. Andrady, C., Sharma, S. K. & Chester, K. A. Antibody-enzyme fusion proteins for cancer therapy. *Immunotherapy* **3**, 193–211 (2011).

110. Polak, A., Eschenhof, E., Fernex, M. & Scholer, H. J. Metabolic studies with 5-fluorocytosine-6-14C in mouse, rat, rabbit, dog and man. *Chemotherapy* **22**, 137–53 (1976).

111. Zhang, J., Kale, V. & Chen, M. Gene-Directed Enzyme Prodrug Therapy. *AAPS J.* **17**, 102–110 (2014).

112. Biela, B. H., Khawli, L. A., Hu, P. & Epstein, A. L. Chimeric TNT-3/human beta-glucuronidase fusion proteins for antibody-directed enzyme prodrug therapy (ADEPT). *Cancer Biother. Radiopharm.* **18**, 339–353 (2003).

113. Fong, V. *et al.* Adenoviral Vector Driven by a Minimal Rad51 Promoter Is Selective for p53-Deficient Tumor Cells. *PLoS One* **6**, e28714 (2011).

114. Tian, D. *et al.* Human telomerase reverse-transcriptase promoter-controlled and herpes simplex virus thymidine kinase-armed adenoviruses for renal cell carcinoma treatment. *Onco. Targets. Ther.* **6**, 419–426 (2013).

115. Wang, H., Zhou, X.-L., Long, W., Liu, J.-J. & Fan, F.-Y. A Fusion Protein of RGD4C and β-Lactamase Has a Favorable Targeting Effect in Its Use in

Antibody Directed Enzyme Prodrug Therapy. *Int. J. Mol. Sci.* **16**, 9625–9634 (2015).

116. Bildstein, L., Dubernet, C. & Couvreur, P. Prodrug-based intracellular delivery of anticancer agents. *Advanced Drug Delivery Reviews* **63**, 3–23 (2011).

117. Caussinus, E., Kanca, O. & Affolter, M. Fluorescent fusion protein knockout mediated by anti-GFP nanobody. *Nat. Struct. Mol. Biol.* **19**, 117–122 (2012).

118. Banaszynski, L. A., Sellmyer, M. A., Contag, C. H., Wandless, T. J. & Thorne, S. H. Chemical control of protein stability and function in living mice. *Nat. Med.* **14**, 1123–1127 (2008).

119. Johnsson, N. & Varshavsky, A. Split ubiquitin as a sensor of protein interactions in vivo. *Proc. Natl. Acad. Sci. U. S. A.* **91**, 10340–10344 (1994).

120. Stagljar, I., Korostensky, C., Johnsson, N. & Te Heesen, S. A genetic system based on split-ubiquitin for the analysis of interactions between membrane proteins in vivo. *Proc. Natl. Acad. Sci. U. S. A.* **95**, 5187–5192 (1998).

121. Holst, J., Burton, A. R., Vignali, K. M. & Vignali, D. A. A. Rapid analysis of T-cell selection in vivo using T cell-receptor retrogenic mice. *Nat. Methods* **3**, 191–197 (2006).

122. Wright, C. M., Wright, R. C., Eshleman, J. R. & Ostermeier, M. A protein therapeutic modality founded on molecular regulation. *Proc. Natl. Acad. Sci. U. S. A.* **108**, 16206–16211 (2011).

123. Mann, K. & Kullberg, M. Trastuzumab-targeted gene delivery to Her2-overexpressing breast cancer cells. *Cancer Gene Ther.* **23**, 221–8 (2016).

124. Sigoillot, F. D. & King, R. W. Vigilance and Validation: Keys to Success in RNAi Screening. *ACS Chem. Biol.* **6**, 47–60 (2011).

125. Battle, A. *et al.* Impact of regulatory variation from RNA to protein. *Science (80-.).* **347**, 664–667 (2015).

126. Wu, L. *et al.* Variation and genetic control of protein abundance in humans. *Nature* **499**, 79–82 (2013).

127. Vogel, C. & Marcotte, E. M. Insights into the regulation of protein abundance from proteomic and transcriptomic analyses. *Nat. Rev. Genet.* **13**, 227–232 (2012).

128. Mei, L. *et al.* Long-term in vivo recording of circadian rhythms in brains of

freely moving mice. *Proc. Natl. Acad. Sci. U. S. A.* **115**, 4276–4281 (2018).

129. Sjaastad, L. E. *et al.* Distinct antiviral signatures revealed by the magnitude and round of influenza virus replication in vivo. *Proc. Natl. Acad. Sci. U. S. A.* **115**, 9610–9615 (2018).

130. Chen, R. P., Gaynor, A. S. & Chen, W. Synthetic biology approaches for targeted protein degradation. *Biotechnol. Adv.* **37**, 107446 (2019).

131. Sherr, C. J. & Roberts, J. M. CDK inhibitors: positive and negative regulators of G1-phase progression. *Genes Dev.* **13**, 1501–12 (1999).

132. Shemorry, A., Hwang, C. S. & Varshavsky, A. Control of protein quality and stoichiometries by N-terminal acetylation and the N-end rule pathway. *Mol. Cell* **50**, 540–551 (2013).

133. Zhang, Z., Kulkarni, K., Hanrahan, S. J., Thompson, A. J. & Barford, D. The APC/C subunit Cdc16/Cut9 is a contiguous tetratricopeptide repeat superhelix with a homo-dimer interface similar to Cdc27. *EMBO J.* **29**, 3733–3744 (2010).

134. Oh, J.-H., Hyun, J.-Y. & Varshavsky, A. Control of Hsp90 chaperone and its clients by N-terminal acetylation and the N-end rule pathway. *Proc. Natl. Acad. Sci. U. S. A.* **114**, E4379 (2017).

135. Jungbluth, M., Renicke, C. & Taxis, C. Targeted protein depletion in Saccharomyces cerevisiae by activation of a bidirectional degron. *BMC Syst. Biol.* **4**, 176 (2010).

136. Zakeri, B. *et al.* Peptide tag forming a rapid covalent bond to a protein, through engineering a bacterial adhesin. *Proc. Natl. Acad. Sci. U. S. A.* **109**, E690-7 (2012).

137. Shcherbakova, D. M. *et al.* Bright monomeric near-infrared fluorescent proteins as tags and biosensors for multiscale imaging. *Nat. Commun.* **7**, 12405 (2016).

138. Li, S. S. Specificity and versatility of SH3 and other proline-recognition domains: structural basis and implications for cellular signal transduction. *Biochem. J.* **390**, 641–653 (2005).

139. Dueber, J. E., Mirsky, E. A. & Lim, W. A. Engineering synthetic signaling proteins with ultrasensitive input/output control. *Nat. Biotechnol.* **25**, 660–662 (2007).

140. Kubala, M. H., Kovtun, O., Alexandrov, K. & Collins, B. M. Structural and

thermodynamic analysis of the GFP:GFP-nanobody complex. *Protein Sci.* **19**, 2389–2401 (2010).

141. Saerens, D. *et al.* Identification of a Universal VHH Framework to Graft Non-canonical Antigen-binding Loops of Camel Single-domain Antibodies. *J. Mol. Biol.* **352**, 597–607 (2005).

142. Tang, J. C. Y. *et al.* A nanobody-based system using fluorescent proteins as scaffolds for cell-specific gene manipulation. *Cell* **154**, 928–939 (2013).

143. Gaynor, A. S. & Chen, W. Induced prodrug activation by conditional protein degradation. *J. Biotechnol.* **260**, 62–66 (2017).

144. Prakash, S., Inobe, T., Hatch, A. J. & Matouschek, A. Substrate selection by the proteasome during degradation of protein complexes. *Nat. Chem. Biol.* **5**, 29–36 (2009).

145. Stack, J. H., Whitney, M., Rodems, S. M. & Pollok, B. A. A ubiquitin-based tagging system for controlled modulation of protein stability. *Nat. Biotechnol.* **18**, 1298–1302 (2000).

146. Elsasser, S. *et al.* Proteasome subunit Rpn1 binds ubiquitin-like protein domains. *Nat. Cell Biol.* **4**, 725–730 (2002).

147. Yu, H. *et al.* Conserved Sequence Preferences Contribute to Substrate Recognition by the Proteasome. *J. Biol. Chem.* **291**, 14526–14539 (2016).

148. Choi, W. S. *et al.* Structural basis for the recognition of N-end rule substrates by the UBR box of ubiquitin ligases. *Nat. Struct. Mol. Biol.* **17**, 1175–81 (2010).

149. Matta-Camacho, E., Kozlov, G., Li, F. F. & Gehring, K. Structural basis of substrate recognition and specificity in the N-end rule pathway. *Nat. Struct. Mol. Biol.* **17**, 1182–1187 (2010).

150. Bachmair, A., Finley, D. & Varshavsky, A. In vivo half-life of a protein is a function of its amino-terminal residue. *Science (80-.).* **234**, 179–186 (1986).

151. Gonda, D. K. *et al.* Universality and stucture of the N-end rule. *J. Biol. Chem.* **264**, 16700–16712 (1989).

152. Fridy, P. C. *et al.* A robust pipeline for rapid production of versatile nanobody repertoires. *Nat. Methods* **11**, 1253–1260 (2014).

153. Jansma, A. L. *et al.* The high-risk HPV16 E7 oncoprotein mediates interaction

between the transcriptional coactivator CBP and the retinoblastoma protein pRb. *J. Mol. Biol.* **426**, 4030–4048 (2014).

154. Senba, M. & Mori, N. Mechanisms of virus immune evasion lead to development from chronic inflammation to cancer formation associated with human papillomavirus infection. *Oncol. Rev.* **6**, e17 (2012).

155. Moody, C. A. & Laimins, L. A. Human papillomavirus oncoproteins: Pathways to transformation. *Nature Reviews Cancer* **10**, 550–560 (2010).

156. Li, S. *et al.* Nanobody against the E7 oncoprotein of human papillomavirus 16. *Mol. Immunol.* **109**, 12–19 (2019).

157. Papapostolou, D. & Howorka, S. Engineering and exploiting protein assemblies in synthetic biology. *Molecular BioSystems* **5**, 723–732 (2009).

158. Hörner, M., Reischmann, N. & Weber, W. Synthetic biology: Programming cells for biomedical applications. *Perspect. Biol. Med.* **55**, 490–502 (2012).

159. Kelwick, R., MacDonald, J. T., Webb, A. J. & Freemont, P. Developments in the tools and methodologies of synthetic biology. *Frontiers in Bioengineering and Biotechnology* **2**, (2014).

160. Grünberg, R. & Serrano, L. Strategies for protein synthetic biology. *Nucleic Acids Res.* **38**, 2663–2675 (2010).

161. Sadowski, J. P., Calvert, C. R., Zhang, D. Y., Pierce, N. A. & Yin, P. Developmental self-assembly of a DNA tetrahedron. *ACS Nano* **8**, 3251–3259 (2014).

162. Modi, S. *et al.* A DNA nanomachine that maps spatial and temporal pH changes inside living cells. *Nat. Nanotechnol.* **4**, 325–330 (2009).

163. Zhang, D. Y., Turberfield, A. J., Yurke, B. & Winfree, E. Engineering Entropy-Driven Reactions and Networks Catalyzed by DNA. *Science (80-.).* **318**, 1121–1125 (2007).

164. Seelig, G., Soloveichik, D., Zhang, D. Y. & Winfree, E. Enzyme-free nucleic acid logic circuits. *Science (80-.).* **314**, 1585–1588 (2006).

165. Zhang, D. Y. & Seelig, G. Dynamic DNA nanotechnology using strand-displacement reactions. *Nat. Chem.* **3**, 103–113 (2011).

166. Gröger, K., Gavins, G. & Seitz, O. Strand Displacement in Coiled-Coil Structures: Controlled Induction and Reversal of Proximity. *Angew. Chemie* -

Int. Ed. **56**, 14217–14221 (2017).

167. Stein, V. & Alexandrov, K. Protease-based synthetic sensing and signal amplification. *Proc. Natl. Acad. Sci.* **111**, 15934–15939 (2014).

168. Jovčevska, I. & Muyldermans, S. The Therapeutic Potential of Nanobodies. *BioDrugs* **34**, 11–26 (2020).

169. Chanier, T. & Chames, P. Nanobody Engineering: Toward Next Generation Immunotherapies and Immunoimaging of Cancer. *Antibodies* **8**, 13 (2019).

170. McMahon, C. *et al.* Yeast surface display platform for rapid discovery of conformationally selective nanobodies. *Nat. Struct. Mol. Biol.* **25**, 289–296 (2018).

171. Moutel, S. *et al.* NaLi-H1: A universal synthetic library of humanized nanobodies providing highly functional antibodies and intrabodies. *Elife* **5**, (2016).

172. Tijink, B. M. *et al.* Improved tumor targeting of anti-epidermal growth factor receptor Nanobodies through albumin binding: Taking advantage of modular Nanobody technology. *Mol. Cancer Ther.* **7**, 2288–2297 (2008).

173. Li, M., Fan, X., Liu, J., Hu, Y. & Huang, H. Selection by phage display of nanobodies directed against hypoxia inducible factor-1α (HIF-1α). *Biotechnol. Appl. Biochem.* **62**, 738–745 (2015).

174. Groot, A. J. *et al.* Identification by phage display of single-domain antibody fragments specific for the ODD domain in hypoxia-inducible factor 1alpha. *Lab. Investig.* **86**, 345–356 (2006).

175. Giaccia, A., Siim, B. G. & Johnson, R. S. HIF-1 as a target for drug development. *Nat. Rev. Drug Discov.* **2**, 803–811 (2003).

176. Traenkle, B. *et al.* Monitoring interactions and dynamics of endogenous beta-catenin with intracellular nanobodies in living cells. *Mol. Cell. Proteomics* **14**, 707–723 (2015).

177. Clevers, H. & Nusse, R. Wnt/β-catenin signaling and disease. *Cell* **149**, 1192–1205 (2012).

178. Harashima, H., Dissmeyer, N. & Schnittger, A. Cell cycle control across the eukaryotic kingdom. *Trends Cell Biol.* **23**, 345–356 (2013).

179. Satyanarayana, A. & Kaldis, P. Mammalian cell-cycle regulation: several Cdks,

numerous cyclins and diverse compensatory mechanisms. *Oncogene* **28**, 2925–2939 (2009).

Appendix A

LIST OF PRIMERS USED IN CHAPTER 3

All oligonucleotides were ordered from Integrated DNA Technology (Coralville, IA), purified via standard desalting, and ordered as a standard oligo unless otherwise noted.

Name	**Category**	**Sequence (5'→3')**
AflII YFP	Forward PCR Primer	ATATATTTAAGATGGTGAGCAAGGGCGAGGA
YFP *XhoI*	Reverse PCR Primer	ATATATCTCGAGCTTGTACAGCTCGTCCATG
XhoI cODC1-SpyTag *ApaI*	Ultramer (Sense)	TCGAGATGTCTTGTGCCCAAGAGTCAATAACC AGTCTGTATAAGAAAGCTGGAAGTGAAAACCT CTATTTTCAGTCTAGAGCACACATAGTAATGG TAGACGCCTACAAGCCGACGAAGTAAGGGCC
	Ultramer (Antisense)	CTTACTTCGTCGGCTTGTAGGCGTCTACCATTA CTATGTGTGCTCTAGACTGAAAATAGAGGTTT TCACTTCCAGCTTTCTTATACAGACTGGTTATT GACTCTTGGGCACAAGACATC
NheI mCherry	Forward PCR Primer	ATATATGCTAGCATATTAGCTAAGCATGGTGA GCAAGGGCGAGGA
T2A mChery *AflII*	Reverse PCR Primer	ATATATCTTAAGGGGGCCGGGGTTCTCCTCCA CGTCGCCGCAGGTCAGCAGGGAGCCCCTGCCC TCATTCTTGTACAGCTCGTCCA
Human Codon Optimized SpyCatcher	gBlock Gene Fragment	GACAGCGCCACCCACATCAAGTTCAGCAAGA GGGACGAGGACGGCAAGGAGCTGGCCGGCGC CACAATGGAGCTGAGAGACAGCAGCGGCAAG ACCATCAGCACCTGGATCAGCGACGGCCAGGT GAAGGACTTCTACCTGTACCCCGGCAAGTACA CCTTCGTGGAGACCGCCGCCCCCGACGGCTAC GAGGTGGCCACCGCCATCACCTTCACCGTGAA CGAGCAGGGCCAGGTGACCGTGAACGGC
NheI SpyCatcher	PCR Forward Primer	ATATATGCTAGCATGGACAGCGCCACCCACAT CAAGTTCA
SpyCatcher *EcoRI*	PCR Reverse	ATATATGAATTCGCCGTTCACGGTCACCTGGC CCTGC

	Primer	
EcoRI mCherry	PCR Forward Primer	ATATATGAATTCATGGTGAGCAAGGGCGAGG A
NheI miRFP670	PCR Forward Primer	ATATATGCTAGCCGCCACCATGGTGGCTGGAC ACGCTTC
miRFP670 *HindIII*	PCR Reverse Primer	ATATATAAGCTTGCTCTCCAGGGCGGTGATTC
HindIII T2A *AflII*	Oligo (Sense)	AGCTTGAGGGCAGGGGCTCCCTGCTGACCTGC GGCGACGTGGAGGAGAACCCCGGCCCCC
	Oligo (Antisense)	TTAAGGGGGCCGGGGTTCTCCTCCACGTCGCC GCAGGTCAGCAGGGAGCCCCTGCCCTCA
EcoRI miRFP670	PCR Forward Primer	ATATATGAATTCATGGTGGCTGGACACGCTTC
NheI SH3	PCR Forward Primer	ATATATGCTAGCATGGCAGAGTATGTGCGGGC
SH3 *EcoRI*	PCR Reverse Primer	ATATATGAATTCATACTTCTCCACGTAAGGGA
XbaI SH3Lig *ApaI*	Oligo (Sense)	CTAGACCACCACCAGTCCCCCCTAGACGATAA GGGCC
	Oligo (Antisense)	TGGTGGTGGTCAGGGGGGATCTGCTATTC
XbaI SpyTag *BamHI*	Oligo (Sense)	CTAGAGCACACATAGTAATGGTAGACGCCTAC AAGCCGACGAAGG
	Oligo (Antisense)	GATCCCTTCGTCGGCTTGTAGGCGTCTACCATT ACTATGTGTGCT
BamHI GBP1	PCR Forward Primer	ATATATGGATCCATGCAGGTGCAACTGGTGGA
GBP1 *ApaI*	PCR Reverse Primer	ATATATGGGCCCTTACTTGCTGCTCACGGTCA CCTGGGTG
AflII miRFP670	PCR Forward Primer	ATATATCTTAAGATGGTGGCTGGACACGCTTC

miRFP670 *XhoI*	PCR Reverse Primer	ATATATCTCGAGGCTCTCCAGGGCGGTGATTC
NheI BFP	PCR Forward Primer	ATATATGCTAGCATAAGAATTCATGAGCGAGC TGATTAAGGAGAACATGCACA
BFP *ClaI*	PCR Reverse Primer	ATATATATCGATGTTCAGCTTGTGCCCCAGTTT GCTAGGGAGGTC
ClaI T2A *AflII*	Ultramer (Sense)	CGATGGCAGCGGCGAGGGCAGAGGCAGCCTG CTGACCTGCGGCGACGTGGAGGAGAACCCCG GCCCCC
	Ultramer (Antisense)	TTAAGGGGGCCGGGGTTCTCCTCCACGTCGCC GCAGGTCAGCAGGCTGCCTCTGCCCTCGCCGC TGCCAT
EcoRI BFP	PCR Forward Primer	ATATATGAATTCATGAGCGAGCTGATTAAGGA
AflII yCD	PCR Forward Primer	ATATATCTTAAGATGGTGACCGGCGGAATGGC CAG
yCD *XhoI*	PCR Reverse Primer	ATATATCTCGAGGCTGCCGGATCCTTCTCCAA TATCCTCAAACC
NheI EGFP	PCR Forward Primer	ATATAGCTAGCATGGTGAGCAAGGGCGAGGA GCTGT
EGFP *EcoRI*	PCR Reverse Primer	ATATATGAATTCGCTGCCGCCGCCCTTGTACA GCTCGTCCATGCCGAGA
AflII UbL	PCR Forward Primer	ATATATCTTAAGATGCAGGTGACCCTGAAGAC CCTGC
UbL *ClaI*	PCR Reverse Primer	ATATATATCGATAGAACCACCACCAGATCCAC CGTCT
ClaI YFP	PCR Forward Primer	ATATATATCGATGTGAGCAAGGGCGAGGAGCT GTTCA
Ub-M-EGFP	Mutagenesis Forward Primer	CAGAGGTGGGATGGGGAAGCTTGGTCG

Ub-L-EGFP	Mutagenesis Forward Primer	CAGAGGTGGGCTGGGGAAGCTTG
Ub-X-EGFP	Mutagenesis Reverse Primer	AGACGGAGTACCAGGTGC
Ub-X-KpnI_BamHI-EGFP	Mutagenesis Forward Primer	ATATGGATCCATGGTGAGCAAGGGCG
	Mutagenesis Reverse Primer	ATGGTACCTTGTCGACCAAGCTTCCC
KpnI GBP1	PCR Forward Primer	ATATATGGTACCATGCAGGTGCAACTGGTGGA
GBP1 *BamHI*	PCR Reverse Primer	ATATATGGATCCCTTGCTGCTCACGGTCACCT
BamHI miRFP670	PCR Forward Primer	ATATATGGATCCATGGTGGCTGGACACGCTTCCGG
miRFP670 *NotI*	PCR Reverse Primer	ATATATGCGGCCGCTTAGCTCTCCAGGGCGGTGAT
AflII EGFP	PCR Forward Primer	ATATATCTTAAGATGGTGAGCAAGGGCGAGGA
EGFP *XhoI*	PCR Reverse Primer	ATATATCTCGAGCTTGTACAGCTCGTCCATGC
BamHI LaM4	PCR Forward Primer	ATATATGGATCCATGGCTCAGGTGCAGCTCGTGGA
LaM4 *ApaI*	PCR Reverse Primer	ATATATGGGCCCTTAGGTGAAAGGGGAAGACACGG
KpnI LaM4	PCR Forward Primer	ATATATGGTACCATGGCTCAGGTGCAGCTCGT
LaM4 *BamHI*	PCR Reverse Primer	ATATATGGATCCGGTGAAAGGGGAAGACACGG

KpnI nE7	PCR Forward Primer	ATATATGGTACCATGCAGGTTCAGCTGGTGGAAAG
nE7 *BamHI*	PCR Reverse Primer	ATATATGGATCCGCTGCTCACGGTCACCTGGG
AgeI mCherry	PCR Forward Primer	ATATATACCGGTCGCCACCATGGTGAGCAAGGGCGAGGA
mCherry *NotI*	PCR Reverse Primer	ATATATCGCGGCCGCTTTACTTGTACAGCTCGTCCATGC

Appendix B

LIST OF ABBREVIATIONS

Arg (R)	Arginine
ATP	Adenosine Triphosphate
AZ1	Antizyme 1
BFP	Blue Fluorescent Protein
CDR	Complementary Determining Region
CI	Confidence Interval
cODC1	Synthetic ODC-like Degradation Tag
CPR	Conditional Protein Rescue
CRL	Cullin Ring Ligase
CUL	Cullin
DD	Degradation Domain
DDEPT	Degradation Dependent Enzyme Product Therapy
DNA	Deoxyribonucleic Acid
DMEM	Dulbecco's Modified Eagle Medium
DUB	De-Ubiquitination Enzyme
ecDHFR	*E. coli* dihydrofolate reductase
EGFP	Enhanced Green Fluorescent Protein
EGFR	Epidermal Growth Factor Receptor
FBS	Fetal Bovine Serum
FKBP	FK506-Binding Protein
FRB	FKBP12-Rapamycin-Binding Protein
GBP1	GFP Binding Protein 1
HECT	Homology to E6-AP C-Terminus
HEK293T	Human Embryonic Kidney 293 (SV40 Large T Antigen)
HIF-1α	Hypoxia Inducible Factor-1α
HPV	Human Papillomavirus
HRP	Horseradish Peroxidase
IBC	Inflammatory Breast Cancer
IBR	In-Between Ring

K_d	Dissociation Constant
LB	Lysogeny Broth
Leu (L)	Leucine
LID	Ligand-Induced Degradation
LOV2	Light Oxygen Voltage 2
MBP	Maltose Binding Protein
MEM	Minimal Essential Media
Met (M)	Methionine
miRNA	Micro RNA
nE7	Anti-E7 Nanobody
ODC	Ornithine Decarboxylase
PAGE	Polyacrylamide Gel Electrophoresis
PBS	Phosphate Buffered Saline
PCE	Prodrug Converting Enzyme
PCR	Polymerase Chain Reaction
PNK	Polynucleotide Kinase
POI	Protein of Interest
PROTACs	Proteolysis Targeting Chimeras
RBR	Ring-Between-Ring
RING	Really Interesting New Gene
RNA	Ribonucleic Acid
RNAi	RNA Interference
SCF	SKP1-Cullin-F-box protein
SD	Standard Deviation
SDS	Sodium Dodecyl Sulfate
SH3	Src Homology 3
Shld1	Synthetic Ligand 1
SMASh	Small Molecule-Assisted Shutoff
SURF	Split Ubiquitin for Rescue of Function
TIPI	TEV Protease Induced Protein Inactivation
TMP	Trimethoprim
TMSD	Toehold Mediated Strand Displacement
TShld	Traceless Shielding
Ub	Ubiquitin
UbC	C-terminus of Ubiquitin
UbL	Ubiquitin Like
UbN	N-Terminus of Ubiquitin

Val (V)	Valine
wLig	Weak SH3 Binding Ligand
yCD	Yeast Cytosine Deaminase
YFP	Yellow Fluorescent Protein